FINAL REPORT

on

STABILITY OF STRUCTURAL MATERIALS FOR SPACECRAFT APPLICATION

to

GODDARD SPACE FLIGHT CENTER
Contract No. NAS5-10267

APRIL 16, 1968

by

R. E. Maringer, M. M. Cho, and F. C. Holden

BATTELLE MEMORIAL INSTITUTE
Columbus Laboratories
505 King Avenue
Columbus, Ohio 43201

FINAL REPORT

on

STABILITY OF STRUCTURAL MATERIALS FOR SPACECRAFT APPLICATION

to

GODDARD SPACE FLIGHT CENTER
Contract No. NAS5-10267

April 16, 1968

by

R. E. Maringer, M. M. Cho, and F. C. Holden

BATTELLE MEMORIAL INSTITUTE
Columbus Laboratories
505 King Avenue
Columbus, Ohio 43201

SUMMARY

This program has been designed to evaluate the micromechanical properties related to dimensional stability of several selected structural materials of interest for spacecraft applications. The materials investigated were 2024, 5456, and 6061 aluminum alloys; I-400 beryllium; TZM molybdenum; AZ 31 magnesium; and Ti-6Al-4V and Ti-5Al-2.5Sn titanium alloys. The program was divided into three topics: evaluation of (1) microyield strength (MYS) after various heat treatments designed to permit some stress-relief, (2) microcreep properties of some of the heat treated materials at stress levels of about 50, 70, and 90 percent of MYS, and (3) thermal and the stress-cycling effects on dimensional stability. The resultant data indicate that both MYS and microcreep properties are structure sensitive, but that this sensitivity varies widely among different alloy systems. 5456-H34 aluminum showed particularly poor microcreep resistance, exhibiting considerable strain after 1400 hours at a stress of only 50 percent of its MYS. TZM-molybdenum, on the other hand, showed essentially no microcreep in 1400 hours at a stress of 70 percent of its MYS. Thermal and stress-cycling appeared to cause dimensional changes for most of the alloys examined. Data are interpreted in terms of the stress or thermal activation of dislocation sources, with dislocation interaction being negligible.

TABLE OF CONTENTS

STABILITY OF STRUCTURAL MATERIALS FOR SPACECRAFT APPLICATION

by

R. E. Maringer and M. M. Cho

INTRODUCTION

Modern technology is rapidly moving in the direction of greater accuracy and reliability requirements. Precision devices, such as gyros, accelerometers, optical systems, gas-bearings, etc., have become almost exquisitely sensitive, and must frequently operate at their ultimate sensitivity for long periods of time without adjustment. This puts a tremendous burden on the design engineer, who must know and understand the behavior of his materials of construction in order to "build-in" the reliability needed The problem is not a simple one, unfortunately, and it is all too often ignored.

The specific material problem of greatest concern is that of dimensional stability[1, 2], the ability of a material to maintain its dimensions over a period of time in a specified environment. The designer can often ignore or compensate for those dimensional changes which are reversible in nature, such as thermal expansion or purely elastic deformation. However, he must concern himself directly with those factors which lead to permanent changes in dimensions.

During the discussion it will be well to keep in mind the truism that, when one material property changes, others can also be expected to change. For example, when some of the carbon dissolved in iron precipitates in the form of carbides, the dimensions change, and so also does the elastic modulus, the electrical resistivity, the magnetic permeability, the yield behavior, and a host of other properties. Much of the following discussion is thus valid for material property stability, and not necessarily limited to dimensional stability.

There are two primary causes for non-reversible dimensional changes in metals. These are (1) metallurgical instabilities, and (2) stress relaxation.

Metallurgical Instabilities

The example cited above of carbon precipitating from solution in iron represents a form of metallurgical instability. In most alloy systems, the solubility of one element in another is temperature dependent. Even if the alloy has been thoroughly equilibrated at some specific temperature, service at some other temperature will incur the approach toward a new equilibrium, with consequent dimensional changes.

Approach to equilibrium will normally involve the ability of a solute atom to move, or, in other words, its diffusion rate. Since diffusion rates at a particular temperature are generally more rapid in low than in high melting point metals, dimensional changes due to these types of reactions are most common in aluminum, magnesium, or

similar low melting temperature alloys. Many refractory alloys and other high temperature materials can be relatively free of such problems.

Phase changes, that is, changes in the crystal structure of a metal, can also produce significant dimensional changes. The most common of these is the austenite-martensite reaction in many steels. Here, the densely packed face-centered-cubic austenite transforms into a less densely packed tetragonal martensite. To compound this change, tempering allows precipitation of carbon from the martensite to produce a more dense body centered cubic ferrite.

Steels, therefore, together with those other materials which can undergo a phase transformation (e.g., titanium, zirconium, cobalt, etc.) can have some special dimensional stability problems associated with them.

This does not by any means complete the list of metallurgical instabilities. Ordering, clustering, magnetic transformations, grain growth or recrystallization, and a host of other reactions will all, in general, lead to dimensional changes.

Stress Relaxation

In the final analysis, even most of the metallurgical instabilities can be considered in terms of stress relaxation. However, these are normally distinguished from the more conventional stress relaxation which deals with the response of materials to stresses imposed or stored during processing or in use. These usually comprise the residual stresses due to heat treatment, mechanical working, machining, or the externally applied stresses encountered during the operation of a part.

It is the dimensional instability associated with stress relaxation which is most commonly observed in engineering materials and which is of most concern to the designer. To appreciate the effects of stress relaxation, we must first examine the behavior of materials when subjected to stresses. Obviously, when a material is subjected to a stress, it changes dimensions. When the stress changes, the dimensions change. In general, therefore, stress relaxation is accompanied by a dimensional change, and the mechanism of stress relaxation, as well as the magnitude, distribution and causes of the stresses, assumes considerable importance.

Since the dimensional instabilities of concern to precision design are of the order of microinches per inch, one cannot rely on conventional mechanical properties to give reliable guidance to designers. The conventional 0.2 percent offset yield strength, for example, represents the stress at which a plastic strain of 2000 microinches per inch is achieved. The precision designer is much more interested in the stress to cause a plastic strain of 10, or 1, or even 0.1 microinches per inch. It is important that the designer realize that there is no general rule by which he can estimate what we might call "micro-mechanical" properties from the more conventional "macro-mechanical" properties. Indeed, it has been demonstrated[3] that a material can be strengthened in a macro-sense, and at the same time be weakened in a micro-sense.

It is vital, therefore, to know the micro-mechanical properties of materials to be used in precision applications. One micro-mechanical property which is gradually becoming accepted is the microyield strength, or MYS, the stress necessary to cause a residual plastic strain of one microinch per inch after short time tensile loading.

In the past[1] this property has often been called the precision elastic limit (PEL), but the term is a misnomer, for the MYS is in no sense an elastic limit. It is a measure of plastic strain. A second property of increasing interest is microcreep, loosely defined as creep strain of the order of microinches per inch per month under some fixed stress. Knowledge of both of these properties is essential to precision design, for they allow quantitative estimates to be made of maximum allowable design stresses.

Still another factor, environment, is involved in consideration of dimensional instability of materials. It is becoming increasingly clear that certain environments, particularly vibration and temperature cycling, are responsible for some of the observed dimensional instability of materials. Despite the need, micro-mechanical property data and data on the effects of environment on these properties are extremely sparse.

The objectives of this research program were, therefore, to measure the micro-yield strengths of a variety of commercially available materials; to evaluate the effect of several "stress relief" type anneals on the MYS; to measure the microcreep at several stress levels below the MYS; and to perform some initial experiments relative to the effects of thermal and stress cycling on the dimensional stability of these materials.

MATERIALS AND MATERIAL PREPARATION

The materials obtained for this program are characterized by composition, source, and condition, as shown in Tables 1 and 2 respectively. Some physical and mechanical properties of these materials are given in Table 3.

Tensile specimens and rectangular flat specimens, as shown in Figure 1, were machined from each of the materials. The tensile specimens were used for MYS, microcreep, and stress cycling tests, while the rectangular flat specimens were used for thermal cycling tests. After machining, the specimens were given the stress-relief treatments as indicated in Table 4 (for MYS tests) and Table 5 (for microcreep, thermal and stress cycling tests).

The heat treatments described in Table 5 were selected from those given in Table 4 on the basis of maximum stress relief for the least decrease in MYS. To remove any remaining residual stresses in the machined and subsequently heat-treated surface, about 10 mils were removed from the specimen thickness in the reduced section of the tensile specimen, and from the whole flat rectangular specimen by chemical etching. Chemical solutions and bath temperatures for each alloy are listed as follows:

(1) Aluminum Alloys

Sodium hydroxide (NaOH)	100 g
Water	500 cc
Bath temperature	~110 F
Remove smut in 10 percent HNO_3 in water	

TABLE 1A. MATERIAL COMPOSITION

	Al	C	Cu	Cr	Fe	Mg	Mn	Si	Zn	Be	BeO
Aluminum 2024	Bal	--	4.5	<0.01	0.26	1.42	0.62	0.22	<0.2	--	--
Aluminum 5456	Bal	--	<0.01	0.20	0.18	2.30	<0.01	0.09	<0.2	--	--
Aluminum 6061	Bal	--	0.25	0.26	0.52	0.76	0.07	0.60	<0.2	--	--
Beryllium	0.07	0.20	--	--	0.13	0.01	0.01	0.04	--	Bal	5.78

TABLE 1B. MATERIAL COMPOSITION

	Al	C	Fe	Mn	Ti	Zn	Zr	O	H	N	Mo	Mg	Sn	V
Molybdenum TZM	--	0.016	<0.001	--	0.42	--	0.087	<0.0003	<0.0001	<0.0003	Bal	--	--	
Magnesium AZ 31	3.2	--	--	0.43	--	1.05	<0.1	--	--	--	--	Bal	--	--
Ti-6Al-4V	6.1	0.023	0.09	--	--	--	--	0.10	0.007	0.010	--	--	--	4.1
Ti-5Al-2.5Sn	5.1	0.025	0.32	0.011	--	--	--	0.16	0.005	0.014	--	--	2.4	--

TABLE 2. MATERIAL CONDITION, QUANTITY, SIZE, AND SOURCE

Material	As-Received Condition	Quantity	Size, inches	Source
Aluminum				
2024	T4	30 strips	1/8 x 1 x 4*	Williams and Company, Columbus, Ohio
5456	H34	30 strips	1/4 x 1 x 4*	Williams and Company, Columbus, Ohio
6061	T6	30 strips	1/8 x 1 x 4*	Williams and Company, Columbus, Ohio
Beryllium				
I-400	Hot pressed	1 block	1 x 4 x 2.5	Brush Beryllium Company, Cleveland, Ohio
Molybdenum				
T M	Stress relieved	24 strips	1/8 x 1 x 4*	Climax Molybdenum Company of Michigan Ann Arbor, Michigan
Titanium				
6Al-4V	Solution treated and aged	27 strips	1/8 x 1 x 4*	Titanium Metals Corporation of America Cleveland, Ohio
5Al-2.5Sn	Annealed	27 strips	1/8 x 1 x 4*	Titanium Metals Corporation of America Cleveland, Ohio
Magnesium				
AZ 31		2 plates	6 x 6 x 6 14 x 14 x 0.5	Goddard Space Flight Center Greenbelt, Maryland

*Saw cut with 4-inch length parallel to rolling direction.

TABLE 3. MATERIAL CHARACTERISTIZATION BY THEIR PHYSICAL AND CONVENTIONAL MECHANICAL PROPERTIES

Alloy	Density lbs/in^3	Heat Capacity, Cp, BTU/ lb/F	Thermal Conductivity K, BTU/in. (ft^2/F/ft)	Thermal Expansion Coefficient 10^{-6}/F (70-212F)	Elastic Modulus 10^6 psi	0.2% Offset Yield Strength, 10^3 psi
Aluminum						
2024-T4	0.10	0.20	68	12.7	10.5	61.7
5456-H34	0.096	0.23	68	13.3	10.0	28.1
6061-T6	0.098	0.23	67	13.1	10.0	41.6
Beryllium						
I-400	0.067	0.59	87	6.5*	43.6	60.0
Molybdenum						
TZM	0.37	0.07	70-84	3.0	42.8	121.1
Magnesium						
AZ31	0.067	0.24	48-56	14.2**	6.5	7.5
Titanium						
Ti-6Al-4V	0.160	0.135	4.2	4.9***	16.5	134
Ti-5Al-2.5Sn	0.161	0.125	4.5	5.2***	16.0	123

*Be is anisotropic, with TEC differing by about 2 x 10^{-6} per degree F at room temperature.

**Mg is anisotropic, with TEC differing by about 0.4 x 10^{-6} per degree F at room temperature.

*** Ti is anisotropic, with TEC differing by about 1 x 10^{-6} per degree F at room temperature (estimated).

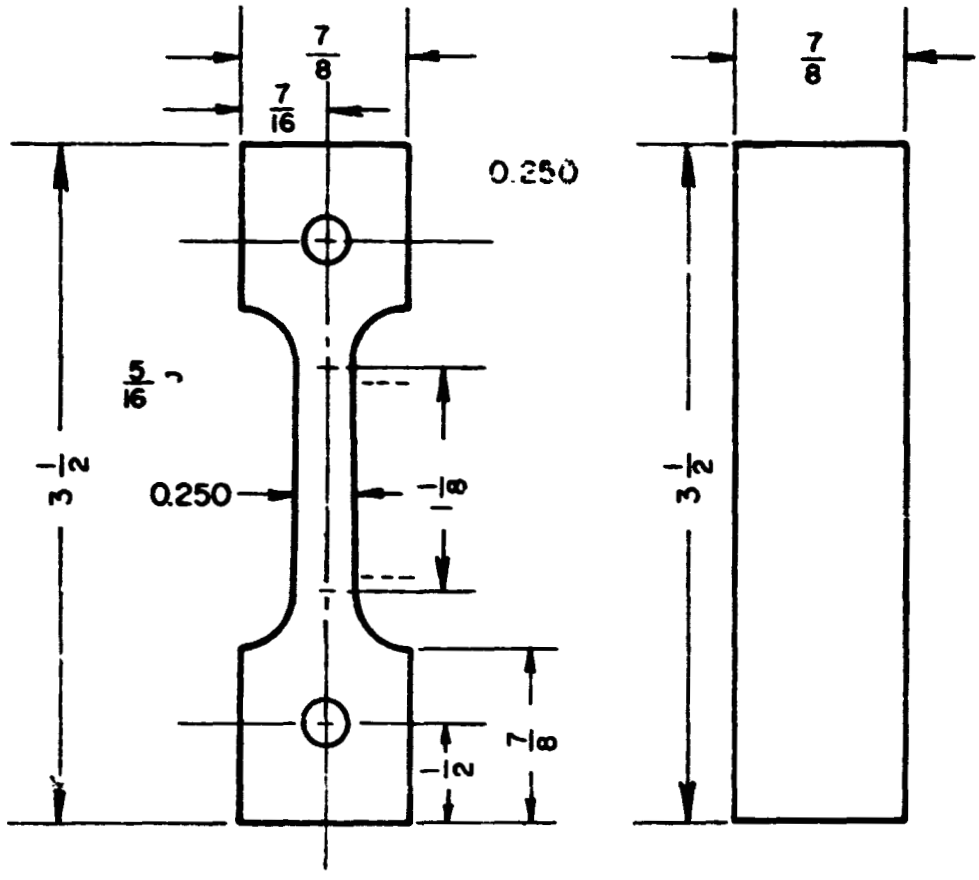

FIGURE 1. SPECIMENS FOR MYS, MICROCREEP, STRESS AND TEMPERATURE CYCLING TESTS

Note: All measurements given in inches; holes are located on axis of reduced section to within 0.0005 inch; specimen thickness is 0.1220 inch or less; specimen ends are lapped flat and parallel.

TABLE 4. SECONDARY HEAT TREATMENT OF SPECIMENS FOR MYS TESTS

Alloys	Secondary Heat Treatment			
	Temperature, F	Time, hours	Cooling	Atmosphere
Aluminum				
2024-T4	400	1	FC*	Air
	450	1	FC	Air
	500	1	FC	Air
5456-H34	400	1	FC	Air
	450	1	FC	Air
	500	1	FC	Air
6061-T6	400	1	FC	Air
	450	1	FC	Air
	500	1	FC	Air
Beryllium				
I-400	1100	1	FC	Vacuum
	1500	1	FC	Vacuum
Molybdenum				
Mo-0.5Ti	2200	1	FC	Hydrogen
	2600	1	FC	Hydrogen
Magnesium				
AZ 31	450	1	FC	Air
Titanium				
Ti-6Al-4V	1100	1	FC	Vacuum
	1300	1	FC	Vacuum
	1500	1	FC	Vacuum
Ti-5Al-2.5 Sn	1100	1	FC	Vacuum
	1300	1	FC	Vacuum
	1500	1	FC	Vacuum

*FC denotes furnace cooling. Cooling rate not to exceed 300 F/hr from 2600, 200 F/hr from 1600 to 500 F, and 100 F/hr from 500 F to room temperature.

TABLE 5. SECONDARY HEAT TREATMENT OF SPECIMENS FOR MICROCREEP, THERMAL AND STRESS CYCLING TESTS

Material	Stress-Relief Heat Treatment	Cooling	Atmosphere
2024-T4, 5456-H34, and 6061-T6 aluminum	400 F, for 1 hour	FC*	Air
AZ 31 Mg	450 F, for 1 hour	FC	Air
TZM Mo	2200 F, for 1 hour	FC	H_2
I-400 Be	1100 F, for 1 hour	FC	Vacuum
Ti-6Al-4V	1100 F, for 1 hour	FC	Vacuum
Ti-5Al-2.5Sn	1100 F, for 1 hour	FC	Vacuum

*Furnace cooled.

(2) Beryllium I-400

Sulphuric acid (96% H_2SO_4)	27 cc
Phosphoric acid (85% H_3PO_4)	410 cc
Chromic acid (CrO_3)	70 g
Water	130 cc
Bath temperature	~170 F

(3) Molybdenum TZM

Water	225 cc
Nitric acid (70% HNO_3)	150 cc
Sulphuric acid (96% H_2SO_4)	150 cc
Bath temperature	RT

(4) Titanium Alloys

Lactic acid (88.4% CH CHOHCOOH)	240 cc
Nitric acid (70% HNO_3)	80 cc
Hydrofluoric acid (48.7 HF)	80 cc
Bath temperature	RT
Slowly stirred on a magnetic stirrer	

(5) Magnesium AZ 31

5 percent nitric acid in water	
Bath temperature	RT

Chemical etching was accomplished by the following procedure. Stop-off materials (such as Microstop lacquer, which was applied by brushing or dipping, and Microwax, which melts at 125 F and was applied by dipping) were used to mask the heads of the specimens. The masked specimens were placed in the constantly agitated etching bath for various periods of time. The specimens were periodically removed from the bath, washed, and measured. Complete etching cycles ranged from 10 to 30 minutes for each specimen. Microstop was removed by washing with acetone. Microwax was removed by cutting the wax off with a razor blade, and removing the residue with trichlorethylene.

Foil gages of Type MA-XX-250 BG-120, manufactured by the Micro-Measurements Company, were used throughout this study. Some of the details of these gages are given in Figure 2.

Two types of cements were employed for MYS tests; Eastman 910, a cyanoacrylate cement, and BR-600, an epoxy cement. Eastman 910 is convenient for application, and cures at relatively low temperature. BR-600 requires an elevated-temperature cure to achieve the desired degree of stability and strength.

Eastman 910 was used for MYS tests on 5456-H34 Al, 6061-T6 Al, I-400 beryllium, molybdenum TZM, and magnesium AZ 31; BR600 was used for MYS tests on 2024-T4 Al, and on all microcreep tests.

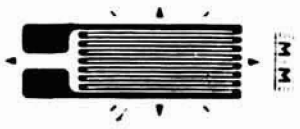

FIGURE 2. MA-XX-250BG-120 FOIL GAGE

Physical Properties:

Dimensions

Gage length 0. 250 inch
Overall length 0. 375 inch
Grid width 0. 125 inch
Overall width 0. 125 inch

Grid Alloy

Constantan foil with a temperature compensation for 3, 6, 13, or 15 μin./in./F

Backing

A tough epoxy resin film with a 0. 0009-inch thickness

Electrical Properties

Gage resistance 120 ohms
Gage factor 2. 095
Linearity better than 0. 05 percent

With Eastman 910, the chemically milled surface of the specimen was cleaned with alcohol, metal conditioner, and neutralizer. A terminal strip (GS-3 from Budd Company) was placed about 1/16 inch from the tab end of the gage. A piece of cellophane tape (3/4 inch wide and 1.5 to 2.5 inches long) was placed over the open face of the gage and terminal strip for handling. The gage and terminal-strip backings were cleaned with a cotton swab or Q-tip slightly moistened with the neutralizer. A thin film of accelerator was then applied, and one to two minutes drying time was allowed. The tape was oriented on the specimen in the area for gaging. One end of the tape was then attached to the specimen. One drop of cement was placed on the specimen near the end of the gage, and another drop in the middle of the gage area. With some pressure from the thumb, one wiping motion was made from the taped end to the terminal-strip end. The gage was held with moderate pressure for two to four minutes. Then the tape was peeled off at 90 degrees to the gage plane, the specimens were placed in an oven at 105 F, and allowed to post-cure for 24 hours. A protective coating, designated as Gagekote No. 1 by W. T. Bean Company, was applied over the gage, except for the gage tab and terminal strip, as soon as the specimen had been cured. Small soldered flexible leads connect the gage to the terminal strips. The main leads were soldered to the terminal strips. The resin of the solder was dissolved with solvent prior to final and overall coating of the gage and the lead wires. The gaged specimens were ready for testing after drying the coating for one hour or longer.

With BR-600, surface preparation of the specimen was the same as above. The GS-3 terminal strips were again placed on the cellophane tape, 1/8 inch from the tab of the gage. With a neutralizer-moistened Q-tip both faces of the gage and the terminal-strip backing were cleaned and allowed to dry. A thin film of BR-600 was applied to the surfaces of the gage and the terminal-strip backing, and allowed to dry for 5 minutes in air. The gage was then oriented in the designated area and held on the specimen by tape. A 2-inch long by 3/4-inch wide 1-mil thick Teflon sheet was held down on the tape end. With some pressure from the thumb, one wiping motion was made from the tape end to the end of the gage. Similarly, a gage on the opposite face of the specimen was applied. The gages were sandwiched with Teflon. Then a silicone rubber pad, 1-12/ inches long, 3/4 inch wide, and 1/8 inch thick was placed over the Teflon. Aluminum pressure distributors of equal size were placed on the pads and a clamp force of 12 to 60 psi was applied with a small C-clamp. The whole assembly was placed in an oven to be cured at 350 F for 5 hours, followed by furnace cooling. The application of the protective coating and the installation of lead wires were performed in the same manner as above. An example of a prepared specimen is shown in Figure 3.

EXPERIMENTAL RESULTS

Microyield Strength Measurement

Experimental Method

The system devised to load the specimens in uniaxial tension is shown in Figures 4 and 5. The details of the assembly can be seen in the drawing of Figure 6. The uppermost fitting (in the exploded view) is a ball-thrust-bearing system to eliminate the possibility of significant torque being applied to the specimen during loading.

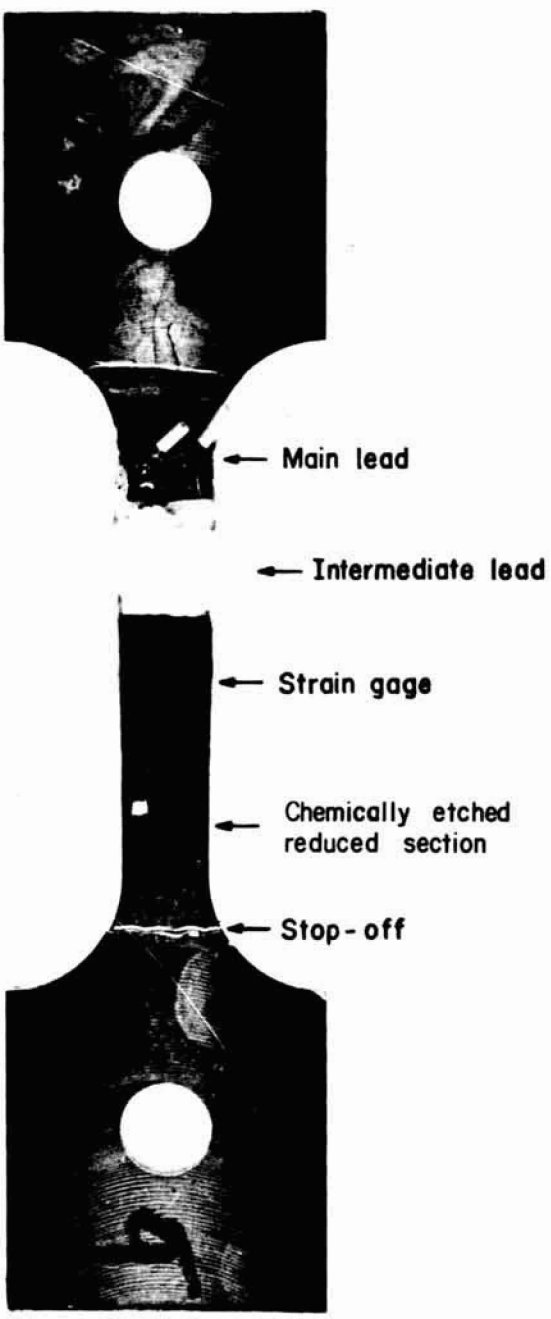

FIGURE 3. TYPICAL SPECIMEN SHOWING STRAIN GAGE DETAILS

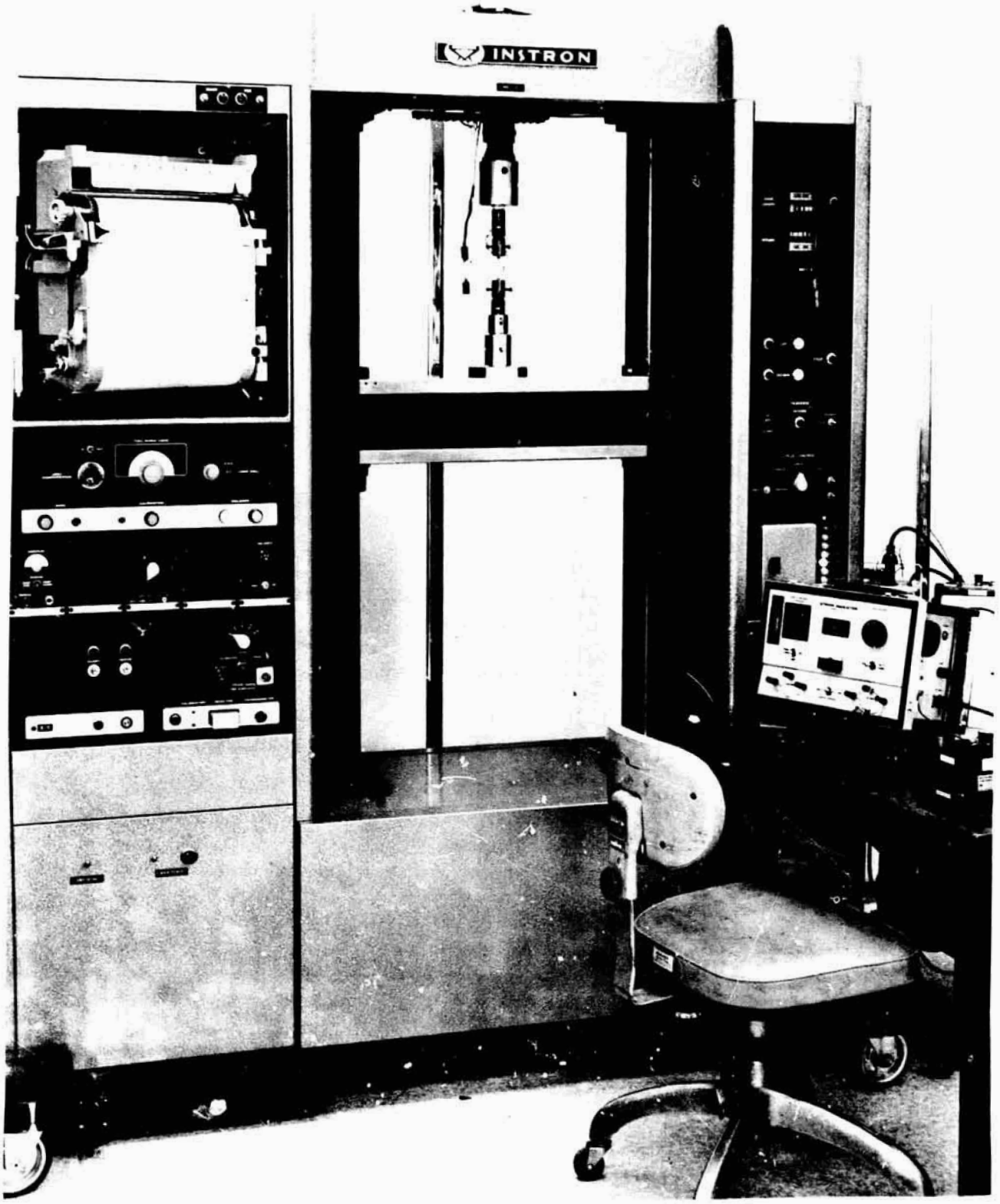

FIGURE 4. MYS TEST SET-UP

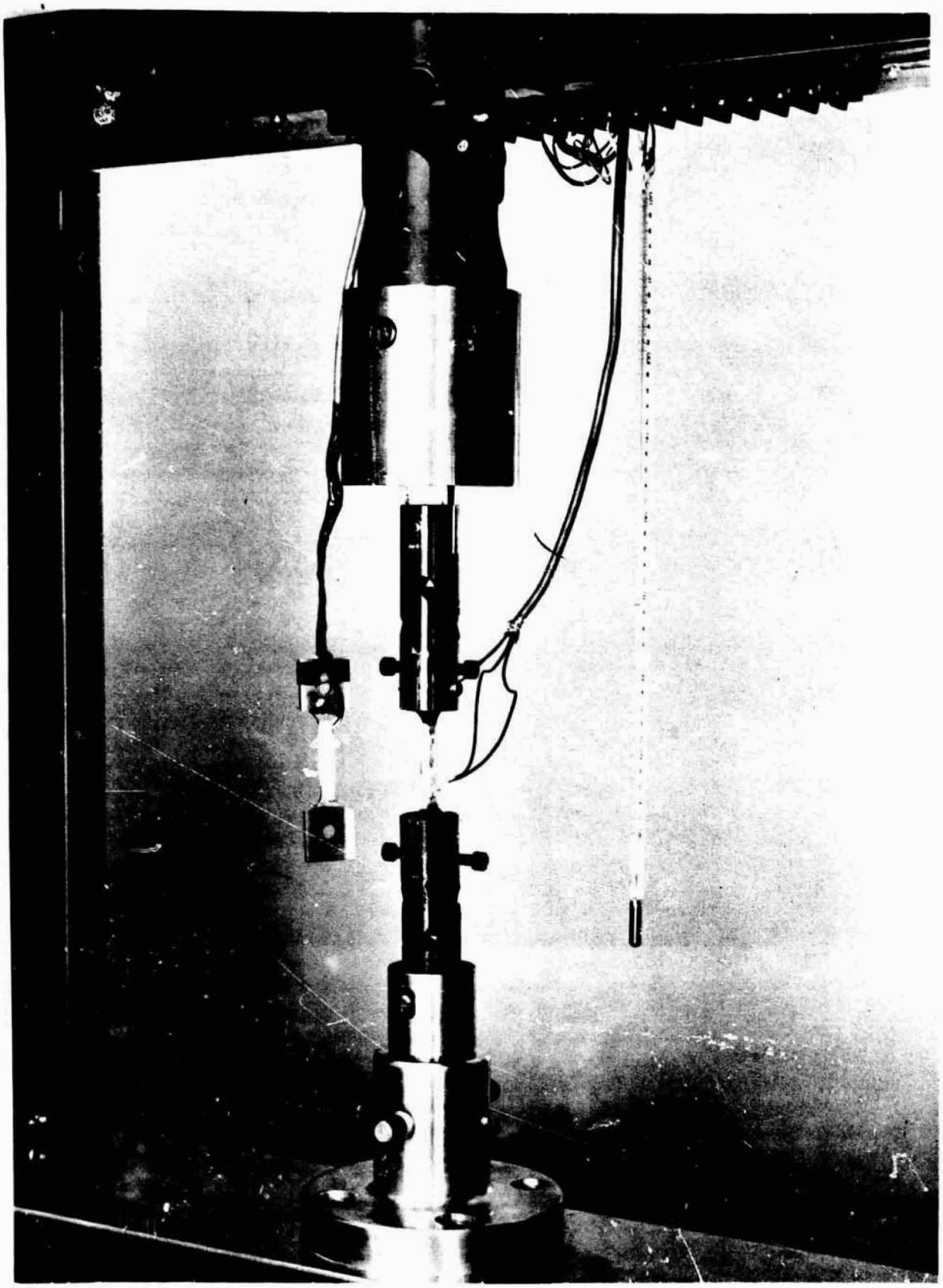

FIGURE 5. CLOSE-UP VIEW OF MYS LOAD TRAIN

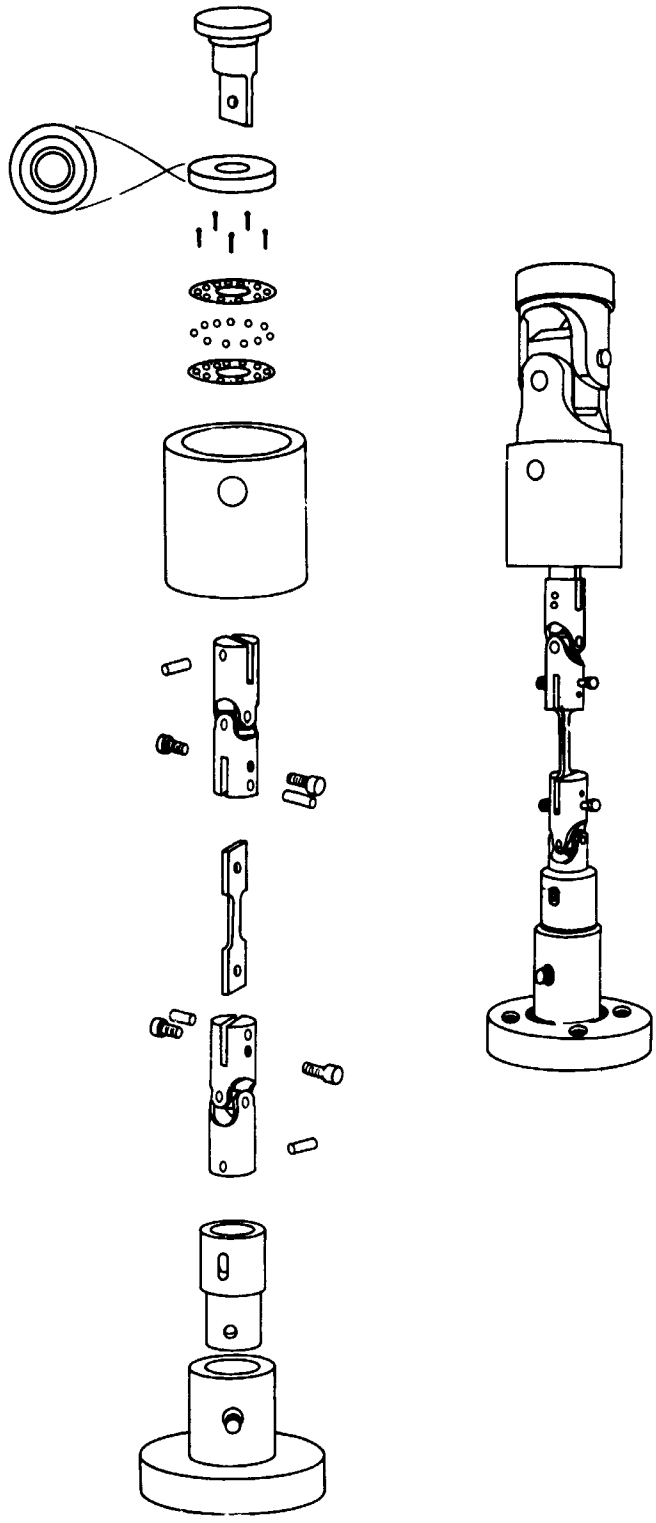

FIGURE 6. EXPLODED VIEW OF MYS LOAD TRAIN

This device supports a universal joint in which the specimen is gripped. The lower end of the specimen is gripped in another universal joint attached to the moving platen of the tensile machine by a pinned joint. In this lower joint, the pin is confined in a slotted hole. Therefore, when the tensile load is removed, there is no compressive load applied to the specimen.

Active and dummy gages are connected in a full-bridge circuit with Number 25 AWG four conductor wire, shielded in pairs. Bridge connections were made to a terminal strip attached rigidly to the loading frame as shown in Figure 5. Strain measurements were made with a BLH Model 120 strain indicator, factory modified to increase its sensitivity by a factor of 5. The indicator was modified still further by using a highly sensitive galvanometer in place of the normal null indicator.

A full-bridge circuit was used (as shown in Figure 7) with the inactive bridge resistors being gages of the same type mounted on the same material as the active gages. All the gages were kept close together physically to minimize temperature variations. The use of temperature-compensated gages also aided in minimizing the effects of temperature fluctuations. All tests were conducted in a constant-temperature room (68± 1/4 F).

In practice, the specimen is loaded several times up to 5 to 10 percent of its estimated MYS. Both gages are read individually in a half-bridge circuit, any observed eccentricity is corrected by adjustments of the screws on the sides of the universal joints. When fully adjusted the full-bridge circuit is used (see Figure 7), and the specimen is again loaded several times to 5 to 10 percent of its estimated MYS to assure stability in the strain readings. The load is then raised to a higher value and immediately removed. In the unloaded state, the lower pin is disengaged in the slot so that only a nominal load (~1/2 lb) remains on the specimen. At this reference load, the strain is read. This procedure is repeated, with the load increasing incrementally with each cycle, until a total permanent elongation of the order of 50 microinches per inch is read under the reference load.

At the conclusion of the MYS test, the specimen was normally loaded incrementally, and strain readings were taken at each stress level. From these data, elastic moduli were calculated. Finally, the same specimen was tested conventionally to obtain the 0.2 percent offset yield strength.

The same procedure was followed for measuring the MYS of the titanium alloys, except that an Instron Extensometer, Model 51 was used as the strain sensor for above described circuit, since total strains at the MYS exceeded the useful range of the foil strain gages.

Microyield Strength Data

A typical example of the data generated is given in Figure 8. There is normally a stress range over which plastic deformation is not measurable (less than 0.1 x 10^{-6} in./in.). Once measurable deformation begins, the curve begins to break over sharply. The stress to produce a residual strain of one microinch per inch represents the microyield strength. The test is normally continued until a residual strain of the order of 50 microinches per inch is achieved, as this gives some indication of the rate

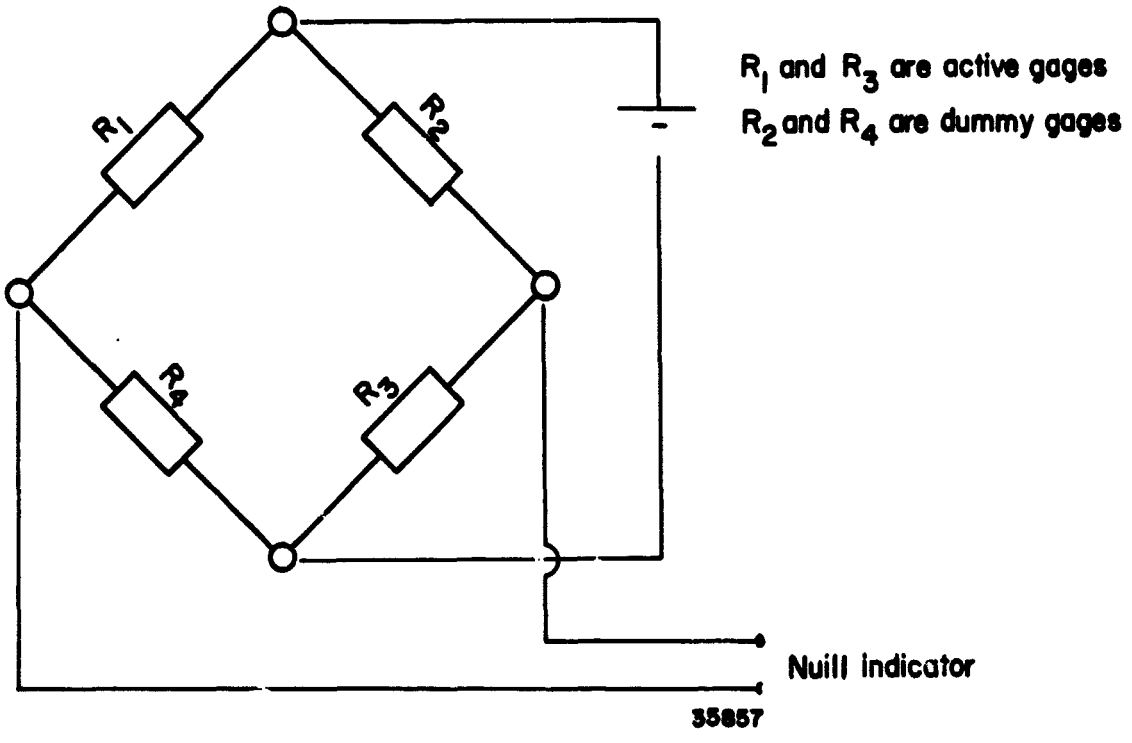

FIGURE 7. A FULL BRIDGE MEASURING CIRCUIT

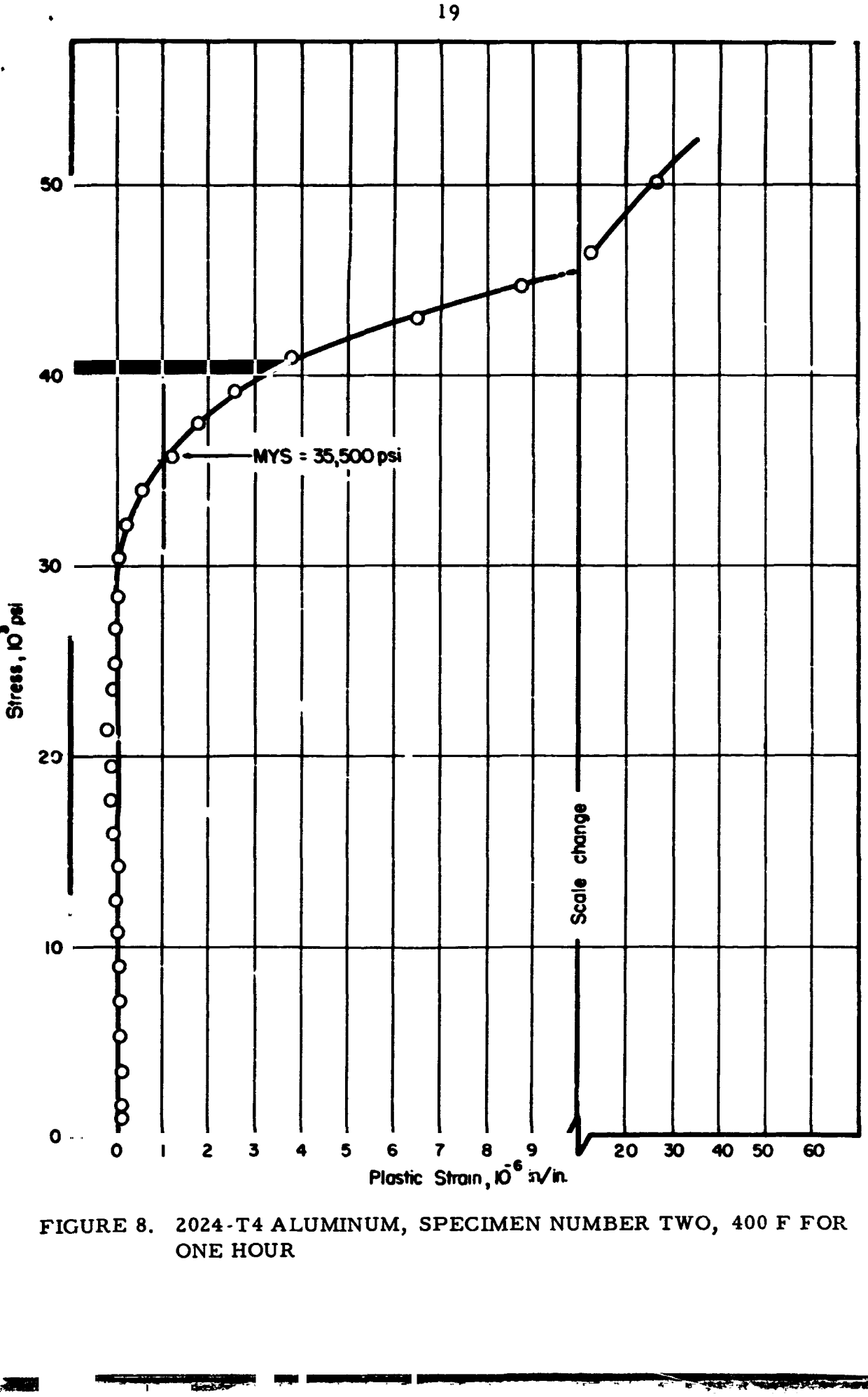

FIGURE 8. 2024-T4 ALUMINUM, SPECIMEN NUMBER TWO, 400 F FOR ONE HOUR

of strain hardening and may relate to creep resistance. These data, in addition to the conventional 0.2 percent offset yield, and measured elastic moduli are given in Table 6. For comparison, the stresses to cause plastic strains (ϵ_p) of 5 and 10 microinches per inch are also given in Table 6. The actual MYS curves are given in Appendix A.

Microcreep Measurements

Experimental Methods

Figure 9 shows the basic strain-measurement circuit – a "chevron" type – for a group of two to three specimens in a train of four to six specimens. The strain-indication system employed was the same as that described for the MYS testing. However, in some cases, the strain level exceeded the range of the modified BLH strain indicator, necessitating the incorporation of an external bridge in the measuring bridge network, as shown in Figure 10. All lead wires of the circuits were kept to a practical minimum length.

Each specimen and gage network was checked prior to creep loading for any instability due to circuit frailties, gage instabilities, etc., and thermal equilibrium of the strain-measurement system was achieved. Figure 11 shows the results of a stability check on one specimen.

Specimens were loaded for microcreep studies in a dead-weight A-frame or through a 20:1 lever-arm system in conventional creep frames (Figure 12). Specimens were loaded in strings, each specimen being separated from its neighbor by a universal joint. Each string contained a thrust bearing to relieve any torque that might develop in the string. All testing was done in a constant-temperature room at 68 ± 1/4 F.

Loading was accomplished in small steps, with strain readings taken on each gage. Where possible, eccentricity was adjusted to a minimum. In some cases, heat treatment had bent the specimens slightly, and a relatively high eccentricity had to be accepted. Loading times were normally from twenty to thirty minutes. A summary of specimens and loading conditions is given in Table 7. Data were taken from each specimen at time intervals varying from minutes early in the tests to days at later stages of testing.

Microcreep Data

A typical example of a creep strain versus log time curve is given in Figure 13. The remainder of the curves are given in Appendix B. For most of the materials, the creep behavior appeared normal (i.e., creep strain increased with time in a monotonic fashion). For one AZ 31 Mg sample (Figure B-16), and for one I-400 Be sample (Figure B-25), discontinuities were observed which are believed to be associated with the strain gages or the gaging circuitry. The TZM molybdenum showed indication of both negative creep (Figures B-21, B-22, B-24) and positive creep (Figures B-20 and B-23), most of which totaled less than two microinches per inch over the entire two-month testing period. Creep experiments using strain-gage techniques on the Ti alloys were unsuccessful. This was due to strain-gage limitations which will be discussed shortly.

Notations:

A_1 = active gage of Specimen No. 1

D_1 = dummy gage for Specimen No. 1

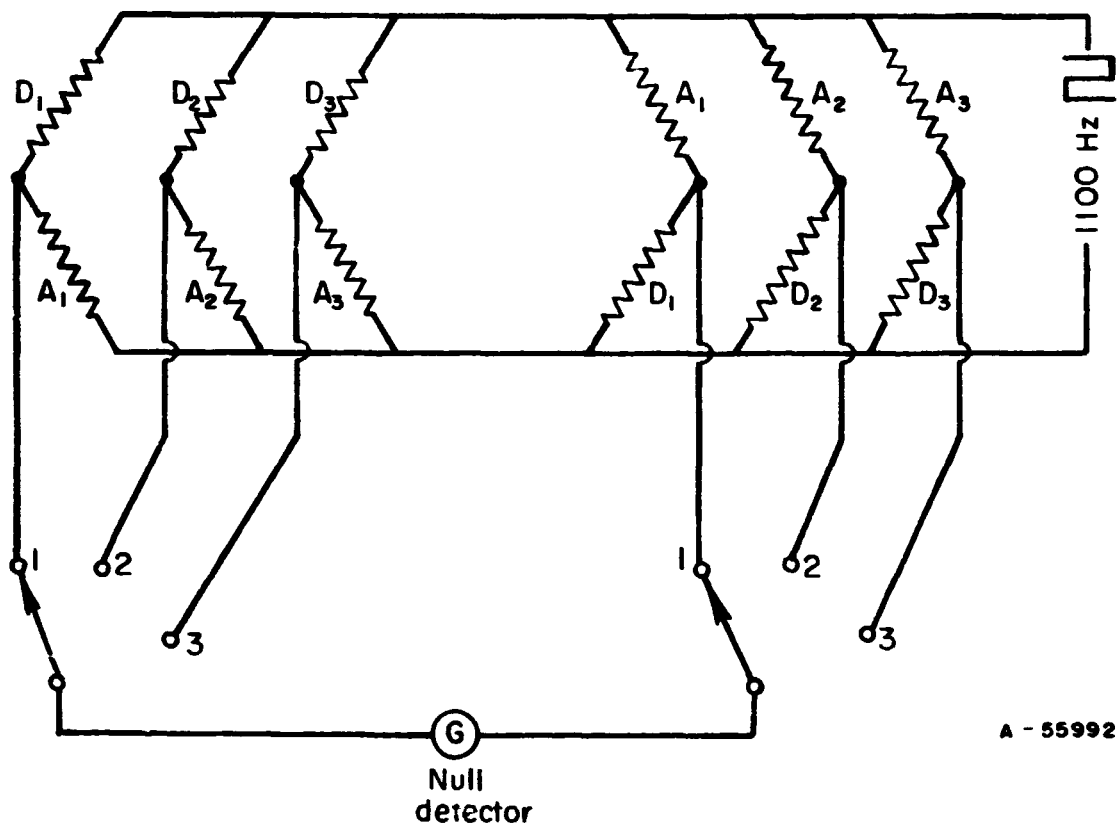

FIGURE 9. BASIC STRAIN MEASUREMENT CIRCUIT

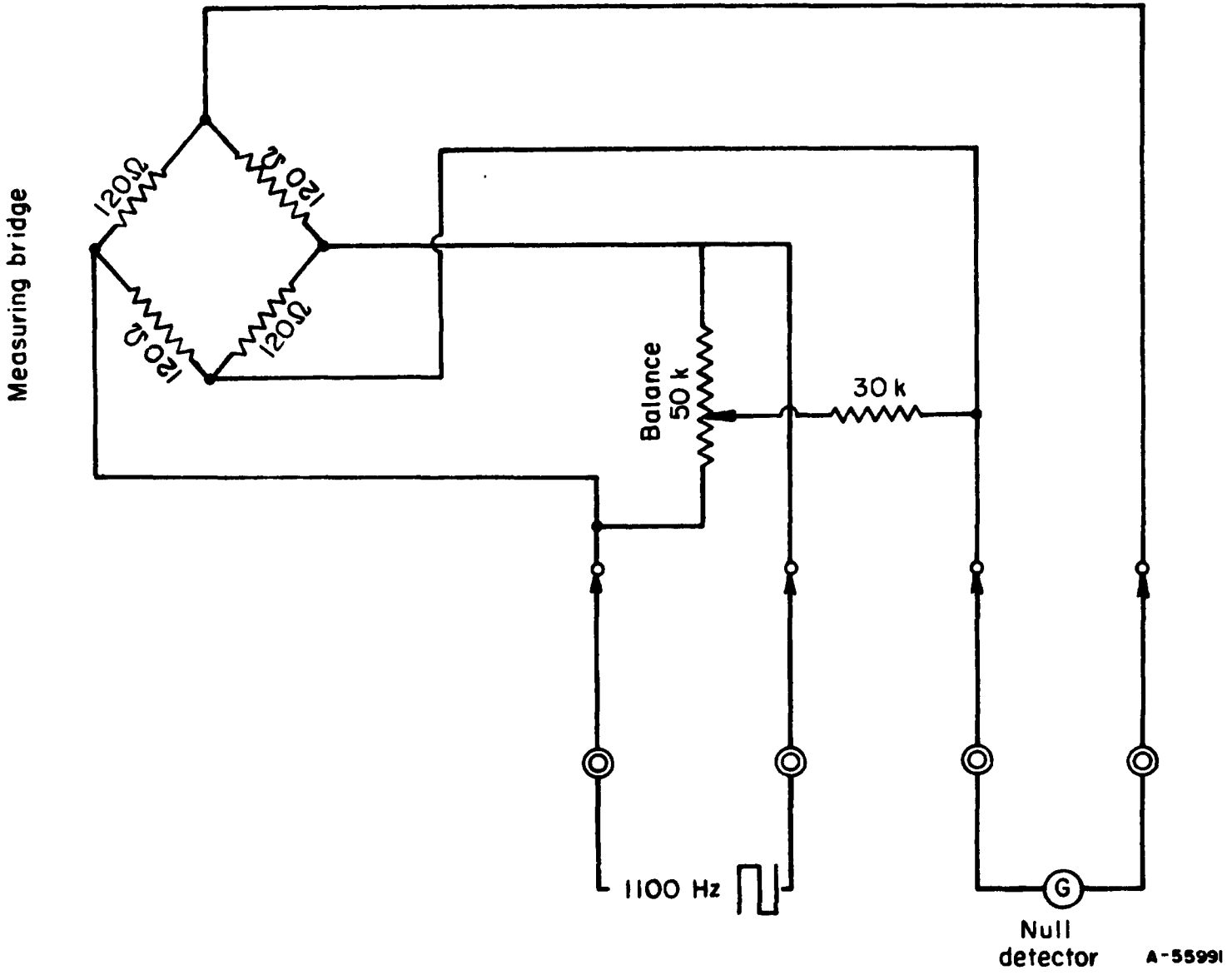

FIGURE 10. CIRCUIT FOR AN EXTENSION OF STRAIN RANGE

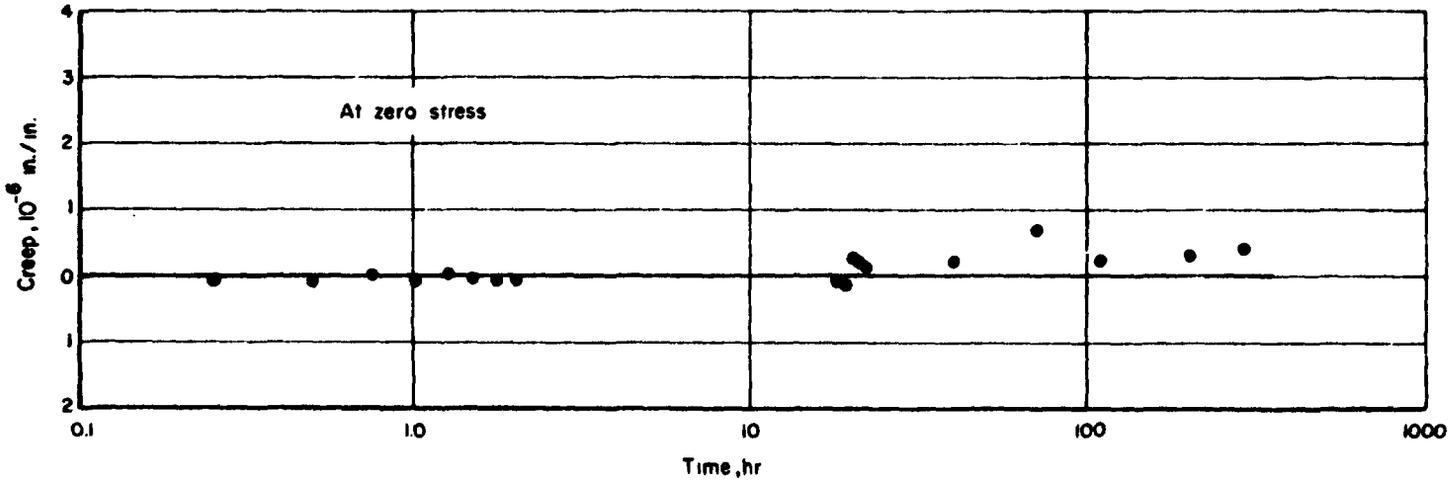

FIGURE 11. STRAIN-TIME RELATIONSHIP OBTAINED FROM A TEST SET-UP (AZ31 Mg, Specimen No. 3) FOR MICROCREEP AT ZERO LOAD

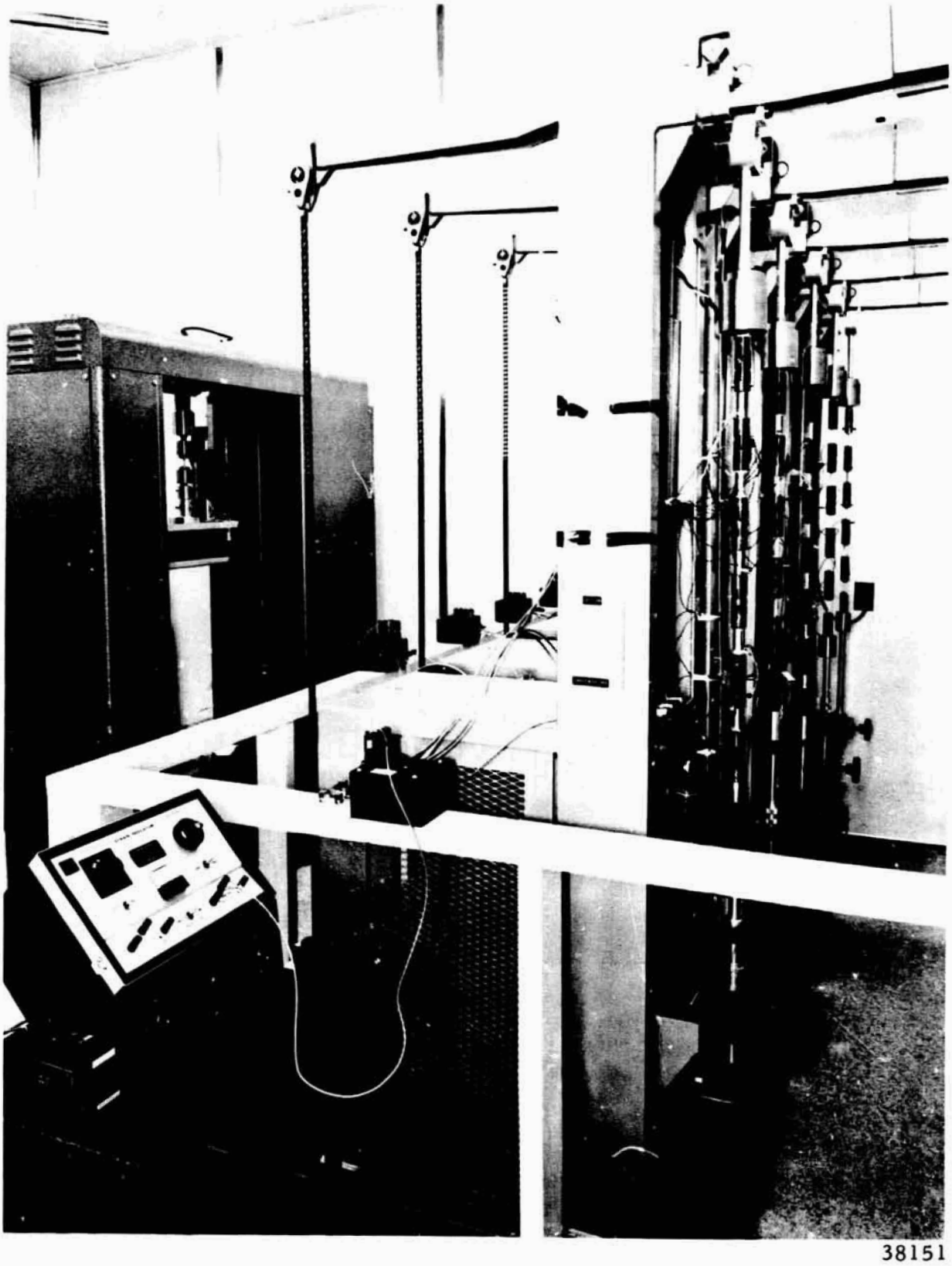

38151

FIGURE 12. MICROCREEP TEST STANDS

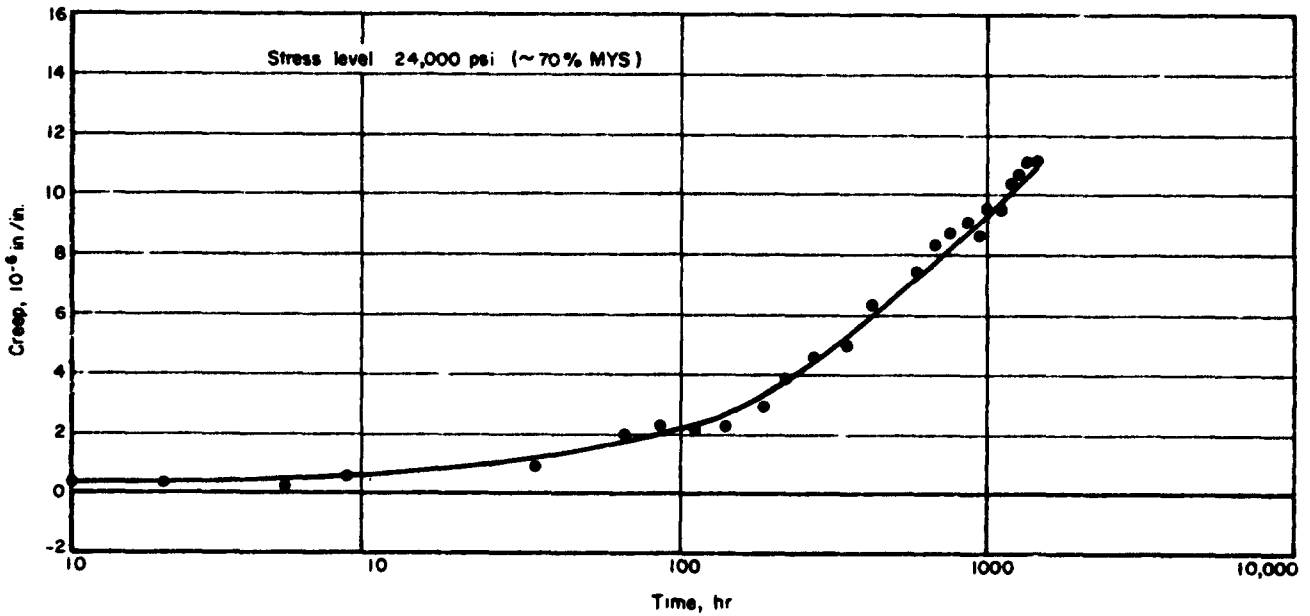

FIGURE 13. MICROCREEP TEST ON 2024-T4 A1, SPECIMEN NO. 10, HEAT TREATED AT 400 F FOR 1 HOUR

TABLE 6A. SUMMARY OF MICRO AND CONVENTIONAL MECHANICAL DATA OBTAINED BY STRAIN GAGE

Material	Specimen Number	Heat Treatment	MYS, 1 μin./in. psi	Stress for ε_p of MYS, 5 μin./in. psi	Stress for ε_p of MYS, 10 μin./in. psi	0.2% Offset Yield, 10^3 psi	Elastic Modulus, 10^6 psi
2024-T4 Al	8	As received	38,000	45,000	46,200	50.0	10.2
	7	As received	39,000	42,500	44,500	51.8	9.9
	2	1 hr at 400 F	35,500	42,000	45,500	59.9	10.3
	3	1 hr at 400 F	29,000	39,500	44,500	63.5	10.7
	19	1 hr at 450 F	28,800	37,000	41,200	63.5	10.2
	18	1 hr at 450 F	32,400	39,000	43,000	--	10.0
	21	1 hr at 500 F	20,200	28,200	32,200	52.2	10.2
	20	1 hr at 500 F	22,500	30,000	33,500	--	10.2
5456-H34 Al	4	As received	17,500	19,800	--	30.8	10.0
	5	As received	17,500	19,400	20,900	28.2	10.2
	10	1 hr at 400 F	21,600	22,300	22,800	27.0	10.2
	11	1 hr at 400 F	19,500	21,000	21,600	29.2	9.8
	17	1 hr at 450 F	22,200	24,800	25,600	29.2	10.0
	16	1 hr at 450 F	19,800	21,000	21,700	28.0	10.0
	22	1 hr at 500 F	19,700	20,800	21,000	26.5	10.0
	23	1 hr at 500 F	18,600	20,000	20,400	28.0	10.3
6061-T6 Al	2	As received	19,000	26,400	30,400	--	10.0
	1	As received	18,400	26,800	30,400	42.0	10.0
	9	1 hr at 400 F	25,400	29,900	31,600	41.2	10.0
	8	1 hr at 400 F	27,200	31,600	33,900	42.0	10.0
	15	1 hr at 450 F	20,800	25,000	27,100	43.5	10.0
	14	1 hr at 450 F	21,400	26,400	28,400	37.8	9.9
	25	1 hr at 500 F	10,200	16,200	19,200	31.0	9.8
	24	1 hr at 500 F	17,200	19,900	22,000	30.8	9.6
AZ 31 Mg	1	As received	3,200	4,400	4,800	7.0	6.3
	2	As received	3,200	4,200	4,700	7.8	6.5
	3	1 hr at 450 F	3,340	3,880	4,080	7.0	6.3
	4	1 hr at 450 F	3,850	5,240	5,840	7.9	6.7
TZM Mo	1	As received	24,000	52,000	61,000	126.0	44.0
	2	As received	35,500	58,000	65,000	126.0	--
	4	1 hr at 2200 F in H_2	52,200	60,500	63,000	120.2	42.6
	5	1 hr at 2200 F in H_2	52,700	62,500	67,000	123.5	43.2
	6	1 hr at 2200 F in H_2	52,700	61,000	67,000	122.0	43.2
	7	1 hr at 2200 F in H_2	58,000	63,500	67,500	119.0	42.4
	8	1 hr at 2600 F in H_2	49,700	54,000	61,500	75.5	43.0

TABLE 6A. (Continued)

Material	Specimen Number	Heat Treatment	MYS, 1 μin./in. psi	Stress for ϵ_p of MYS, 5 μin./in. psi	Stress for ϵ_p of MYS, 10 μin./in. psi	0.2% Offset Yield, 10^3 psi	Elastic Modulus, 10^6 psi
M Mo	9	1 hr at 2600 F in H_2	50,000	53,000	56,000	76.8	44.4
	10	1 hr at 2600 F in H_2	49,000	52,000	54,000	79.0	45.0
	11	1 hr at 2600 F in H_2	52,000	56,500	58,000	78.2	44.4
400 Be	1	As received	7,400	14,200	20,000	60.0	41.8
	2	As received	5,000	10,400	15,500	59.5	42.7
	6	1 hr at 1100 F in vacuum	9,000	18,600	24,000	Fractured at grip	43.5
	7	1 hr at 1100 F in vacuum	6,800	17,000	24,000	60.0	43.8
	4	1 hr at 1500 F in vacuum	9,200	17,600	22,700	58.5	41.0
	5	1 hr at 1500 F in vacuum	5,200	12,100	16,800	59.0	41.0

TABLE 6B. SUMMARY OF MICRO AND CONVENTIONAL MECHANICAL DATA OBTAINED BY INSTRON EXTENSOMETER

Material	Specimen Number	Heat Treatment	MYS 1 μin./in. psi	Stress for ϵ_p of MYS, 5 μin./in. psi	Stress for ϵ_p of MYS, 10 μin./in. psi	0.2% Offset Yield, 10^3 psi	Elastic Modulus, 10^6 psi
i-6Al-4V	10	As received	80,000	119,000	120,000	140.0	15.6
	11	As received	76,000	88,000	96,000	--	--
	3	1 hr at 1100 F in vacuum	92,000	97,000	104,000	166.0	15.6
	2	1 hr at 1100 F in vacuum	95,500	99,000	106,000	170.0	15.6
	8	1 hr at 1300 F in vacuum	66,500	69,000	71,000	145.0	15.6
	3	1 hr at 1300 F in vacuum	58,000	63,000	66,000	--	--
	5	1 hr at 1500 F in vacuum	48,000	54,000	58,000	145.0	15.8
	4	1 hr at 1500 F in vacuum	42,000	57,000	65,000	134.5	16.0

TABLE 6B. (Continued)

Material	Specimen Number	Heat Treatment	MYS 1 μin./in. psi	Stress for ϵ_p of MYS, 5 μin./in. psi	Stress for ϵ_p of MYS, 10 μin./in. psi	0.2% Offset Yield 10^3 psi	Elastic Modulus, 10^6 psi
Ti-5Al-2.5Sn	18	As Received	86,000	104,000	114,000	124.0	15.0
	19	As received	80,000	93,000	102,000	121.0	15.2
	2	1 hr at 1100 F in vacuum	83,000	91,000	96,000	--	--
	3	1 hr at 1100 F in vacuum	73,000	80,000	85,000	124.0	15.0
	15	1 hr at 1300 F in vacuum	72,000	78,000	85,000	124.0	15.0
	7	1 hr at 1300 F in vacuum	76,500	79,500	85,000	126.0	16.3
	12	1 hr at 1500 F in vacuum	66,500	78,000	84,000	121.0	16.7
	13	1 hr at 1500 F in vacuum	73,000	82,000	88,000	121.0	16.5

TABLE 7. SUMMARY OF MICROCREEP TEST PARAMETERS

Material	Specimen Number	Load Level Stress	Load Level Percent MYS	Young's Modulus, E, 10^6 psi	Percent Eccentricity, C**	Machine Number	Date of Loading
2024-Al	9	18,000	50	10.8	4.5	1	12/21/66
	10	24,000	70	10.6	4.5	2	12/23/66
	12	24,000	70	10.8	3.9	2	12/23/66
	11a	34,600	90	10.9	4.5	3	2/7/67
	11b	34,600	90	10.8	0.9	3	2/7/67
5456-Al	17	11,000	50	10.7	0	A-frame	2/21/67
	18	11,000	50	10.7	36	A-frame	2/21/67
	15	14,800	70	10.4	0.9	4	2/8/67
	16	14,800	70	10.7	9.9	4	2/8/67
	13	17,800	90	10.4	3.9	1	12/21/66
	14	18,000	90	10.6	6.9	1	12/21/66
6061-Al	7	14,800	50	10.2	1.8	4	2/8/67
	8	14,800	50	10.2	1.8	4	2/8/67
	3	18,500	70	10.6	21.9	1	12/21/66
	4	18,000	70	10.4	6.9	1	12/21/66
	5	24,600	90	10.5	0.9	2	12/23/66
	6	24,600	90	10.6	1.8	2	12/23/66
AZ 31-Mg	1	1,720	60	6.0	49.3	A-frame	11/21/66
	2	1,700	50	6.1	3.6	A-frame	11/21/66
	3	2,540	70	5.8	77.6	A-frame	11/21/66
	4	2,490	70	5.8	11.3	A-frame	11/21/66
	5	3,000	90	5.8	61.0	A-frame	11/21/66
	6	2,990	90	5.8	49.0	A-frame	11/21/66
TZM-Mo	1	27,000	50	43.4	15.0	2	12/23/66
	3	29,600	60	45.0	60.0*	5	3/29/67
	8	29,600	60	45.0	90.0*	5	3/29/67
	2	38,000	70	45.0	22.8	5	3/29/67
	4	38,000	70	44.0	60.0*	5	3/29/67
I-400 Be	2	4,500	50	44.2	75.0	A-frame	2/21/67
	3	5,600	70	45.4	75.0	A-frame	2/21/67
	1	7,000	90	46.0	87.0	A-frame	2/21/67
Ti-6Al-4V	1	29,629	40	16.4	37.8	5	3/27/67
	3	39,600	50	17.5	73.8*	3	2/7/67
	4	39,600	50	17.6	99.0*	3	2/7/67
Ti-5Al-2.5Sn	1	3,200	40	16.4	13.8	5	3/27/67
	16	39,600	50	17.6	81.0*	3	2/7/67
	17	39,600	50	17.6	60.0*	3	2/7/67

Note: Sources of eccentricity are (1) misalignment of load, and (2) initially curved specimens.

*Specimens were visibly bent initially, presumably as a result of heat treatment.

**Eccentricity calculated according to $C = \frac{\text{max strain - min. strain}}{\text{max strain + min. strain}}$ which is equal to the ratio of the surface strain due to bending to the average strain.

All materials were kept under load for two months (1400 hours). On unloading, the strain readings were again monitored to see if strain relaxation or recovery could be observed. These data are summarized in Table 8. An example of the recovery data for 5456-H34 aluminum is given in Figure 14.

Because of the large elastic deformation encountered in the Ti alloys, strain gage techniques for the measurement of microcreep were not practicable. In order to obtain some indication of the creep behavior of these alloys, an alternative method of testing was devised. Tensile specimens as shown in Figure 1 were lapped flat and parallel at the ends. Measurements could then be taken before and after creep loading to detect creep strain. While this specimen configuration is relatively poor for such measurements, the data proved to be sufficiently self-consistent to be of value. These data are given in Table 9.

Because these specimens are not ideally suited for precision length measurements the length changes are probably not accurate to less than 10 to 20 microinches. Taken in this light, the Ti-6Al-4V and TZM, loaded at 77 percent of their MYS values, did not creep detectably. 5456 aluminum, loaded to about 70 percent of its MYS crept appreciably. Ti-5Al-2.5Sn and 2024 Al, loaded at or above their MYS values, also crept appreciably. Thus, the data agree qualitatively with those of the strain gaged samples where the load conditions are comparable. It is important to note that the observed microcreep strains at stresses near or exceeding the MYS are comparatively severe. This justifies the original assumption that the MYS represents a maximum allowable stress for a precision application, and that appreciable creep should be seen at stress levels somewhat below the MYS.

Stress and Thermal Cycling Experiments

A Federal Electronic Comparator, Model 130-B-16-R3 was employed to measure the change in length of the specimens due to stress or thermal cycling. All measurements were made in a controlled temperature room in which the temperature was maintained at 68 ± 0.25 F.

Figure 15 shows the comparator with specimens mounted on the base platen used to advance the specimen into position for measurement. The system consists of an assembly floating on reed springs incorporating one active and one inactive measuring contact. A change in distance between the two contacts (i.e., the inactive reference contact and the active contact) activates an induction transformer that is calibrated for change in length. Figure 15 also shows the assembly of the reference gage block (a wrung stack of known length), the specimens, and a holder fastened in a fixed position on the base platen. The movement of this assembly into the measuring position is guided by a dial gage in contact with the gage block stack. The sensitivity of measuring the differential length between the gage blocks and the specimens with this instrument is 1μin/in. Ample time for attaining temperature equilibrium of the system and specimen was provided (about 24 hours for the specimen to remain in the constant temperature room and 2 hours after the specimens were positioned on the comparator).

Stress Cycling Procedures and Data

In stress cycling tests, specimens were subjected to loads that varied sinusoidally from tension to compression. The stresses were imposed by a Calidyne Shaker,

TABLE 8. MICROCREEP DATA

Material	Specimen Number	Approximate Level of Stress, 10^3 psi	Approximate Level of Strain, 10^{-6} in./in.	Approximate Level of Percent MYS	Total Creep Strain (at about 1400 hrs), 10^{-6} in./in.	Total Strain Recovery (1400 hrs after unloading), 10^{-6} in./in.
2024-Al	9	18.0	1800	50	5	<1
	10	24.0	2400	70	11	~1
	12	24.0	2400	70	6	~1
5456-Al	17	11.0	1100	50	35	20
	18	11.0	1100	50	42	22
	15	14.8	1500	70	40	30
	16	14.8	1500	70	49	32
	13	18.0	1800	90	67	46
	14	17.8	1800	90	62	52
6061-Al	7	14.8	1500	50	1	1
	3	18.5	1800	70	6	2
	4	18.0	1800	70	4	2
	5	24.6	2400	90	10	4
	6	24.6	2400	90	11	3
AZ 31-Mg	1	1.7	270	50	5	<1
	2	1.7	270	50	2	
	3	2.5	420	70	7	<1
	5	3.0	500	90	10	
	6	3.0	500	90	11	3
TZM-Mo	1	27.0	630	50	1.8	0
	3	29.6	700	60	-2.4	0
	8	29.6	700	60	-0.2	0
	2	33.0	900	70	1.2	0
	4	38.0	900	70	-0.2	0
I-400-Be	2	4.5	100	50	>10	(-6)*
	3	5.6	130	70	5	(-3)
	1	7.0	160	90	7	(-4)

*Recovery strain was in the same direction as creep strain.

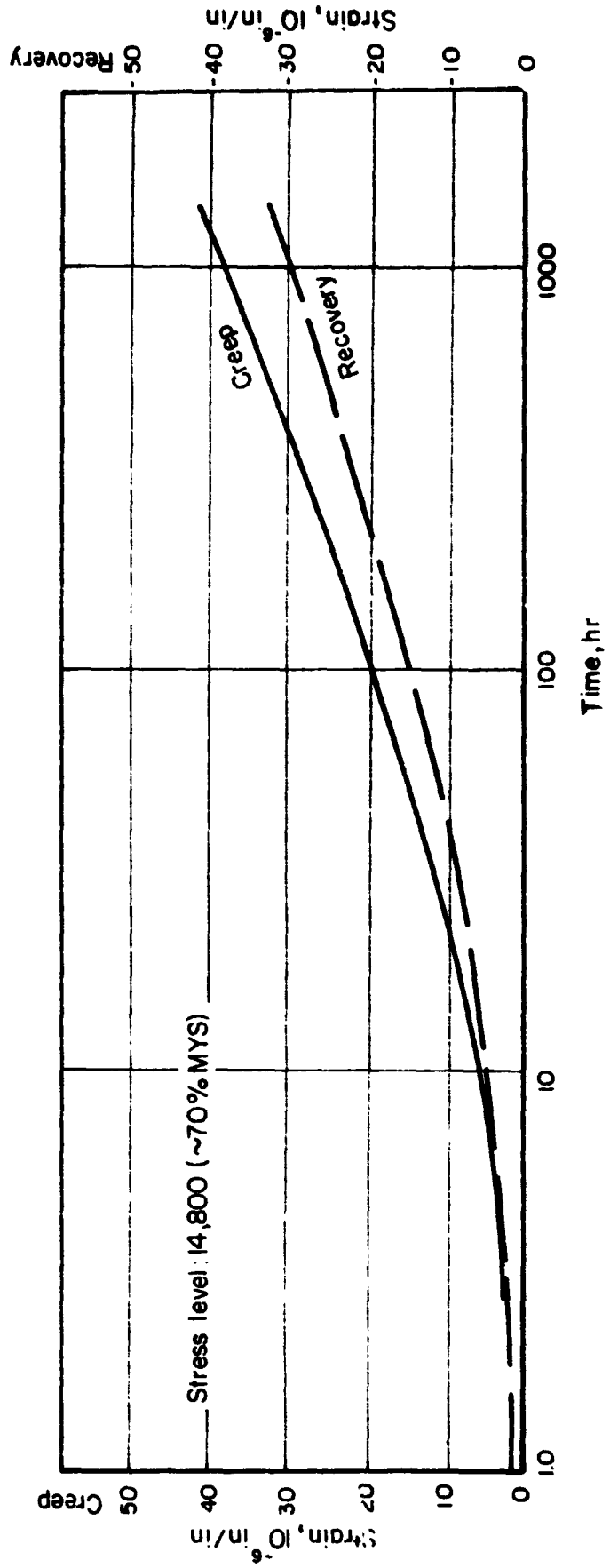

FIGURE 14. MICROSCOPIC CREEP AND RECOVERY CURVES FOR 5456-H34 A1, SPECIMEN No. 16, HEAT TREATED AT 400 F FOR 1 HOUR

TABLE 9. SUMMARY OF "END MEASUREMENT" MICROCREEP DATA

Material	Specimen Number	Stress, psi	Percent MYS	Total Time Under Load, hours	Total Length Change After Unloading
Ti-6Al-4V	11	72,000	77	742	1
Ti-5Al-2.5Sn	4	76,700	98	742	80
	5	80,800	104	742	125
TZM	6	40,400	77	742	-5
	7	40,400	77	742	10
2024Al	8	36,400	117	742	120
	9	36,400	117	742	75
5456Al	14	14,800	72	466	50
	16	14,500	71	466	115

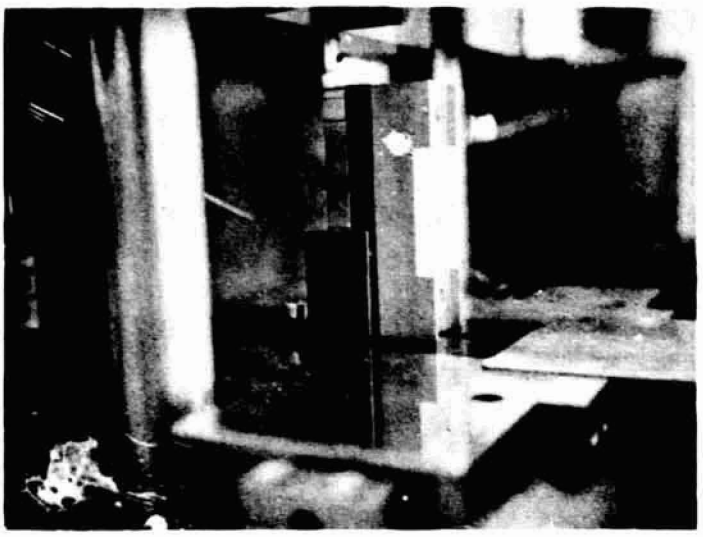

FIGURE 15. THE ASSEMBLY OF SPECIMENS AND WRUNG STACK OF GAGE BLOCKS MOUNTED FOR ADVANCEMENT INTO GAGING POSITION

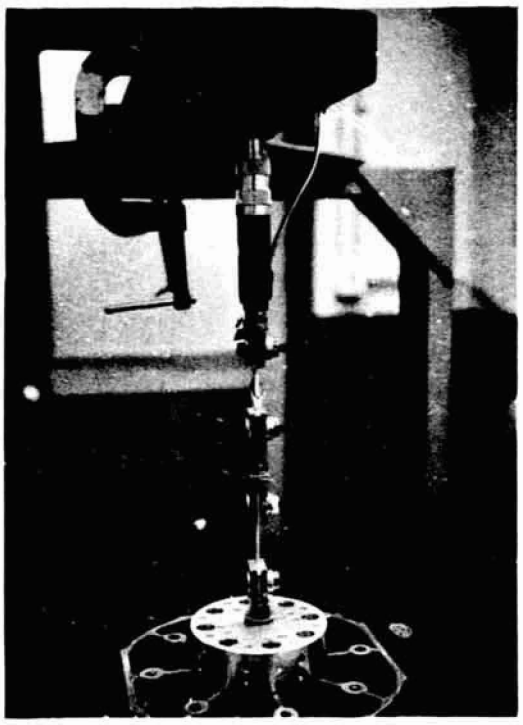

Universal joint

TZM specimen transducer

Test specimen

Calidyne shaker

FIGURE 16. ASSEMBLY OF SPECIMEN IN THE VIBRATION TEST

Model 174, which is an electromechanical device for applying cyclic stresses at controllable frequencies.

The method of gripping the specimen and measuring the load is shown in Figure 16. A test specimen and a load cell were connected in series between the Calidyne Shaker and a universal joint. In gripping the specimen and mounting the assembly, care was exercised to avoid twisting and bending. Tightening of the grips was performed in a vise that facilitated axial alignment of the specimen. After tightening the grips, stiffening plates were attached around the specimens (as shown in Figure 17 and 18) to avoid twisting or bending during assembly of the loading train.

After the loading train was assembled and connected to the Calidyne Shaker, the axial alignment of the system was adjusted to minimize load eccentricity. This was accomplished by adjusting the position of the 1/2-inch threaded rod in a 1-1/4 inch hole of the channel beam, to which the rod is connected with nuts and washers, until the strains measured with gages on either side of the load cell were approximately equal.

The Calidyne Shaker was adjusted to operate at a frequency of approximately 200 cps. This allowed the tests to be conducted in a reasonably short time period (approximately 80 minutes to reach one-million cycles); at the same time, this frequency produced no discernible lateral vibrations in the loading train.

The alternating stress amplitude was adjusted to the desired level (with a dummy specimen in the loading train) by feeding the output of the load cell to an oscilloscope. During an actual stress cycling test, the stress amplitude was monitored continuously on the oscilloscope and was observed to vary within approximately ± 500 psi of the desired value. The resultant data are given in Table 10.

Once again, it must be emphasized that the specimen configuration does not lend itself well to precision length measurement, and the accuracy of the data is open to question. If the specimen end is burred or if the specimen bends or warps, the measurements become tedious and inaccurate. There are no longer flat parallel ends to measure. Still, the length measurements reflect (except in the case of TZM) rather gross changes, much more than was anticipated, and well beyond the estimated accuracy for the specimens of about ± 20 microinches per inch.

Temperature Cycling Procedures and Data

The apparatus used for temperature cycling consisted of (1) a temperature recorder (2) hot water bath (3) cold bath of dry ice in alcohol and (4) a glass specimen container with a thermocouple inserted through the center hole of its stopper. The temperature cycling operation was performed manually and was guided by the temperature trace on the recorder.

The temperature gradient existing in the container with specimens inside was measured with inserted thermometers. One was located near the container wall and the other at the container center. Resulting temperature measurements are given in Table 11.

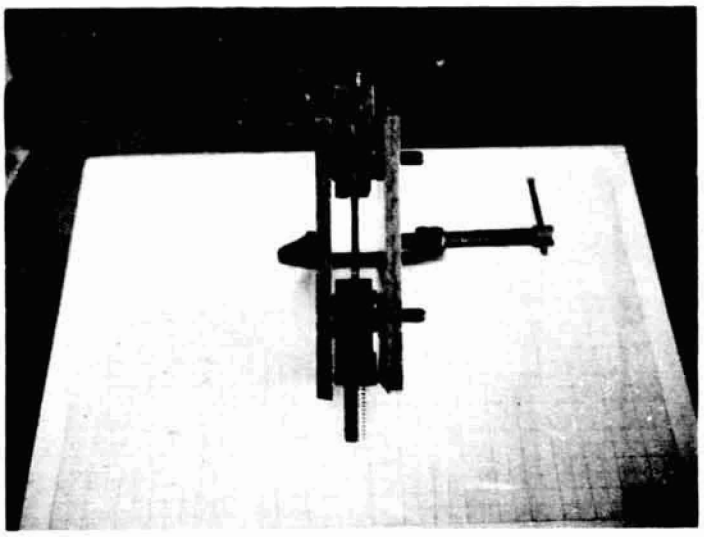

FIGURE 17. SPECIMEN GRIPS AND STIFFENING ASSEMBLY USED TO AVOID TWISTING AND BENDING DURING MOUNTING

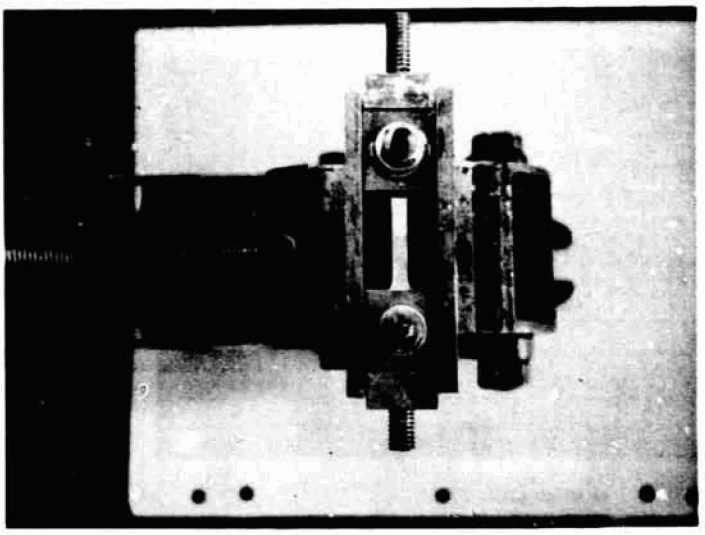

FIGURE 18. GRIP ALIGNMENT FIXTURE

TABLE 10. STRESS-CYCLING DATA

Material	Specimen Number	Alternating Stress Amplitude		Change in Length After ~10^6 Cycles	
		psi	Approximate Percent MYS	ΔL, μin.	Δε, μin./in.
2024 T4Al	A6	4000±500	12	+145	+89
	A7	4000±500		+120	+70
6061-T6Al	T4	4000±500	15	+8	+49
TZM	10	4000±500	7	Damaged	--
	11	4000±500		0	0
Ti-6Al-4V	T1	4000±500	4	+65	+40
	T2	4000±500		+30	+18
Ti-5Al-2.5Sn	E7	4000±500	5	+175	+108
	E1	4000±500		-53	-33
AZ31 Mg	F7	3000±500	83	>+2000	>+1230
				>+2000	>+1230

* The gage length is taken to be 1-5/8 inch.

TABLE 11. TEMPERATURE GRADIENT IN CONTAINER

Time, minutes	Condition	Temperature, degree F	
		Center	Near Wall
0	In air, RT	72.5	72.5
15	Out of water bath after heating to 100 F	100.0	99.5
30	Cooling in air	73.4	73.4
45	In cold bath	-9.6	-9.4
60	Out of cold bath after cooling to -50 F	-49.0	-48.1
75	Warming in air to RT	45.9	44.5

•Specimens were subjected to thermal cycles from -50 to + 100 F, with the temperature varying sinusoidally. The temperature cycle time was normally 90 minutes, with length measurements made before and after cycling. The experimental results are given in Table 12.

Again, the specimen configuration was not ideal, and the accuracy of measurement is estimated to be about ± 20 microinches per inch on all specimens except the I-400 Be. In this case, a specimen of cylindrical cross section was used, and the accuracy of the data is estimated at ± 2 microinches per inch.

Considering the inaccuracies involved, it is probable that 6061 Al and TZM molybdenum are showing little or no effects of thermal cycling. The remainder of the materials appear to be changing dimensions.

DISCUSSION

The discussion can be broken down into two areas, experimental procedures, and material behavior.

Experimental Procedures

The internal consistency of the data indicate that, under the proper test conditions, strain gages can be used to detect creep at the microinch-per-inch range. On the whole, the data are good, showing on the average a scatter of less than ± 1 x 10^{-6}. Humidity appears to have affected the gages, despite the protective coating. It is probable that much of the observed scatter is due to changes in the relative humidity of 5 to 10 percent. As a result, our laboratory has since been modified to provide closer humidity control. Humidity formerly was controlled to 50 percent RH maximum, while currently it is held at 45 percent.

Solder joints and wire leads must be isolated in such a way that there is little or no chance of jarring or moving them. Very slight changes in the resistance of these components inside the strain bridge can introduce considerable and discontinuous changes into the strain readings. When using a single strain indicator to monitor a number of specimens, switching must be done outside the strain bridge; otherwise switching resistance will enter into the bridge readings and degrade the accuracy.

When all the proper precautions have been taken, and the gages are laid down properly, excellent performance can be expected within the limitations of the gages (about 2500 x 10^{-6} in./in.) Overall accuracy appears to be in the range of ± 2 x 10^{-6} in./in. Beyond gage limitations, gage "slippage" occurs. While the actual mechanism of slippage is unknown, it is presumed to involve plastic strain within one of the gage components. This will normally show up experimentally as a negative strain on unloading. The problem of slippage is particularly severe in a material like a titanium alloy, where the elastic modulus is low (~16 x 10^6 psi) and the MYS is high (60,000 to 100,000 psi). In such material, the useful range of the gage is exceeded. This precluded obtaining successful microcreep data by strain-gage methods from the titanium alloys included in the program.

TABLE 12. TEMPERATURE-CYCLING DATA (-50 to +100 F)

Material	Specimen Number	Average MYS, 10^3 psi	Change in Length, $\Delta\epsilon$, μin./in.		
			3 Cycles	9 Cycles	30 Cycles
2024-T4	A12	33	63.5	62.0	65.0
	A22		31.7	31.7	36.0
6061	C32	26	2.8	7.2	21.6
	C33		10.1	23.1	43.3
TZM	1	53	13.0	11.5	13.0
	2		10.1	8.6	27.2
Ti-6Al-4V	E13	93	90.7	69.7	88.5
	E22		58.0	49.4	50.7
Ti-5Al-2.5Sn	D3	78	55.0	58.0	72.5
	D14		20.3	15.9	27.5
AZ31 Mg	F24	3.6	58	80.0	--
	F34		-14.6	-11.6	--
I 400 Be	6	7.9	-2.5(5 cycles)	-6 (10 cycles)	-10 (20 cycles)

Experience dictates that both gages and gage cement should be purchased from the same manufacturer. There are apparently compatability problems which affect the bonding between the gage and the cement. These can lead to total failure of the bond and render the gage useless.

MYS measurements are now routine for most materials. Some negative artifacts are occasionally observed, but these rarely exceed 0.2 - 0.4 microinch per inch. This is largely attributed to the improvement of strain gage mounting procedures, especially in terms of surface cleanliness. We feel strongly that it is also, in part, attributable to the elimination of torsional strains from the load train. Early experiments using dead weight loading demonstrated that consistently better MYS data could be generated if one end of the specimen were free to rotate. It was concluded that, in many or perhaps most cases, a small torque was applied to the specimen through torsional relaxation of various parts of the load train. If the specimen end is not free to rotate, these torsional strains contribute to the load experienced by the specimen in an apparently unreproducible and unpredictable way. Incorporation of the thrust bearing in both the MYS and microcreep load trains appears to have eliminated this problem.

End length measurements have been refined considerably during and since the above described experimental work was completed. In essence it can be stated that the specimens described in Figure 1 are eminently suitable for MYS and microcreep measurements using strain gage techniques, but they are relatively unsuitable for end length measurements. This is largely due to the inability to maintain the end (measuring) surfaces flat and parallel. Most current experiments are being conducted with cylindrical specimens having a length to diameter ratio of about 6. These appear to be far superior to the flat specimens.

Both specimens, however, are limited in the sense that only uniaxial dimension changes are observable. In actual application, biaxial stressing and biaxial dimensional instability are more often encountered. A third type of specimen, a disk with a thickness to diameter ratio of about 0.12, is now being studied. In this case, deviations from the initial flatness of the disk surface are being studied using interferometer techniques and Talysurf measurements.

Material Behavior

MYS Data

There is a significant scatter in the experimental results among what are nominally identical specimens. For example, the MYS values for presumably identical I-400 Be samples differed by 40 percent or more in all three modifications tested. There is little doubt that these variations are far beyond the experimental errors involved in making the measurements. The implication is that there are some uncontrolled factors involved. These may be material inhomogeneity, processing variations, surface variations, or even more subtle differences. Obviously, therefore, one must accept MYS values for what they are, namely, structure-sensitive numbers which are subject to considerable variability.

Examples of the structure sensitivity of the MYS are becoming numerous. Examples can be seen in the response of several of the alloys studied to modest heat treatment.

In 5456-H34 Al, 6061-T6 Al, and TZM molybdenum, moderate heat treatment produces a significant increase in MYS. However, for TZM, even a heat treatment sufficient to cause recrystallization did not significantly lower the MYS, although it did lower the stress necessary to cause strains of 10 or more microinches per inch.

On another program, sponsored by the Air Force[3] it was shown that a prior tensile strain in Ni-Span-C (an iron-nickel alloy) could actually lower the MYS, despite the fact that, at plastic strains greater than 4 or 5 microinches per inch the material had been work hardened.

It is abundantly clear from these and other data that there is no general rule of thumb available to estimate MYS from macro-yield data. It is also abundantly clear that great care must be used in the selection of pertinent data. Older data, especially when reported as an "elastic limit", cannot generally be equated with the MYS, and will frequently differ from the MYS by significant amounts. This results largely because the "elastic limit" was defined as the stress at which the strain became non-elastic, and the experimental results depended entirely on the sensitivity of the strain measuring device. This sensitivity is characteristically between 1 and 50 microinches per inch. Thus, MYS values will normally fall below reported "elastic limit" values.

No effort was made in this program to obtain information relative to the dislocation mechanisms related to the onset of yield. However, some clues to this mechanism have been observed on an Air Force Program[4] currently being conducted at Battelle-Columbus. It appears from transmission electron microscopy that the initial yielding results from the generation of dislocations at grain boundaries or inclusions. These travel until they reach a barrier, such as another grain boundary, at which point they stop. Thus yielding in the micro-region appears to be a function of the stress dependence of the dislocation sources available. Dislocation tangles were not observed. The increase in stress as the strain increases is therefore not a strain hardening, but rather a dislocation source exhaustion. One could predict, on this basis, a rather pronounced micro-Bauschinger effect, caused by the ease with which the dislocations trapped in a given grain could, under the influence of a reverse stress move backwards toward the source and annihilate themselves.

Microcreep Data

If the MYS represents the stress sufficient to cause a residual plastic strain of one microinch per inch in the relatively short-time tensile test, then it is reasonable to assume that the same stress, applied for a longer time, would cause continued strain. This, indeed, appears to be the case. Of the stress levels studied (mostly 50, 70, and 90 percent of the MYS) all were successful in producing microcreep in at least some of the materials. The 5456-H34 alloy was by far the most susceptible to creep, so much so that it was eliminated from further consideration in the program. The reason for the excessive creep in this alloy is not clear. No transmission electron metallography results similar to those discussed above are available for materials which have been subjected to microcreep.

One might be tempted to reason that, in the 5456 alloy, once the dislocations are generated, they are not seriously impeded by grain boundaries or other barriers. Therefore, aided by thermal activation, they continue to move and to produce deformation. However, when the load is removed, the specimen relaxes with time almost back

its original length. This seems likely to be a manifestation of the micro-Bauschinger effect discussed above, and suggests that the barriers are effective in producing a back-stress on the dislocations. Thus creep seems more likely to be associated with the thermally-activated generation of dislocations.

This idea is reasonably consistent with the observed microcreep behavior. When the data are replotted against linear time, as in Figure 19, the curves are invariably concave downward. Within the accuracy of the data, it is not possible to state absolutely whether the creep rate is approaching a steady state, or continuing to decrease. A continuing decrease in creep rate would agree with a mechanism of dislocation source exhaustion.

Within limits of approximately ± 2 microinches per inch, the creep data appear to be consistent and meaningful. Two questions then arise.

(1) Is it possible to predict microcreep data from MYS data?

(2) Is it possible to extrapolate the creep data to obtain strains at greater times or at given times with lesser loads?

It seems reasonable to hope that, if the increasing load required to produce greater strain in the MYS test is the result of the activation of dislocation sources, the slope of the stress versus plastic strain portion of the MYS data might be associated with the amount of microcreep one could expect at some fixed stress. There does indeed appear to be a crude relationship, with the creep rate being generally higher (at some fixed percentage of the MYS) for materials with a low stress-strain ratio (at some fixed strain). Beyond this, no relationship has been observed.

Prediction of microcreep to times 5 to 10 times those actually observed is hazardous for most of the materials studied. The data are too close to the "noise" level. However, the fact that the creep strain versus linear time curves are concave downward, or at worst, linear, makes it possible to predict that the total microcreep after 10,000 hours should be considerably less than 10 times the observed microcreep after 1000 hours.

For the 5456 aluminum, for which the microcreep strain was relatively large, extrapolation of the data is easier. When plotted as log strain versus log time, as in Figure 20, these data approximate straight lines. Assuming the straight line relationship to continue (which seems unlikely, since the lines are tending to converge) one would predict creep strains at 10,000 hours to be from two to four times that observed at 1000 hours.

Extrapolating the microcreep data to lower stresses, with the hope of predicting still lower creep rates is also clouded by the fact that the data are too near the "noise" level. A general relationship appears to exist, with the total creep strain at a given time (ϵ_t) being related to the stress level (σ) by a relationship of the form

$$\sigma = K\epsilon_t^n$$

where K and n appear to be material sensitive constants. Some of the creep data (for 1000 hour creep) are plotted in Figure 21, along with some 500 hour data from the Air Force Program[5] and from Hordon and Weihrauch[6] for A 356 aluminum. If the

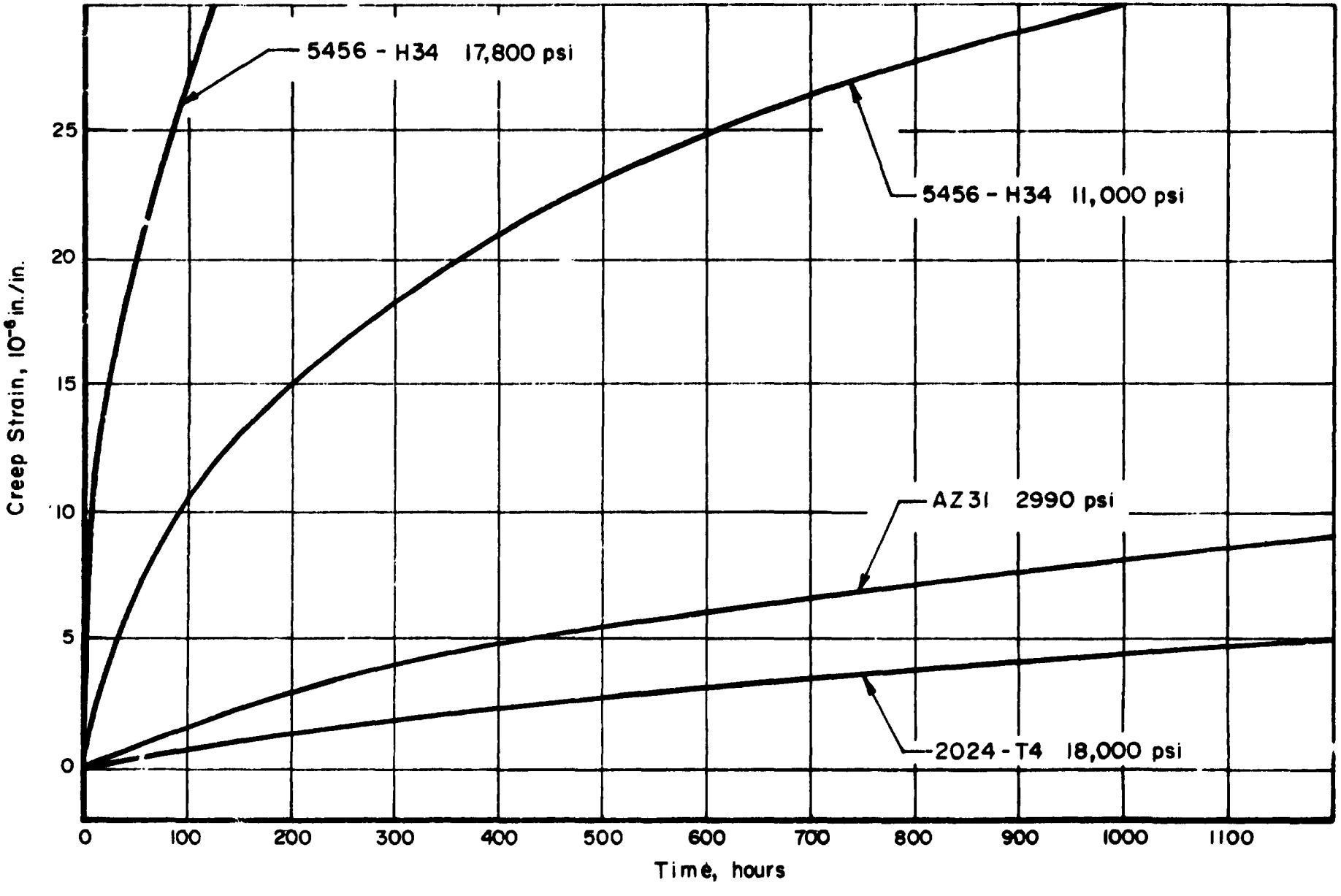

FIGURE 19. CREEP CURVES FOR SEVERAL ALLOYS, REPLOTTED VERSUS LINEAR TIME

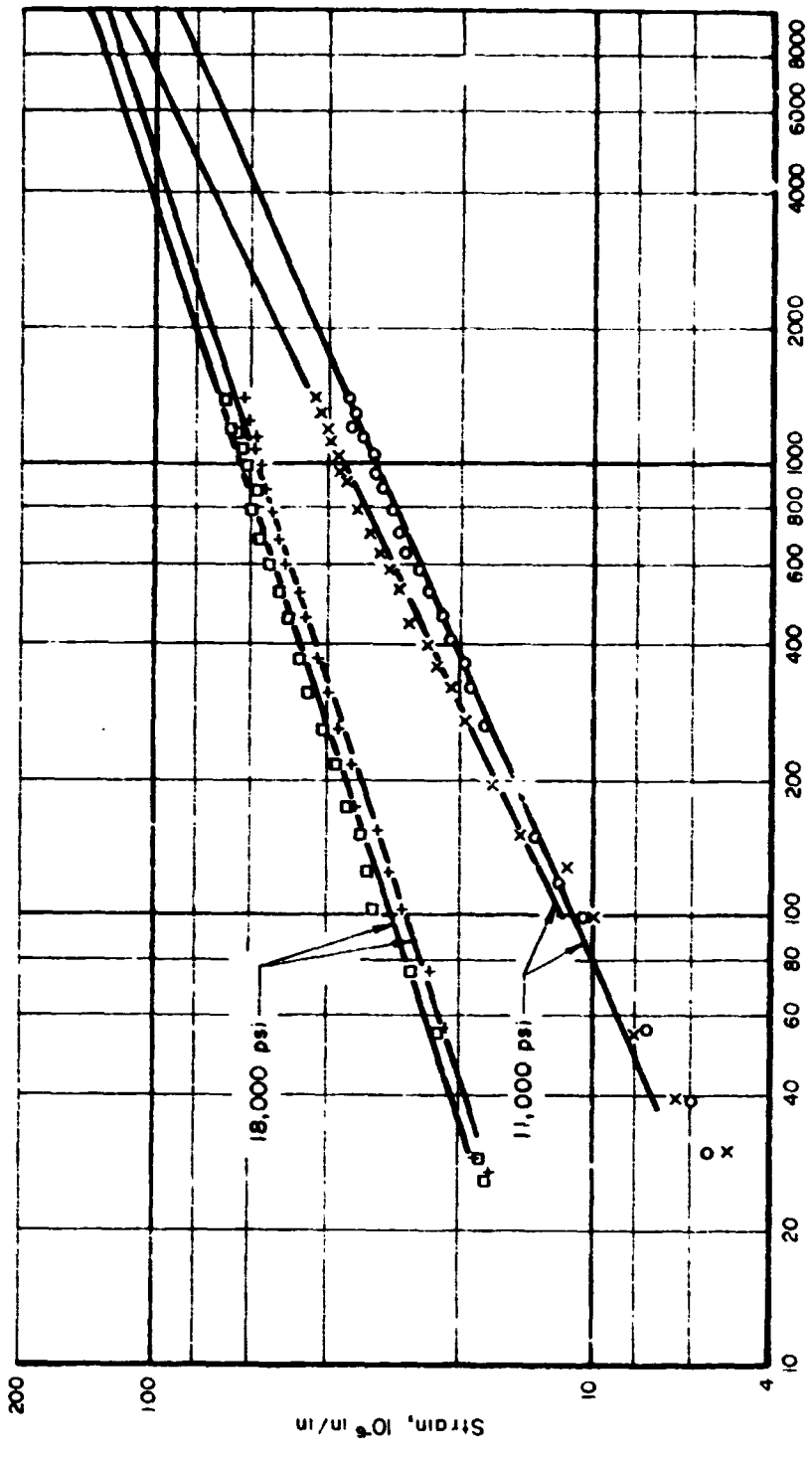

FIGURE 20. MICROCREEP OF 5456-H34A1, HEAT TREATED AT 400 F FOR 1 HOUR

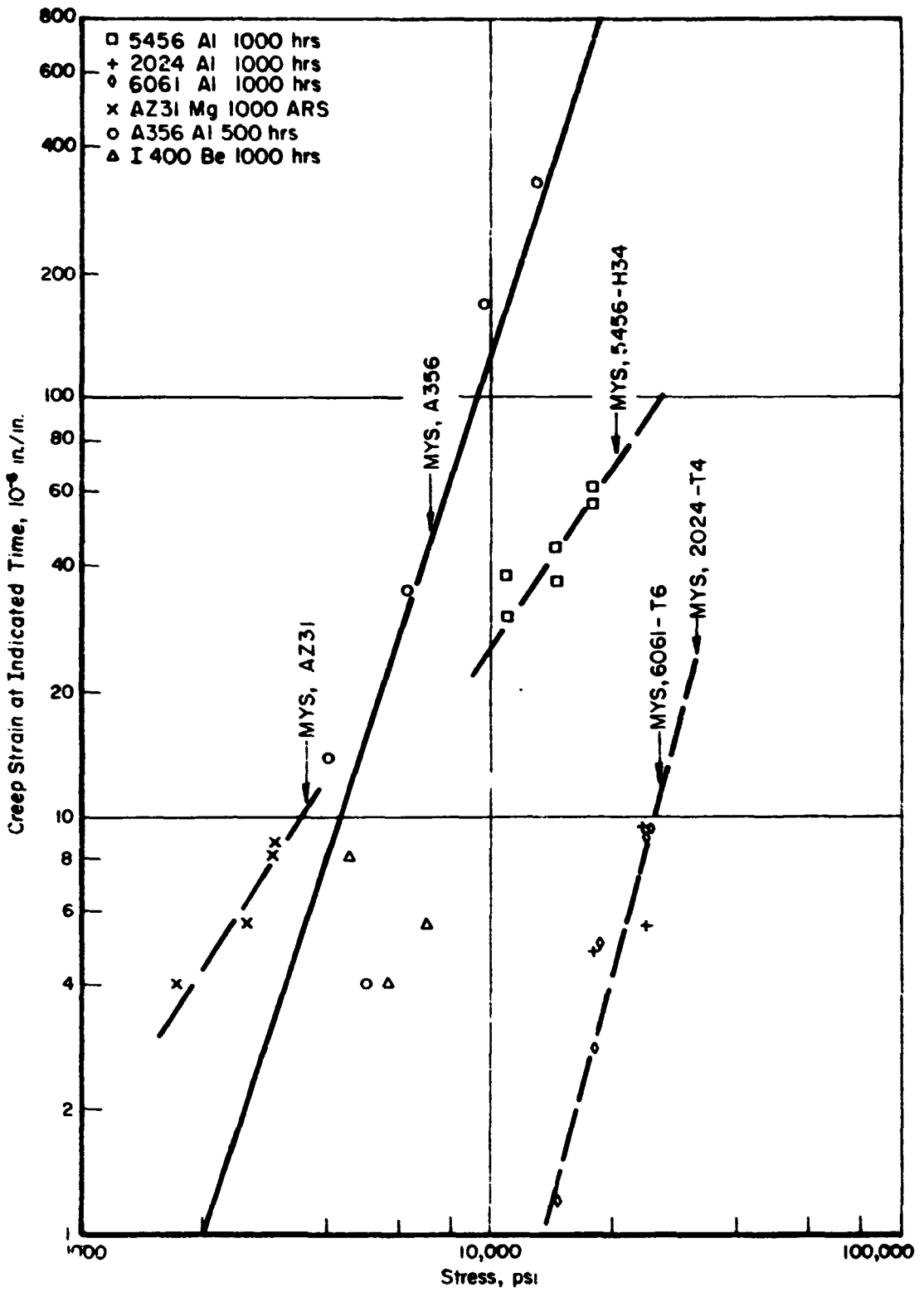

FIGURE 21. TOTAL MICROCREEP STRAIN AT INDICATED TIMES

empirical relationship described above does exist, it clearly indicates the need for microcreep experimentation at stress levels at and somewhat above the MYS.

In any event, it is certain that microcreep can be observed at stress levels well below the MYS for most materials. The sole exception to this observation was TZM molybdenum. It is probable that this alloy, the only body-centered cubic material among those studied, owes its creep resistance to the fact that the binding force between dislocations and interstitial impurities is much higher than in the other crystal structures studied.

Thermal and Stress Cycling Data

The difficulties of end length measurements associated with the specimens used clouds the issue somewhat. However, it seems apparent that both stress cycling and thermal cycling can cause significant dimensional instability. It is not difficult to see why this should happen for stress cycling.

If a residual stress exists in a specimen, then a relaxation of this stress can cause a change in dimensions. The most probable mechanism of stress relaxation is the generation and movement of dislocations. The MYS and the microcreep data suggest that this kind of microdeformation occurs by the stress-induced and thermally activated generation and motion of dislocations. A vibrational stress superimposed on already existing residual stresses could then serve as an "activating" mechanism, simply supplying the small additional stress necessary to start a source operating. If this is the case, then a material not containing residual stresses should be relatively stable with respect to any imposed vibrational stress until those stresses by themselves become high enough to activate dislocation sources.

Thermal cycling can have two effects. If the thermal cycle is rapid enough, then the thermal gradient itself will be enough to generate stress. Even on slow thermal cycling, however, significant stress levels can be generated in the sample if the crystal structure of the alloy is anisotropic with respect to its thermal expansion characteristics or if the alloy is composed of a mixture of phases, each with a different thermal expansion coefficient.

Some current stabilization procedures call for quenching the sample into boiling water, air cooling, then quenching into dry ice and acetone. These are severe conditions, and can be shown experimentally to cause dimensional changes. This procedure will actually deform the specimen plastically. For some applications, however, this seems to be acceptable, especially if the specimen is expected to see severe and rapid thermal cycling in its intended application. For most precision applications, however, quenching as a means of thermal cycling probably does more harm than good.

Differences in thermal expansion coefficients, either with respect to crystal direction or phase relationships, are known to cause severe internal stresses. The thermal cycling of a uranium specimen can cause the length to double or triple. In most materials, however, the stresses are not so severe as to build up stresses which will exceed the MYS. However, in the presence of other residual stresses, the superimposed, thermally-generated stresses can be expected to generate dislocation sources which are already close to operative, with consequent dimensional changes.

In the absence of thermal gradients or differences in the thermal expansion coefficients, thermal cycling is probably effective only in that it exposes a sample to a higher temperature, thereby allowing thermal activation to play a greater role in the generation and movement of dislocations. In this case, of course, the thermal treatment would have no meaning unless a residual stress already existed in the sample.

CONCLUSIONS

Based on the results of this program, the relationship of these results to other programs being conducted at Battelle-Columbus, and the relationship of these combined data with those available in the literature and in current practice, some general conclusions can be drawn. These are

(1) A large fraction, perhaps a majority, of the problems associated with dimensional instability arise from the relaxation of residual or applied stresses rather than from metallurgical changes. The residual stresses most often are introduced into the material during processing.

(2) Because of the importance of stress-induced dimensional changes, MYS and microcreep data are vital to the design of precision equipment.

(3) Current techniques for the measurement of those parameters range from essentially useless to excellent, depending on the nature of the material being examined, and on the nature of the experimental variables under scrutiny. No single method of measurement has the versatility and stability for universal use.

(4) Both MYS and microcreep behavior are very structure sensitive. This combined with limitations of measurement techniques, probably is responsible for the scatter in values reported within and among various laboratories. Designers who intend to use existing data must recognize the inherent scatter and take into account the possible role of structure and measurement technique before using the data.

(5) As a general rule, applied stresses no larger than half the MYS should be permitted if creep and stress relaxation are to be kept at minimum levels. There are exceptions, of course, but the rule appears to be a useful one. Residual stresses exceeding half the MYS are equally unwelcome.

(6) If dimensional instability is largely the result of stress relaxation, then environmental factors such as thermal cycling and vibration should be expected to affect this instability. It should be possible to eliminate much or all of the instability due to stress and thermal cycling by minimizing or removing residual stresses.

FUTURE RESEARCH NEEDS

Since it is becoming apparent that MYS and microcreep are structure sensitive properties, it will be important to define this relationship carefully. Theoretical and experimental work relating MYS and microcreep data to dislocation mechanics and to controllable structural parameters will be helpful in understanding dimensional instability, improving materials for precision uses, and devising stabilization procedures.

Because residual stresses appear to be the driving force behind most dimensional instability, there is a need for a thorough study of the sources of residual stress, its magnitude, its distribution, and its response to its environment. This latter point is perhaps the most pressing from a technological point of view.

Many of our experiments suggest that it is not difficult to produce a dimensionally stable material, so long as its environment does not change. In actual applications, stress and temperature variations are part of the environment. Experiments are urgently needed to define quantitatively as well as qualitatively the role of environment, specifically (for these are in most cases the most important) the effects of stress and thermal cycling. This should be done under conditions in which the magnitude and distribution of the residual stress are known quantitatively.

REFERENCES

(1) Holden, F. C., "A Review of Dimensional Instability in Metals", DMIC Memorandum 189, March 19, 1964.

(2) Maringer, R. E., "Review of Dimensional Instability in Metals", DMIC Memorandum 213, June 23, 1966.

(3) Imgram, A. G., Sovik, J. H., Hoskins, M. E., and Maringer, R. E., "Study of Microplastic Properties and Dimensional Stability of Materials", 4th Quarterly Report from Battelle Memorial Institute, Columbus Laboratories to Air Force Systems Command, WPAFB, September 15, 1967.

(4) Imgram, A. G., Maringer, R. E., and Holden, F. C., Technical Report AFML-TR-67-232, May, 1967.

(5) Imgram, A. G., Hoskins, M. E., Sovik, J. H., and Maringer, R. E., "Study of Microplastic Properties and Dimensional Stability of Materials", 5th Quarterly Report from Battelle Memorial Institute, Columbus Laboratories to Air Force Systems Command, WPAFB, December 15, 1967.

(6) Hordon, M. J., and Weihrauch, P. F., "The Dimensional Stability of Selected Alloy Systems", Alloyd General Corporation, Medford, Massachusetts, December 1, 1963 to April 1, 1964 (Data are also contained in Reference 2).

REM/MMC/FCH:js

APPENDIX A

MICROYIELD STRENGTH CURVES

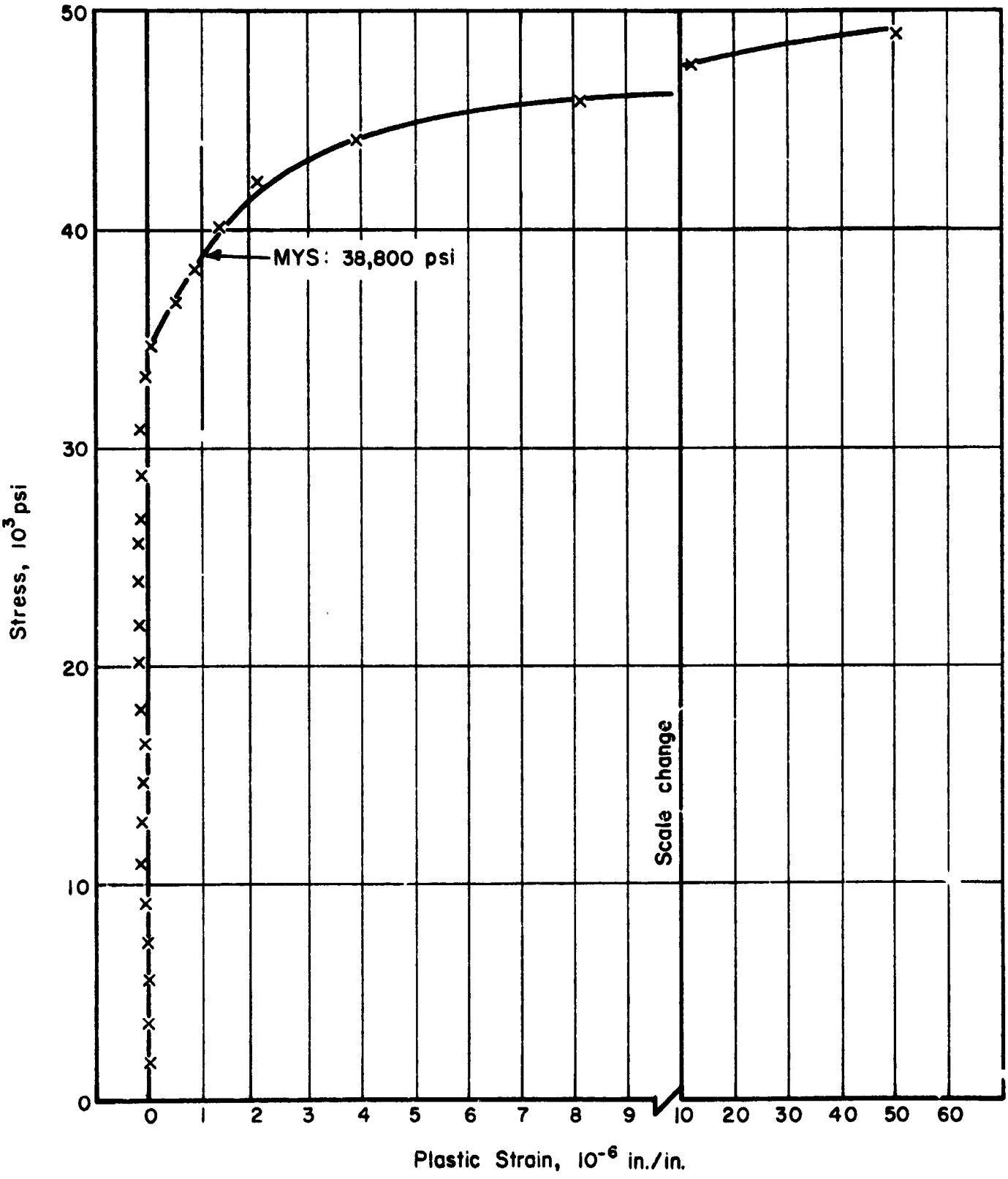

FIGURE A-1. MYS TEST ON 2024-T4 Al, SPECIMEN No. 8, AS RECEIVED

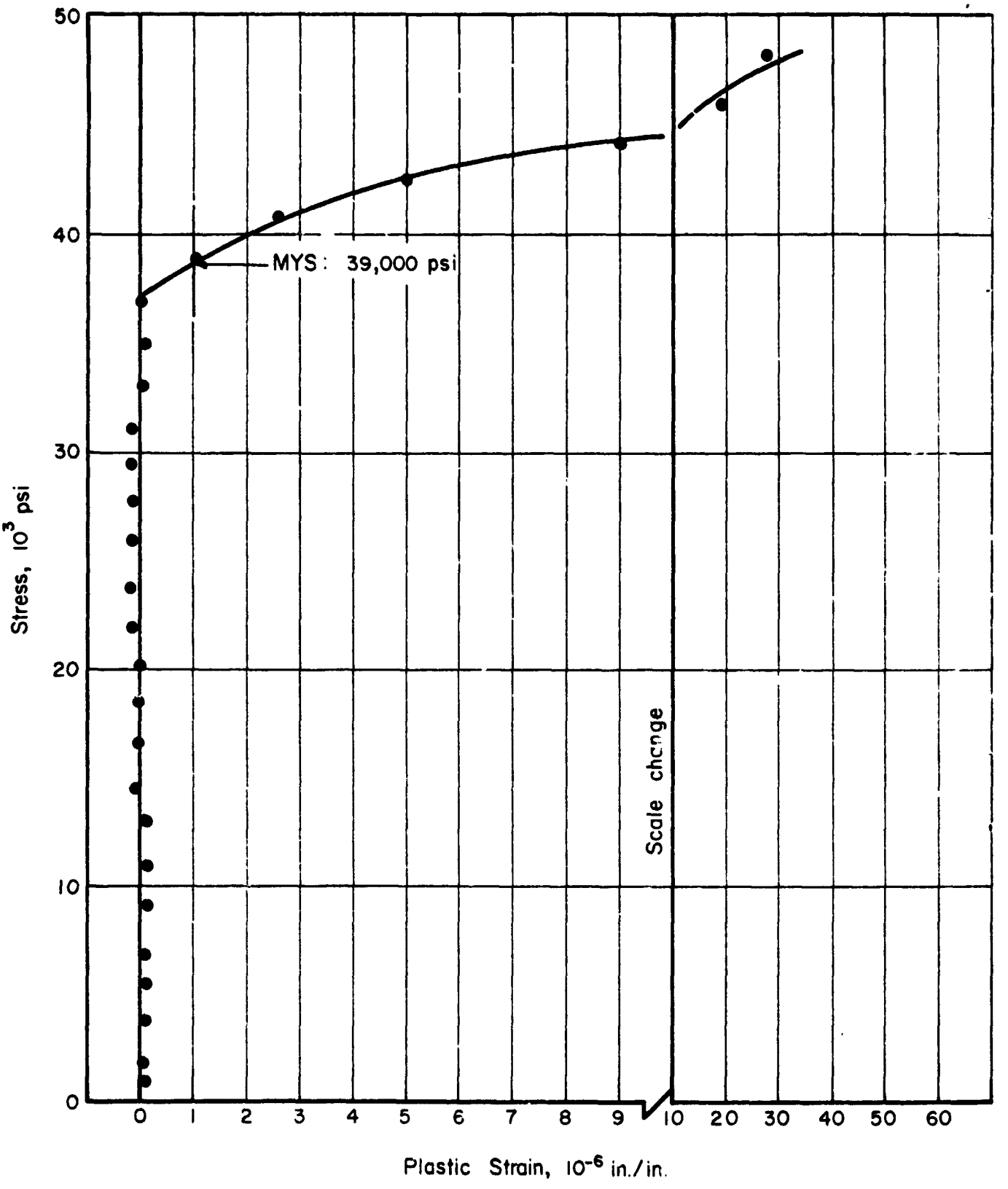

FIGURE A-2. MYS TEST ON 2024-T4 Al, SPECIMEN No. 7, AS RECEIVED

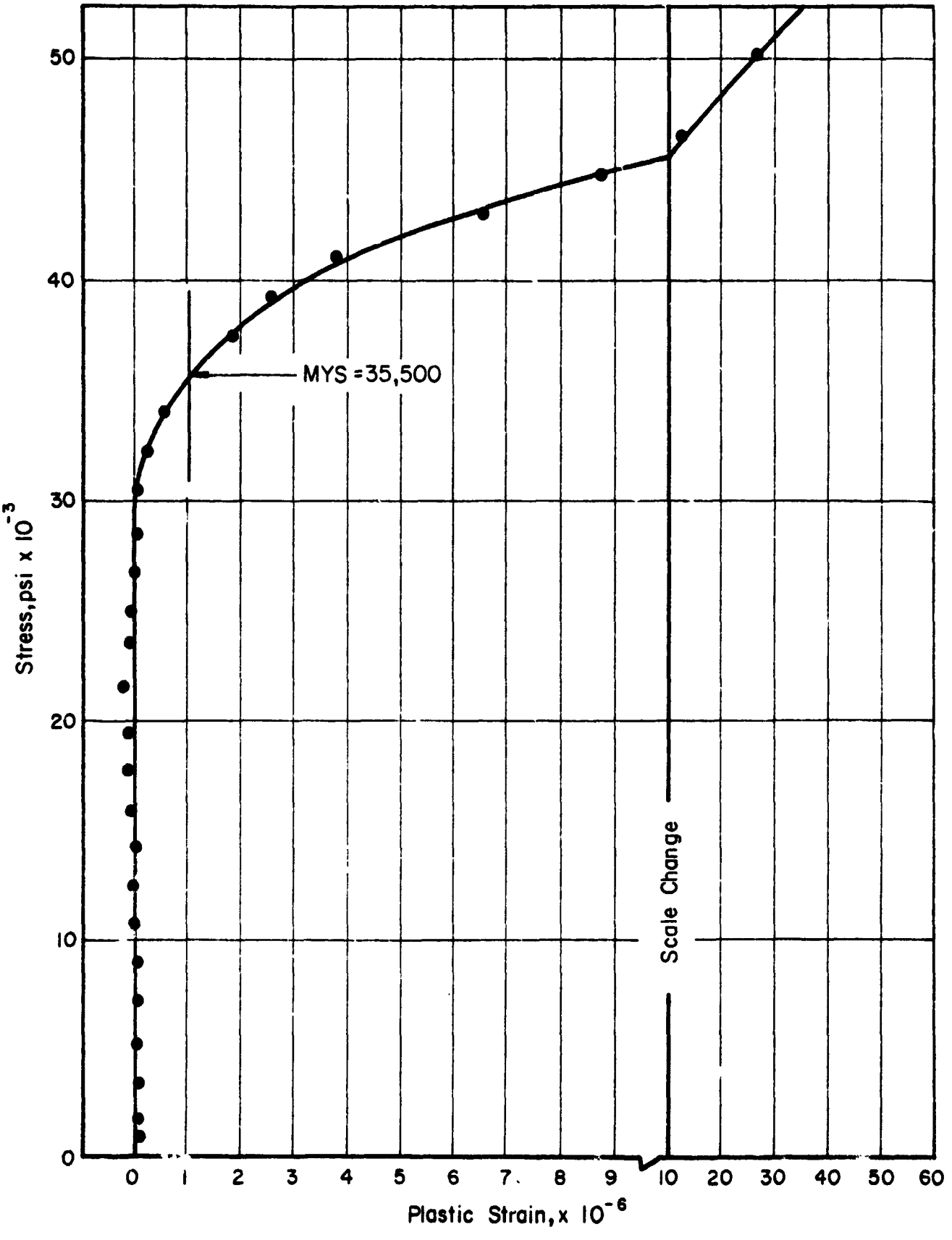

FIGURE A-3. MYS TEST ON 2024-T4 Al, SPECIMEN No. 2,
HEAT TREATED AT 400 F FOR 1 HOUR

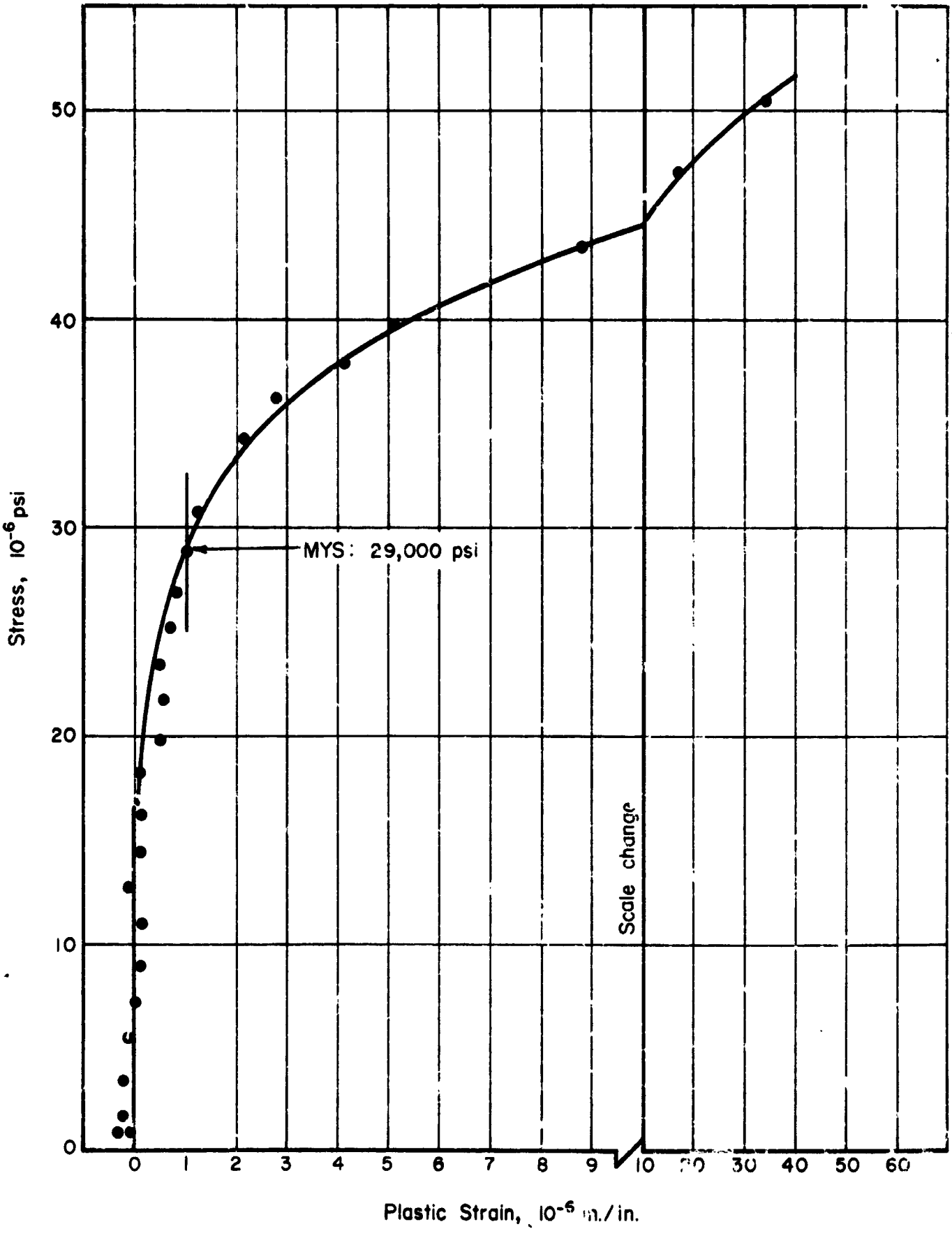

FIGURE A-4. MYS TEST ON 2024-T4 Al, SPECIMEN No. 3, HEAT TREATED AT 400 F FOR 1 HOUR

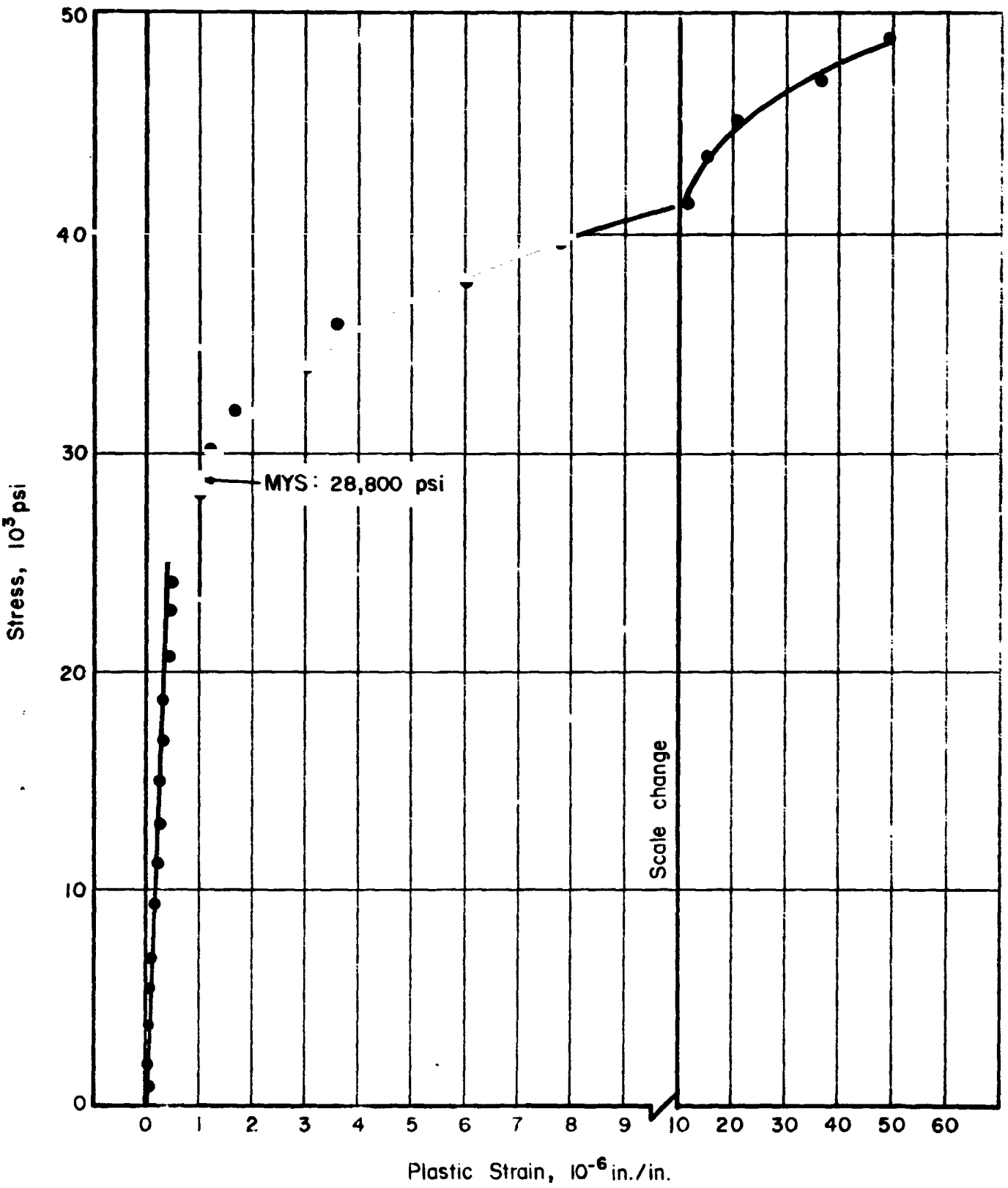

FIGURE A-5. MYS TEST ON 2024-T4 Al, SPECIMEN No. 19, HEAT TREATED AT 450 F FOR 1 HOUR

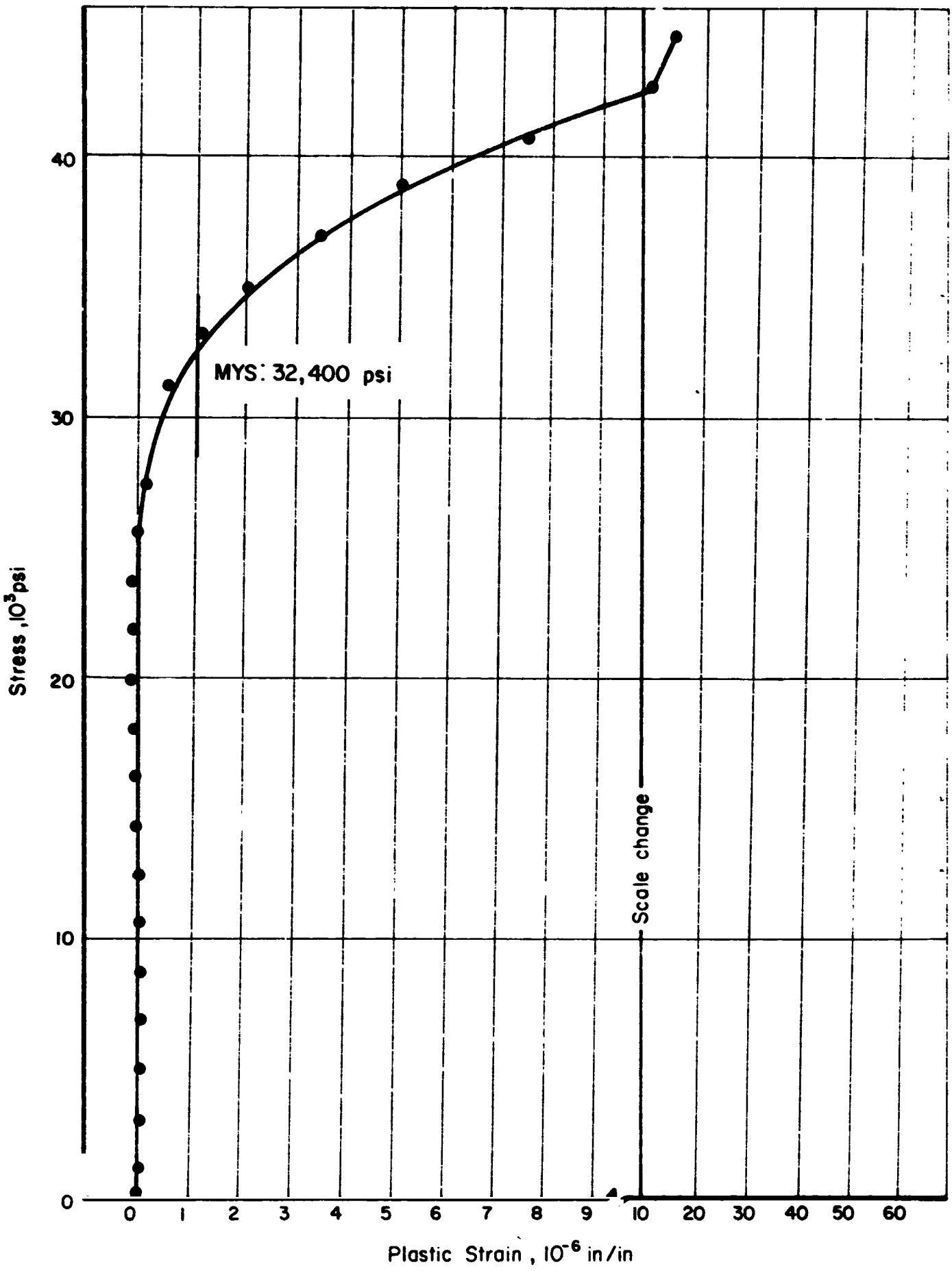

FIGURE A-6. MYS TEST ON 2024-T4 Al. SPECIMEN No. 18, HEAT TREATED AT 450 F FOR 1 HOUR

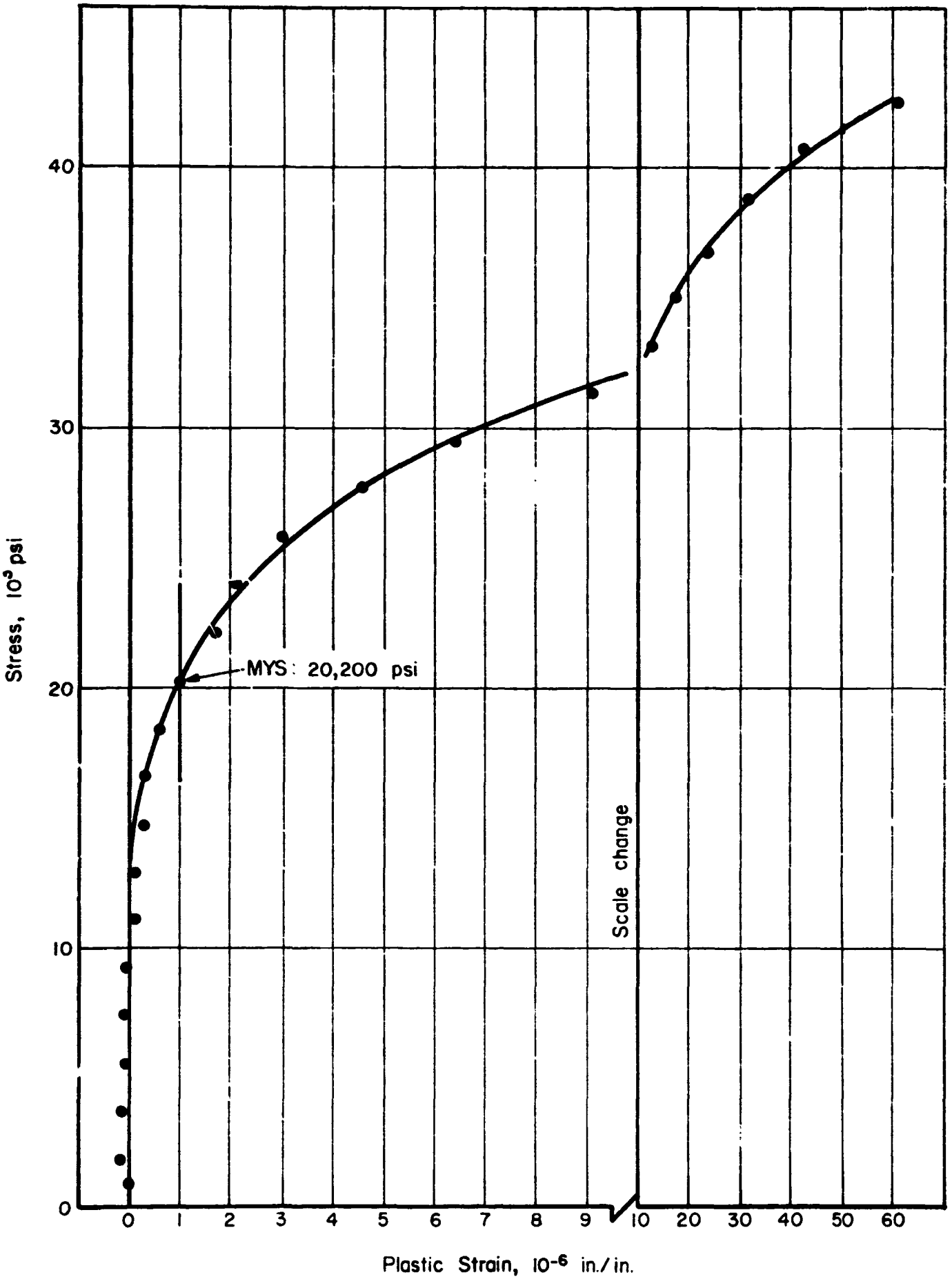

FIGURE A-7. MYS TEST ON 2024-T4 Al, SPECIMEN No. 21, HEAT TREATED AT 500 F FOR 1 HOUR

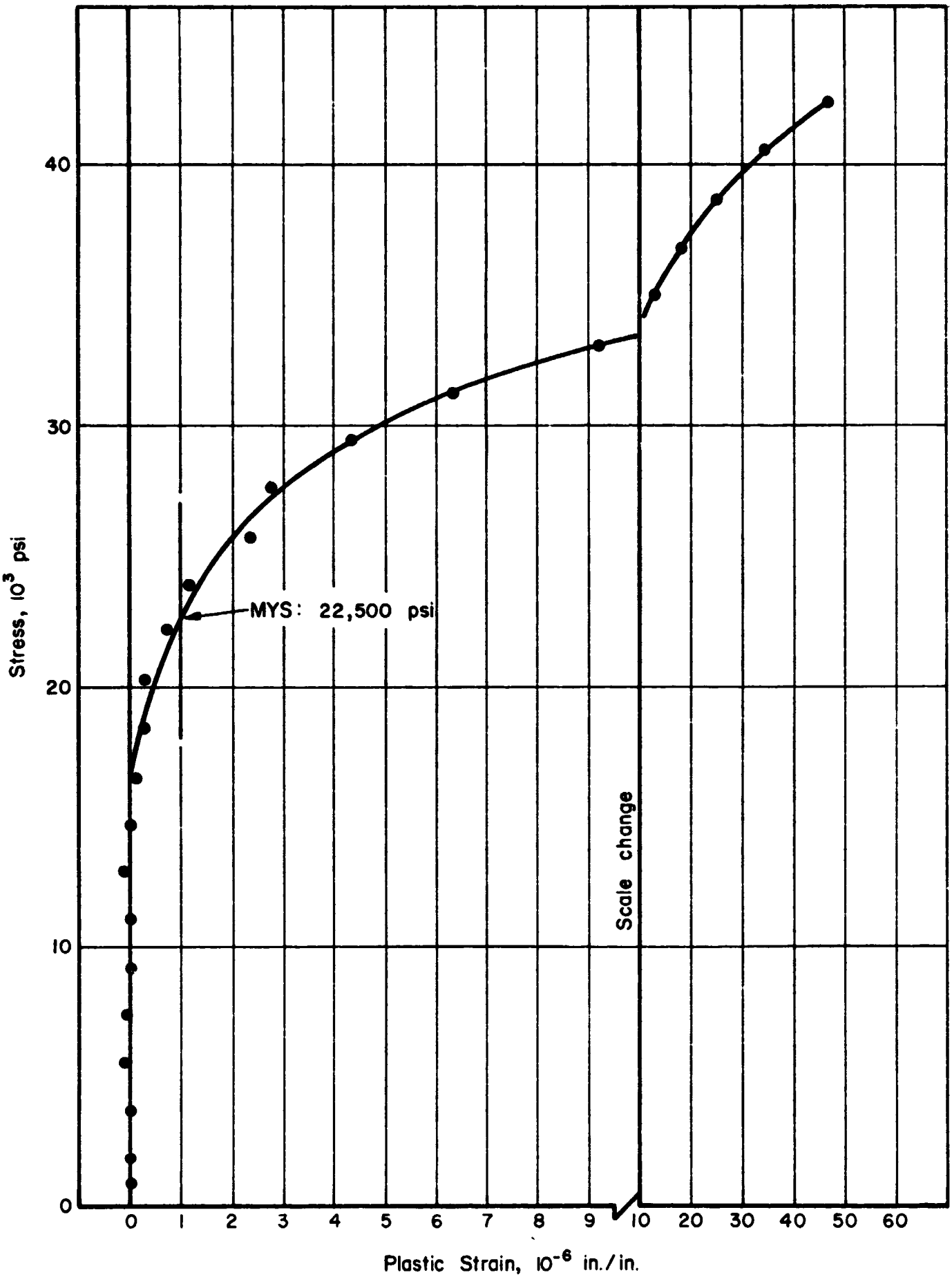

FIGURE A-8. MYS TEST ON 2024-T4 Al, SPECIMEN No. 20, HEAT TREATED AT 500 F FOR 1 HOUR

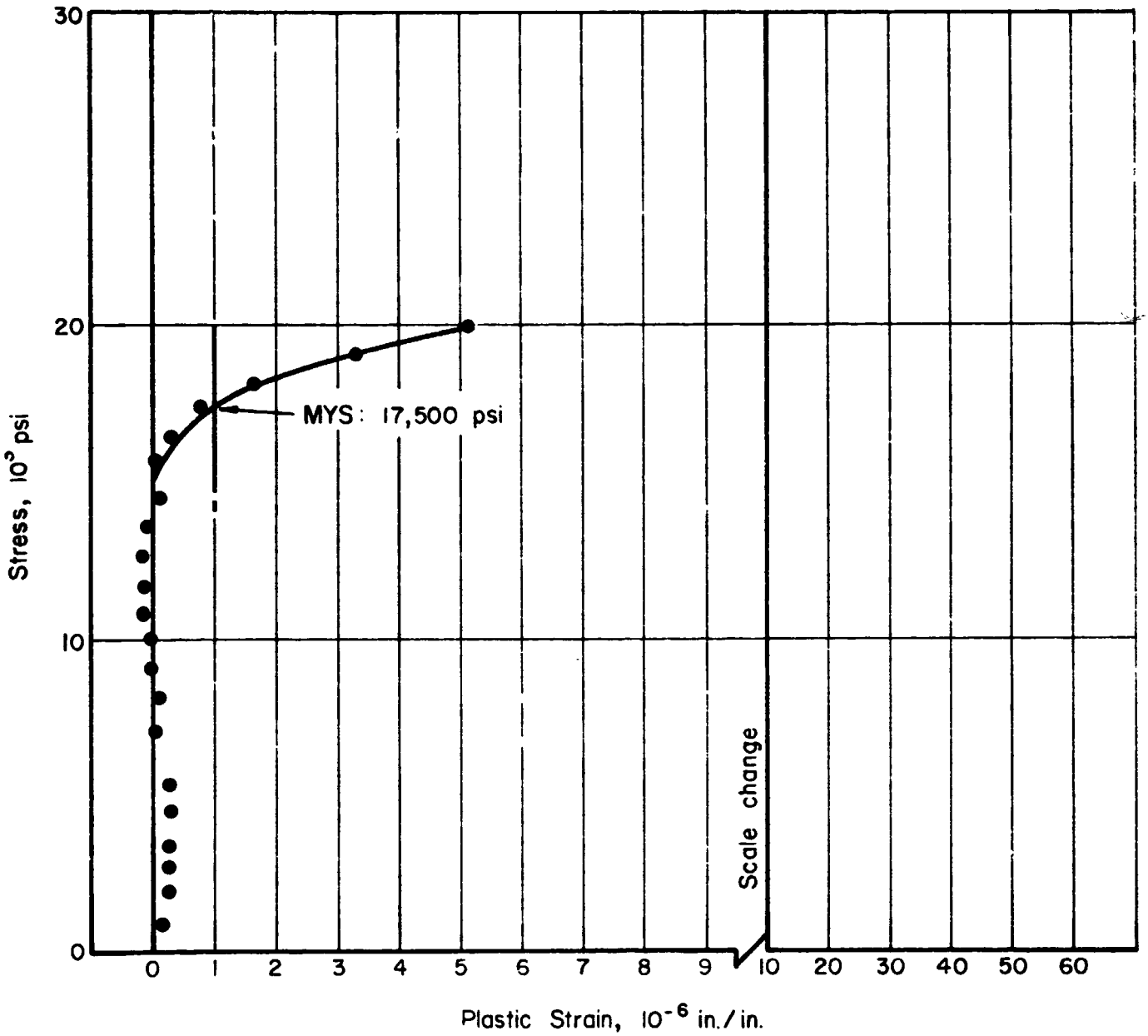

FIGURE A-9. MYS TEST ON 5456-H34 Al, SPECIMEN No. 4, AS RECEIVED

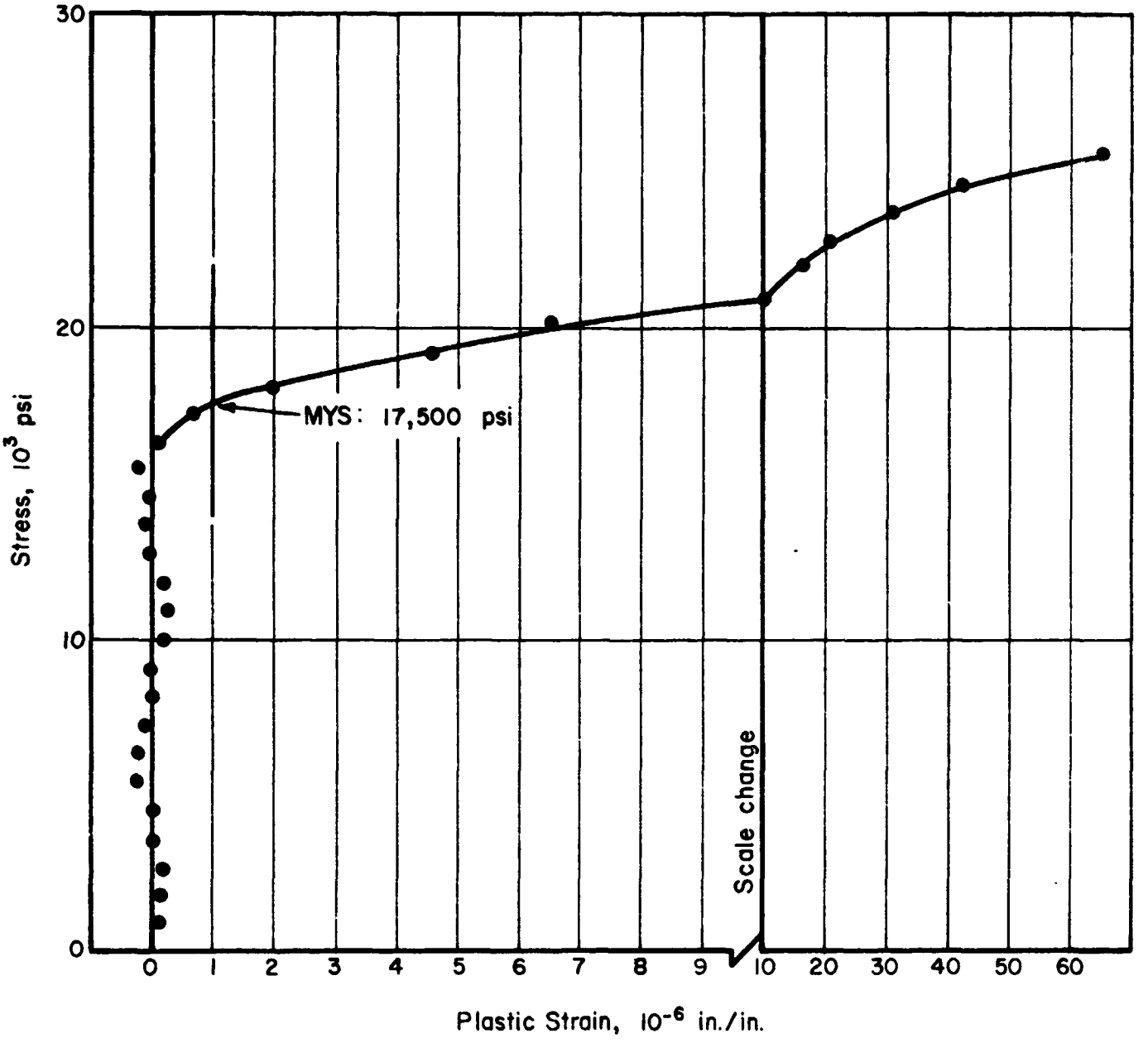

FIGURE A-10. MYS TEST ON 5456-H34 Al, SPECIMEN No. 5, AS RECEIVED

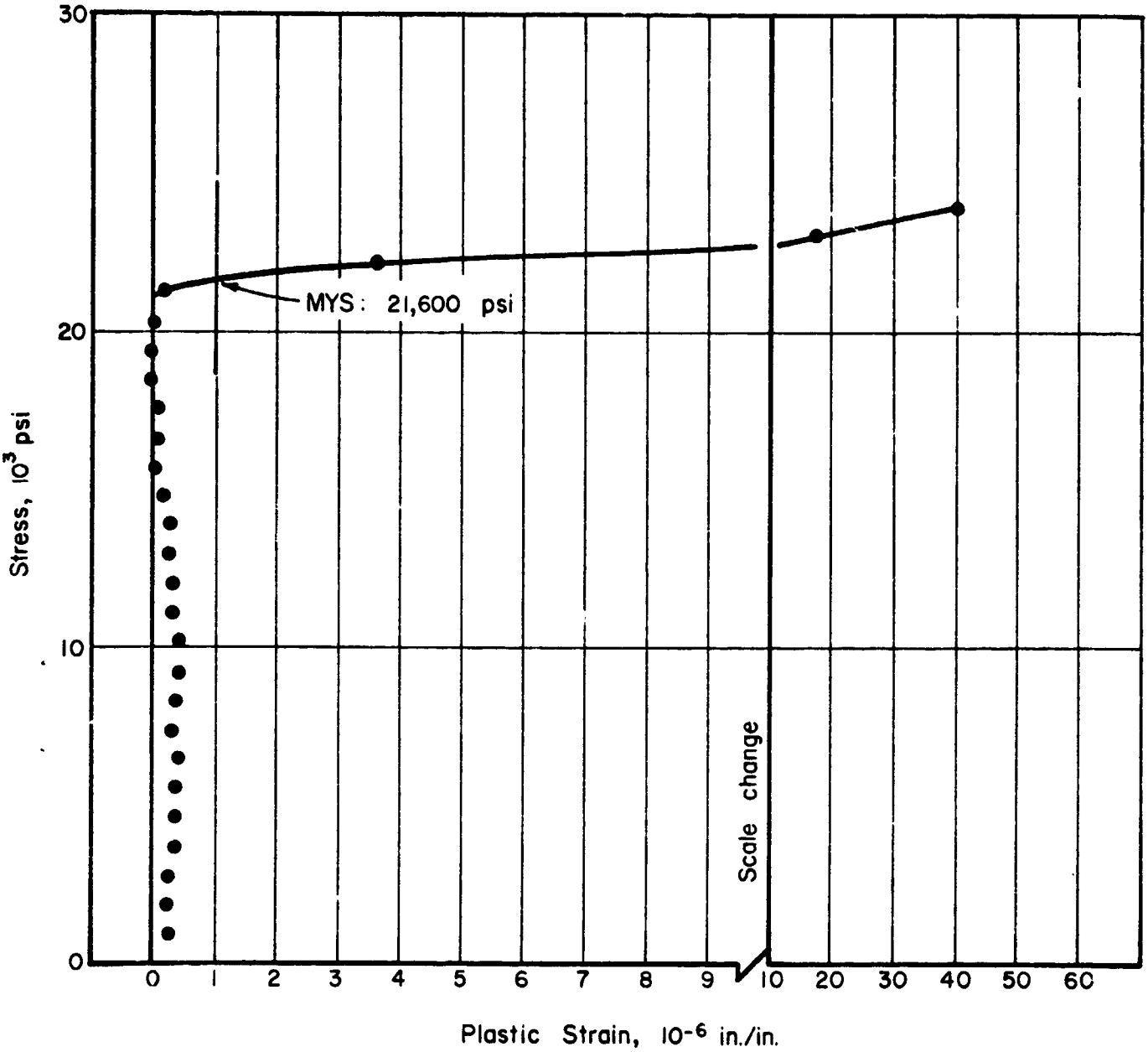

FIGURE A-11. MYS TEST ON 5456-H34 Al, SPECIMEN No. 10, HEAT TREATED AT 400 F FOR 1 HOUR

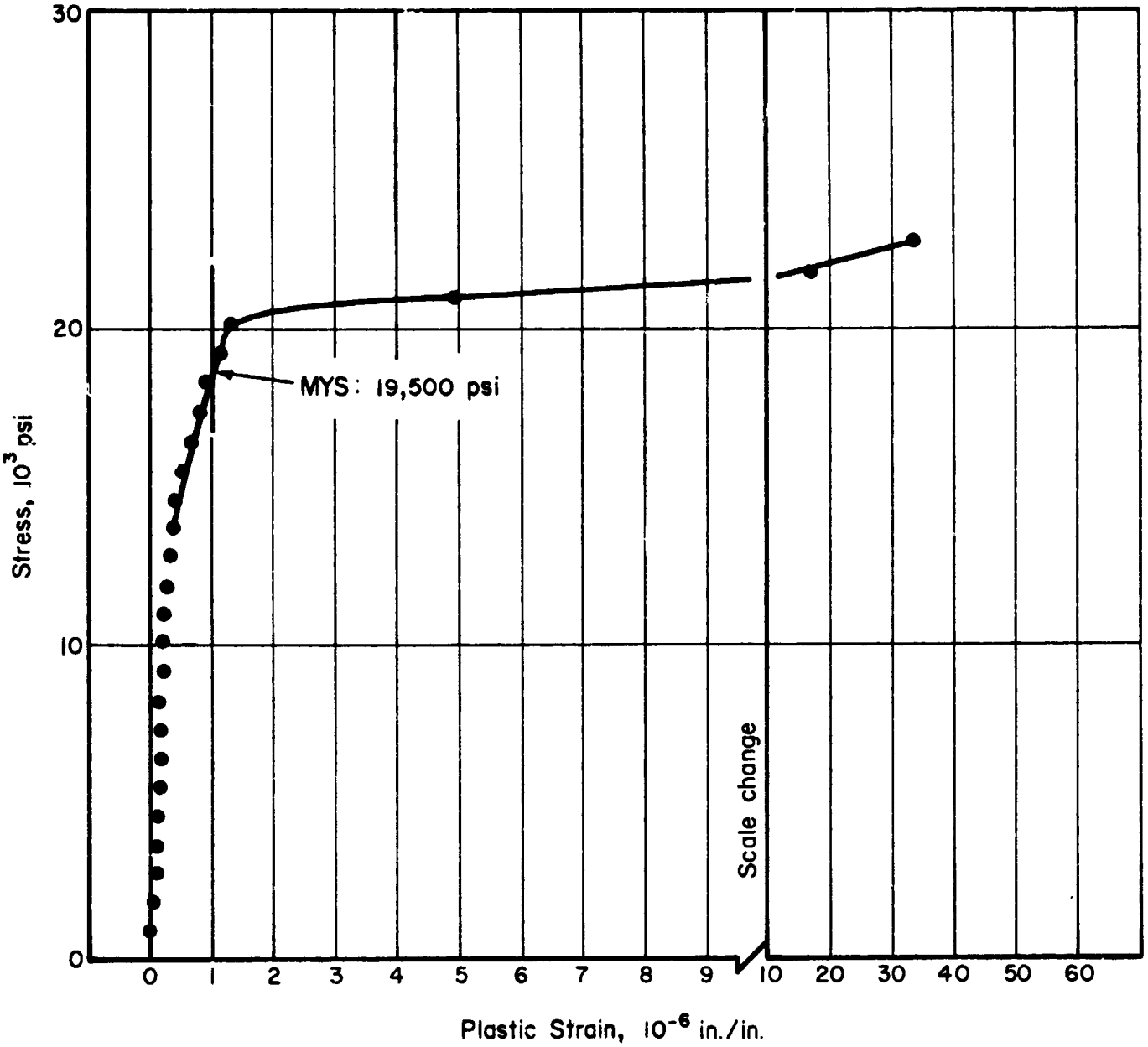

FIGURE A-12. MYS TEST ON 5456-H34 Al, SPECIMEN No. 11, HEAT TREATED AT 400 F FOR 1 HOUR

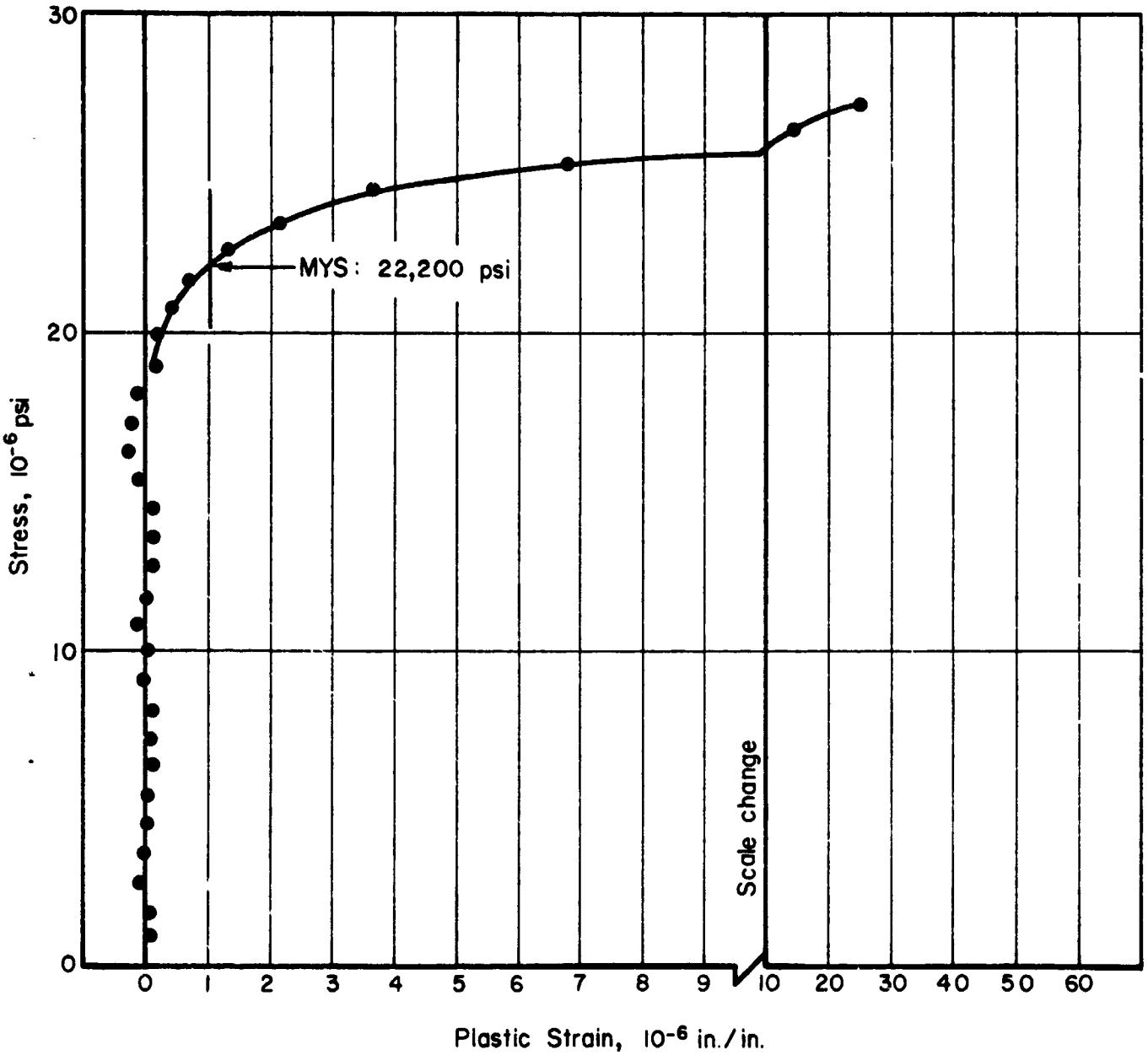

FIGURE A-13. MYS TEST ON 5456-H34 A1, SPECIMEN No. 17, HEAT TREATED AT 450 F FOR 1 HOUR

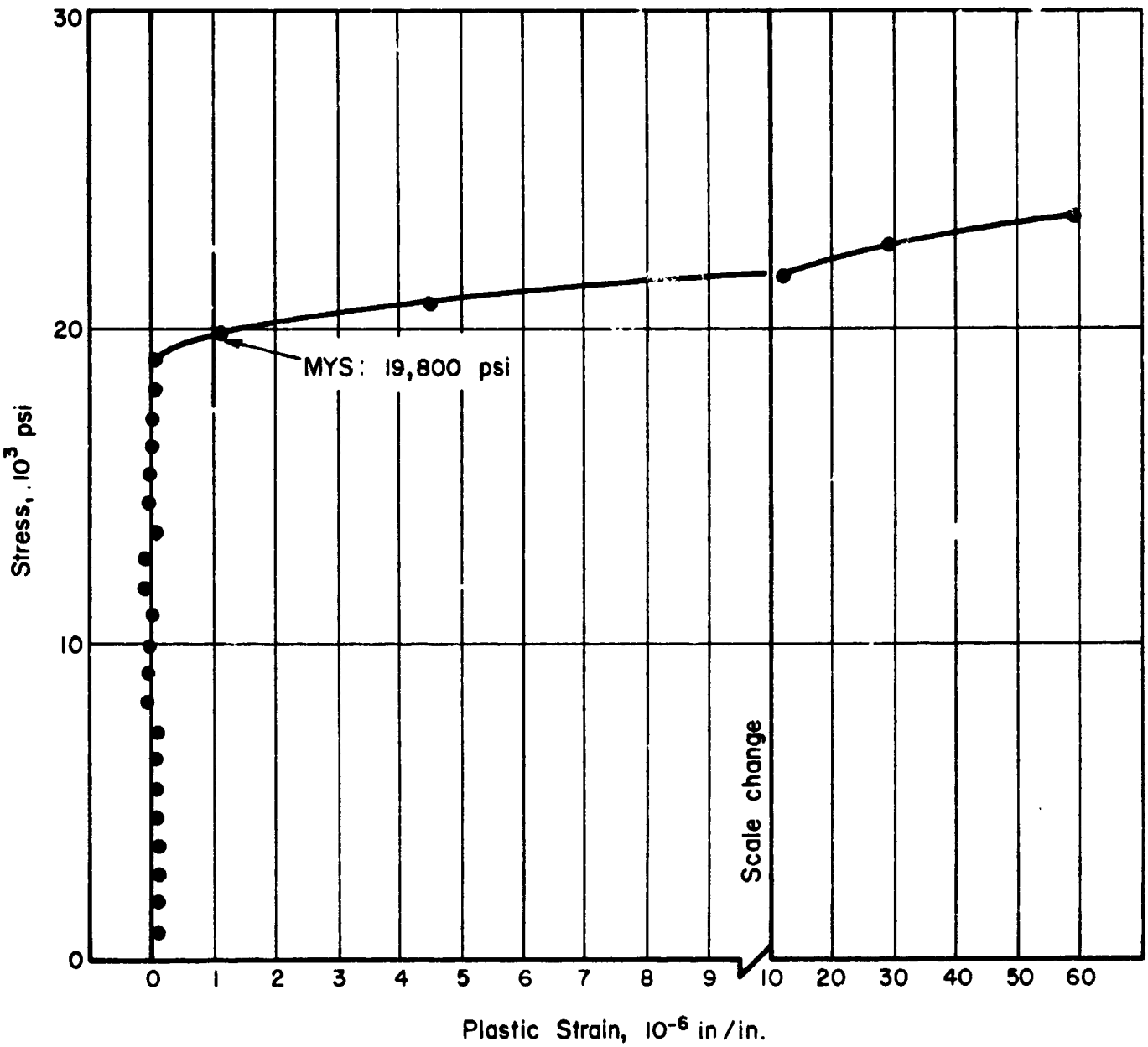

FIGURE A-14. MYS TEST ON 5456-H34 Al, SPECIMEN No. 16, HEAT TREATED AT 450 F FOR 1 HOUR

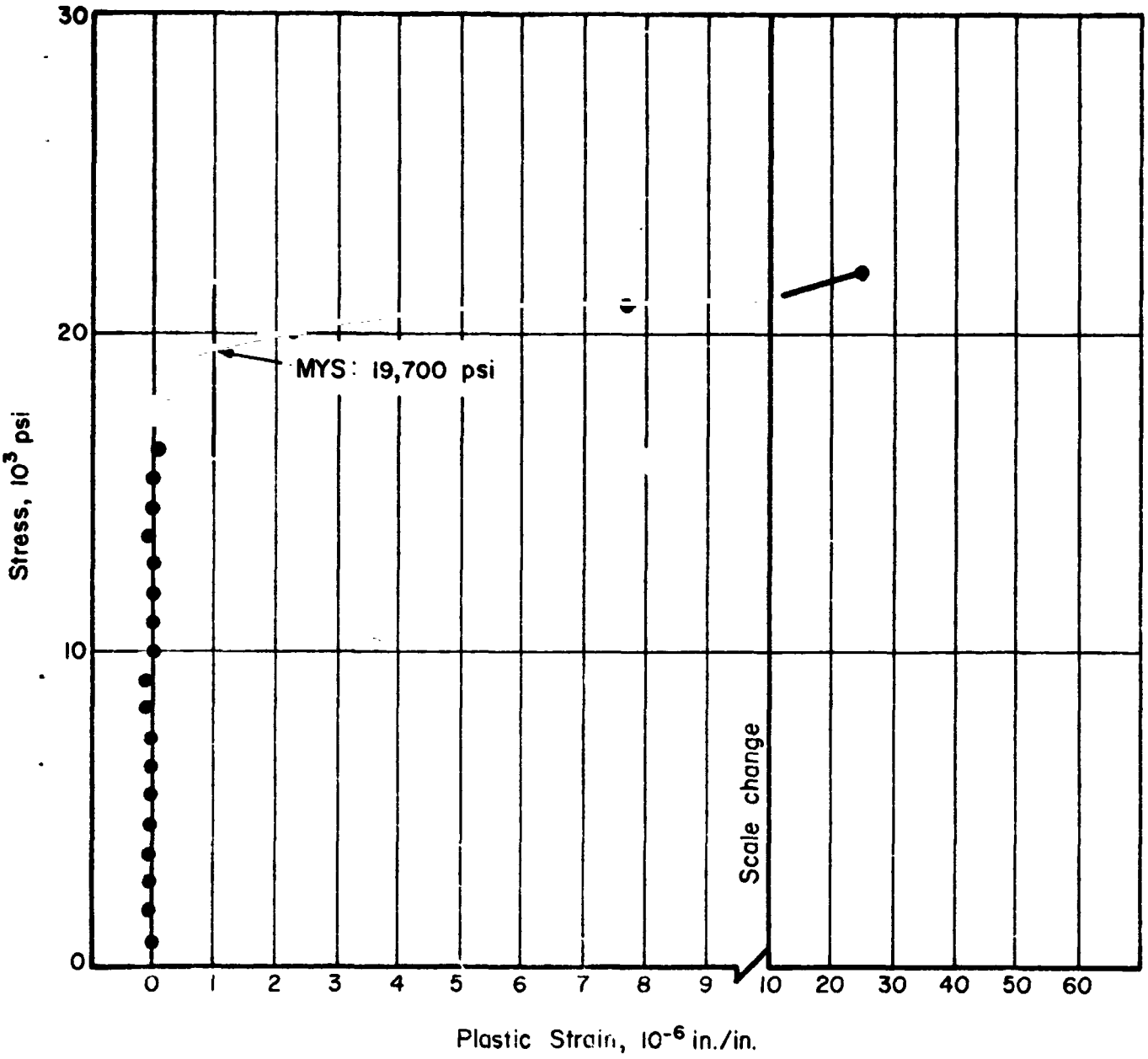

FIGURE A-15. MYS TEST ON 5456-H34 A1, SPECIMEN No. 22, HEAT TREATED AT 500 F FOR 1 HOUR

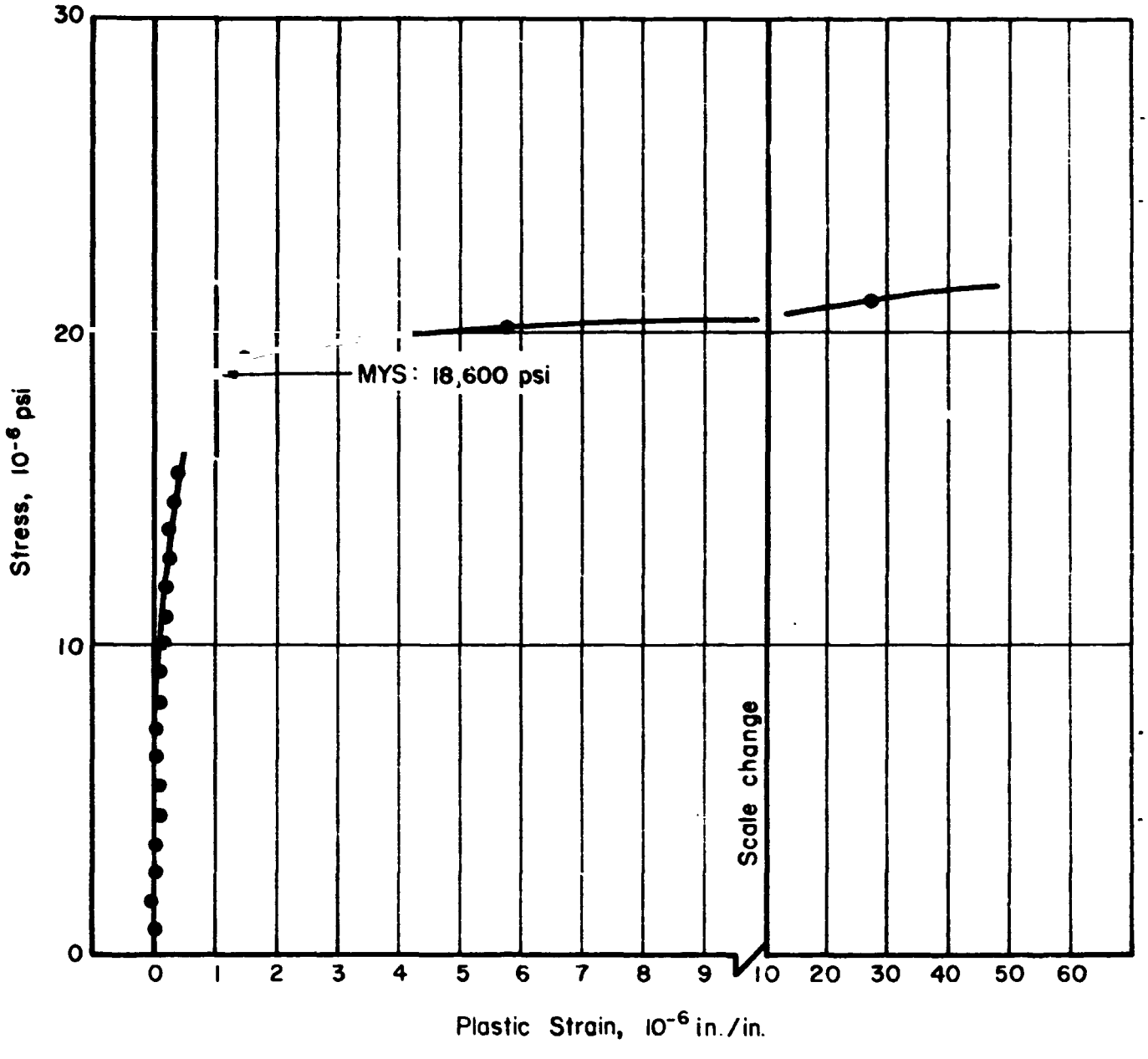

FIGURE A-16. MYS TEST ON 5456-H34 A1, SPECIMEN No. 23, HEAT TREATED AT 500 F FOR 1 HOUR

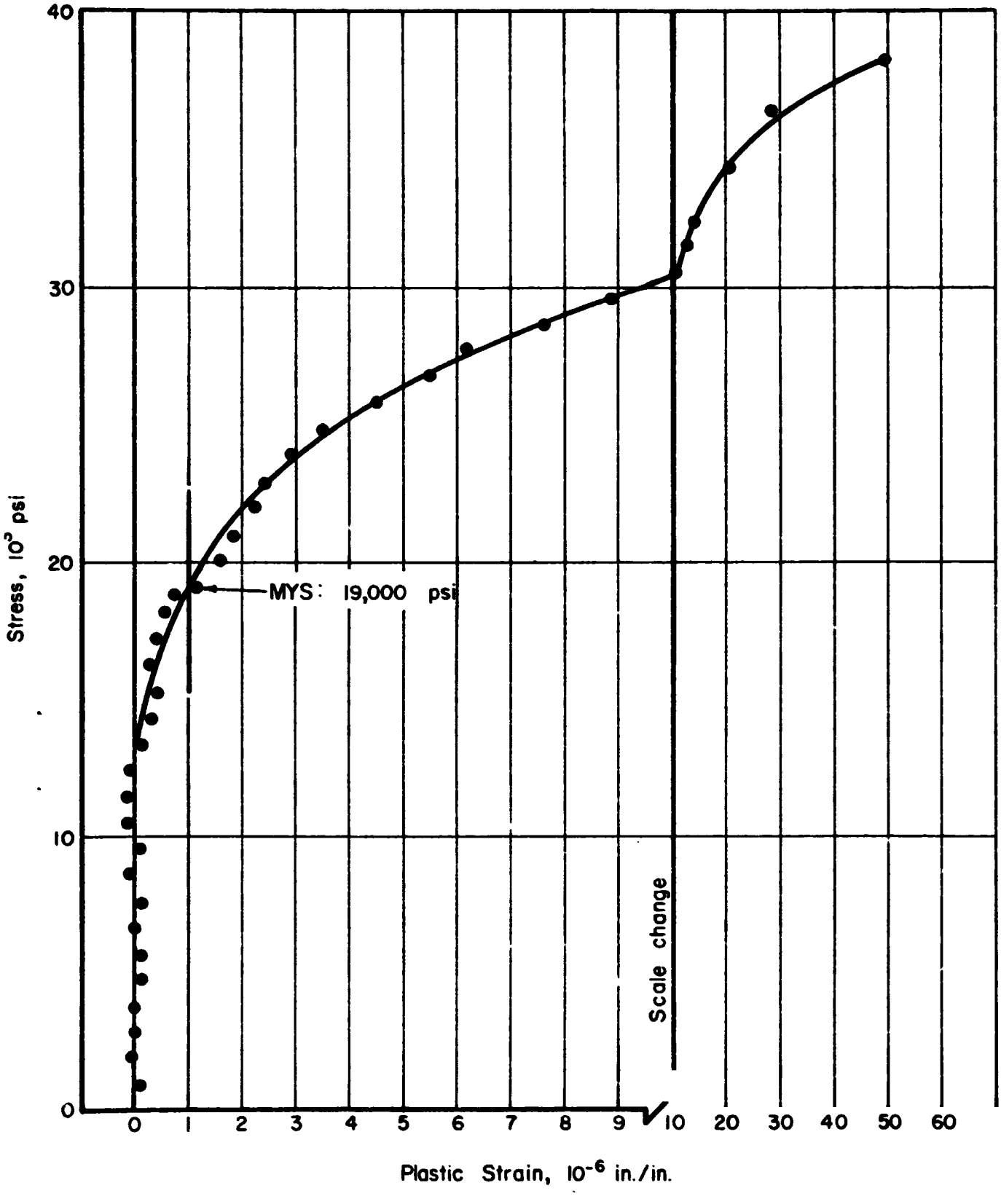

FIGURE A-17. MYS TEST ON 6061-T6 Al, SPECIMEN No. 1, AS RECEIVED

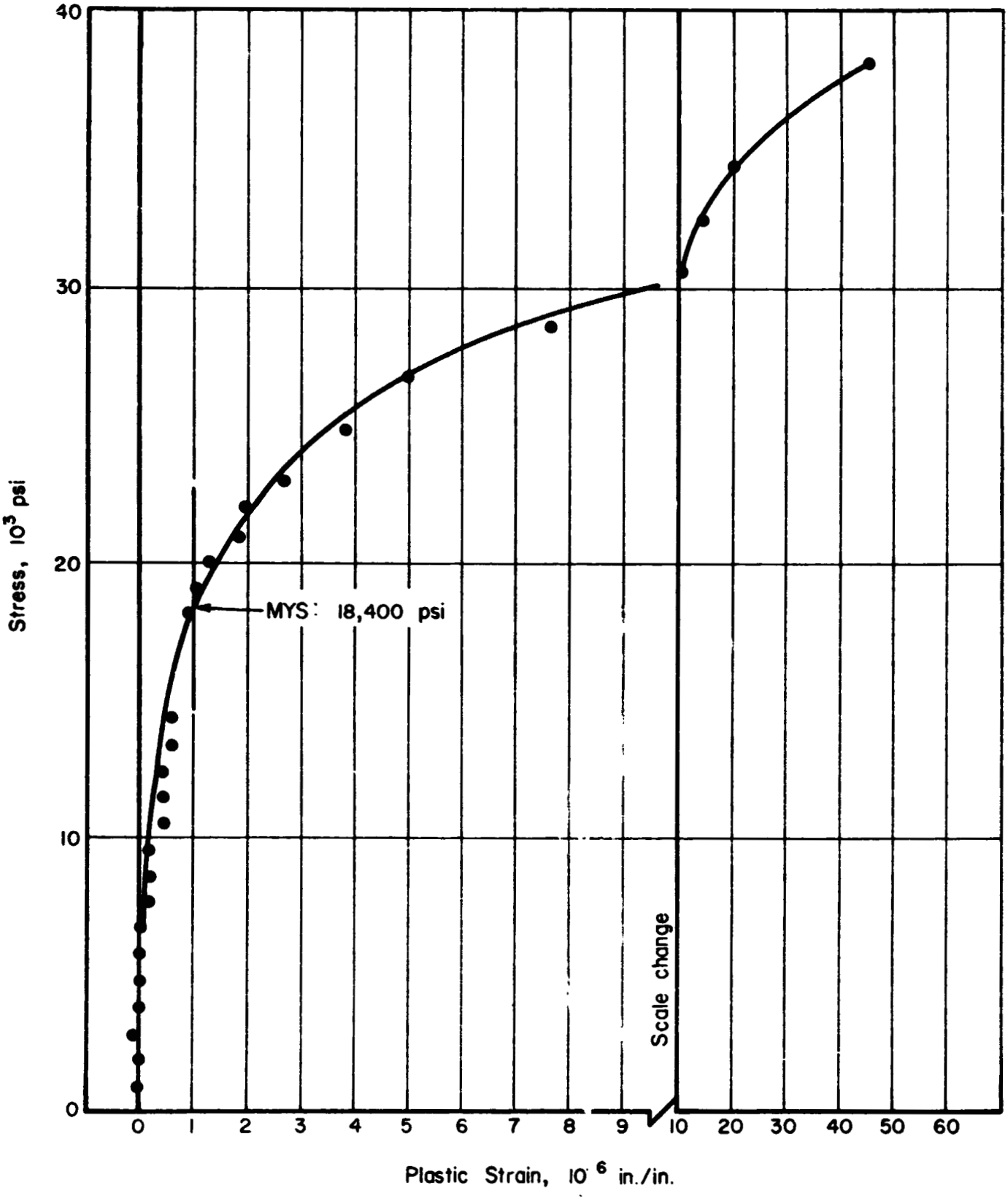

FIGURE A-18. MYS TEST ON 6061-T6 Al, SPECIMEN No 1, AS RECEIVED

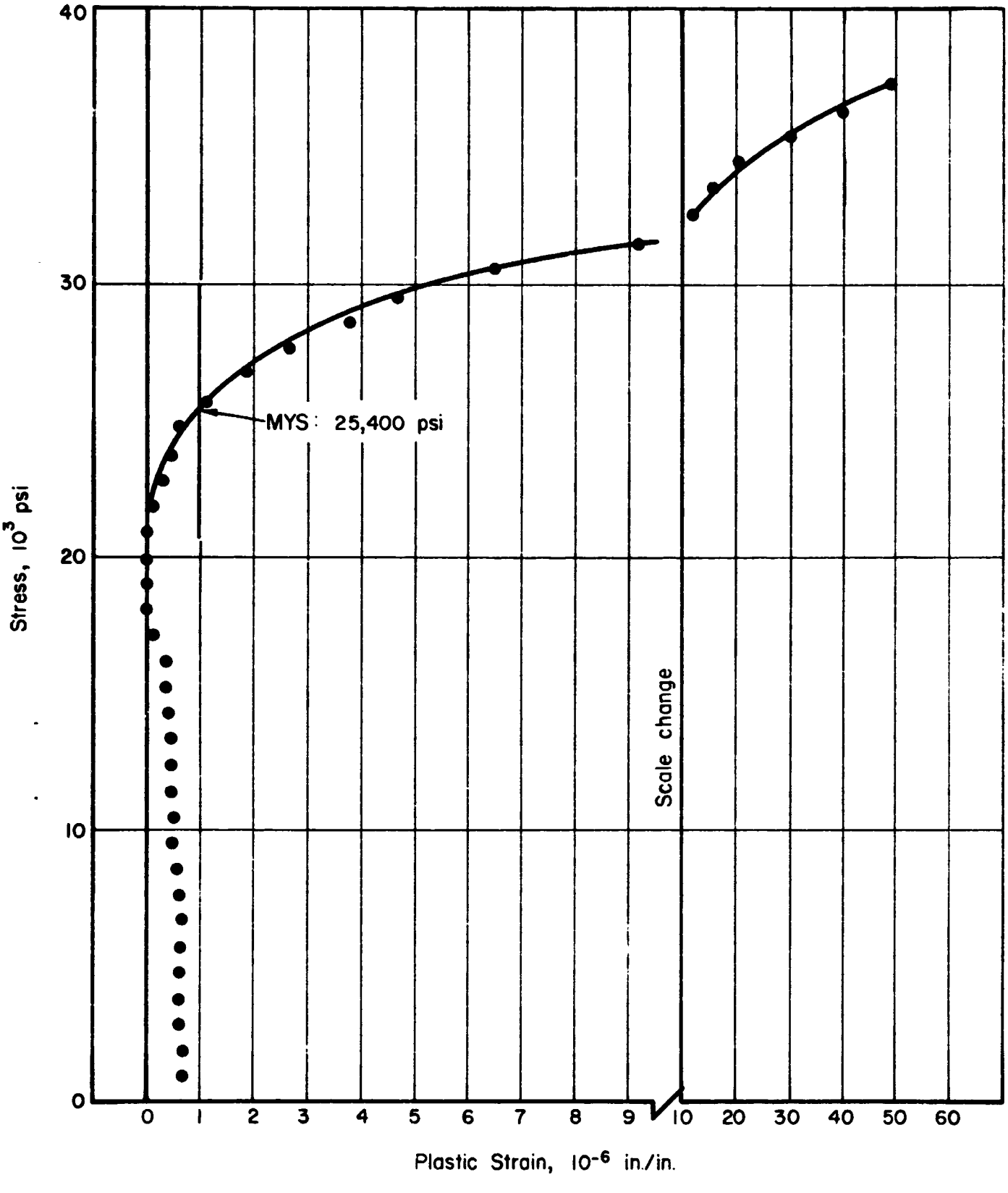

FIGURE A-19. MYS TEST ON 6061-T6 Al, SPECIMEN No. 9, HEAT TREATED AT 400 F FOR 1 HOUR

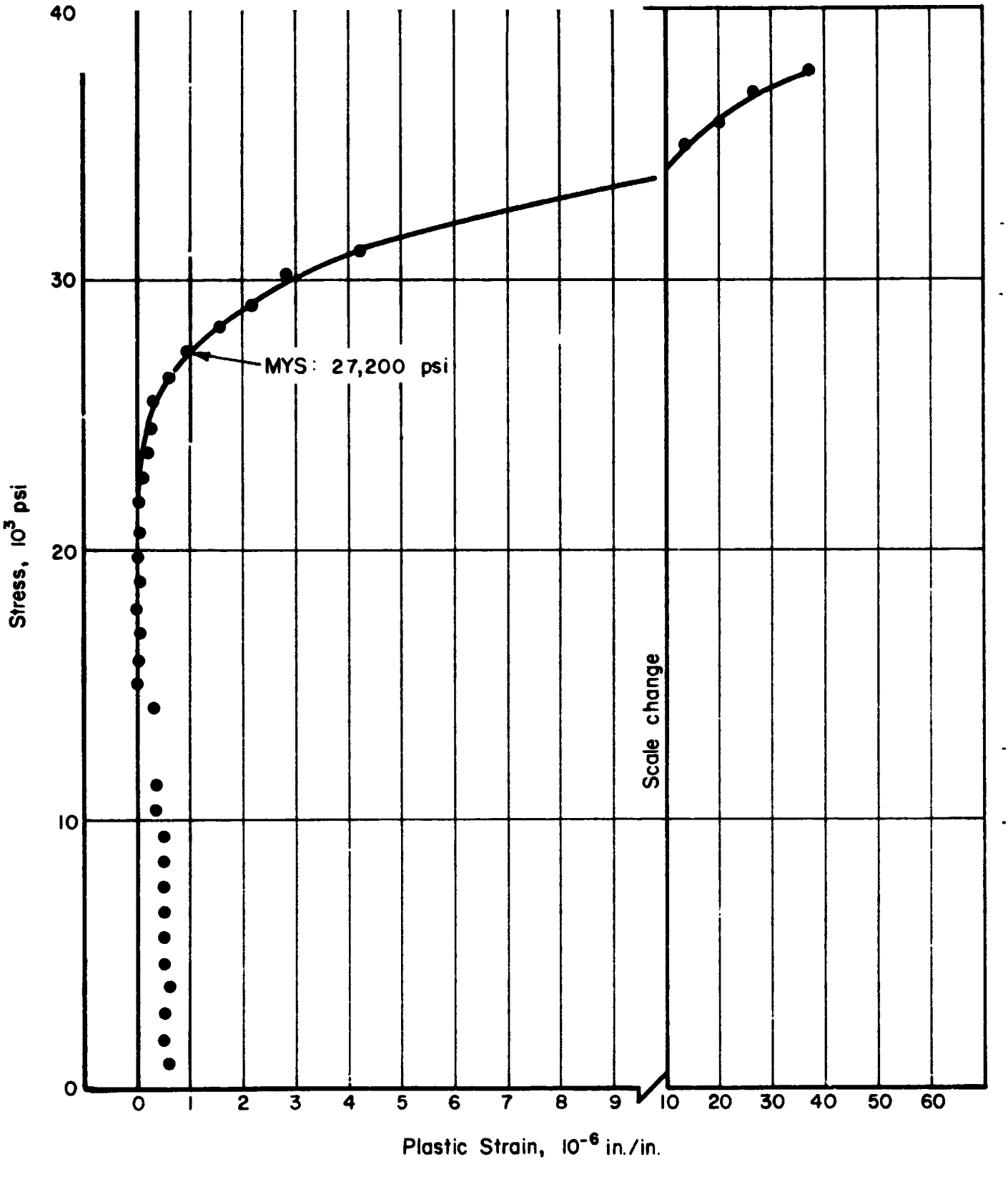

FIGURE A-20. MYS TEST ON 6061-T6 Al, SPECIMEN No. 8, HEAT TREATED AT 400 F FOR 1 HOUR

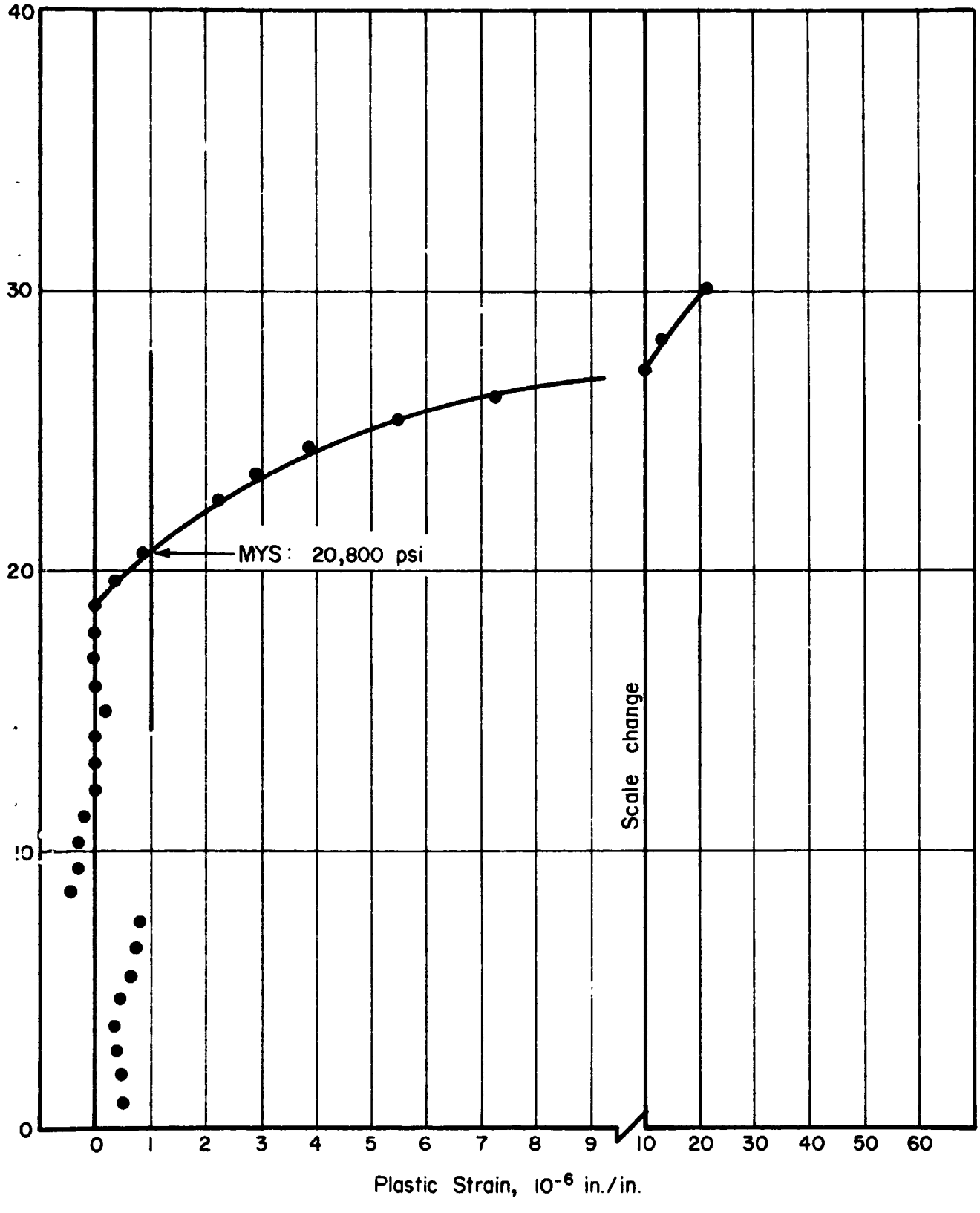

FIGURE A-21. MYS TEST ON 6061-T6 Al, SPECIMEN No. 15, HEAT TREATED AT 450 F FOR 1 HOUR

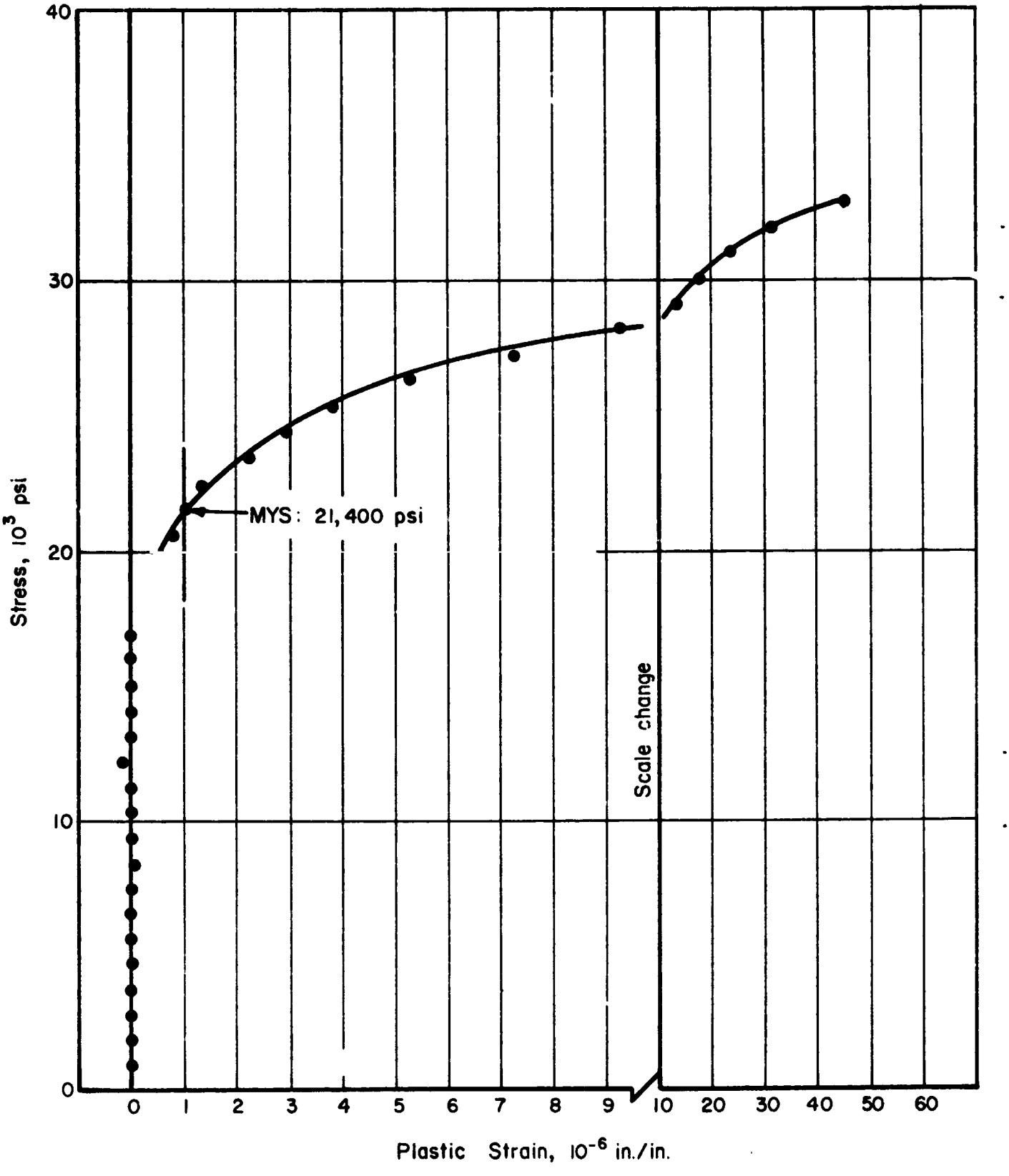

FIGURE A-22. MYS TEST ON 6061-T6 Al, SPECIMEN No. 14, HEAT TREATED AT 450 F FOR 1 HOUR

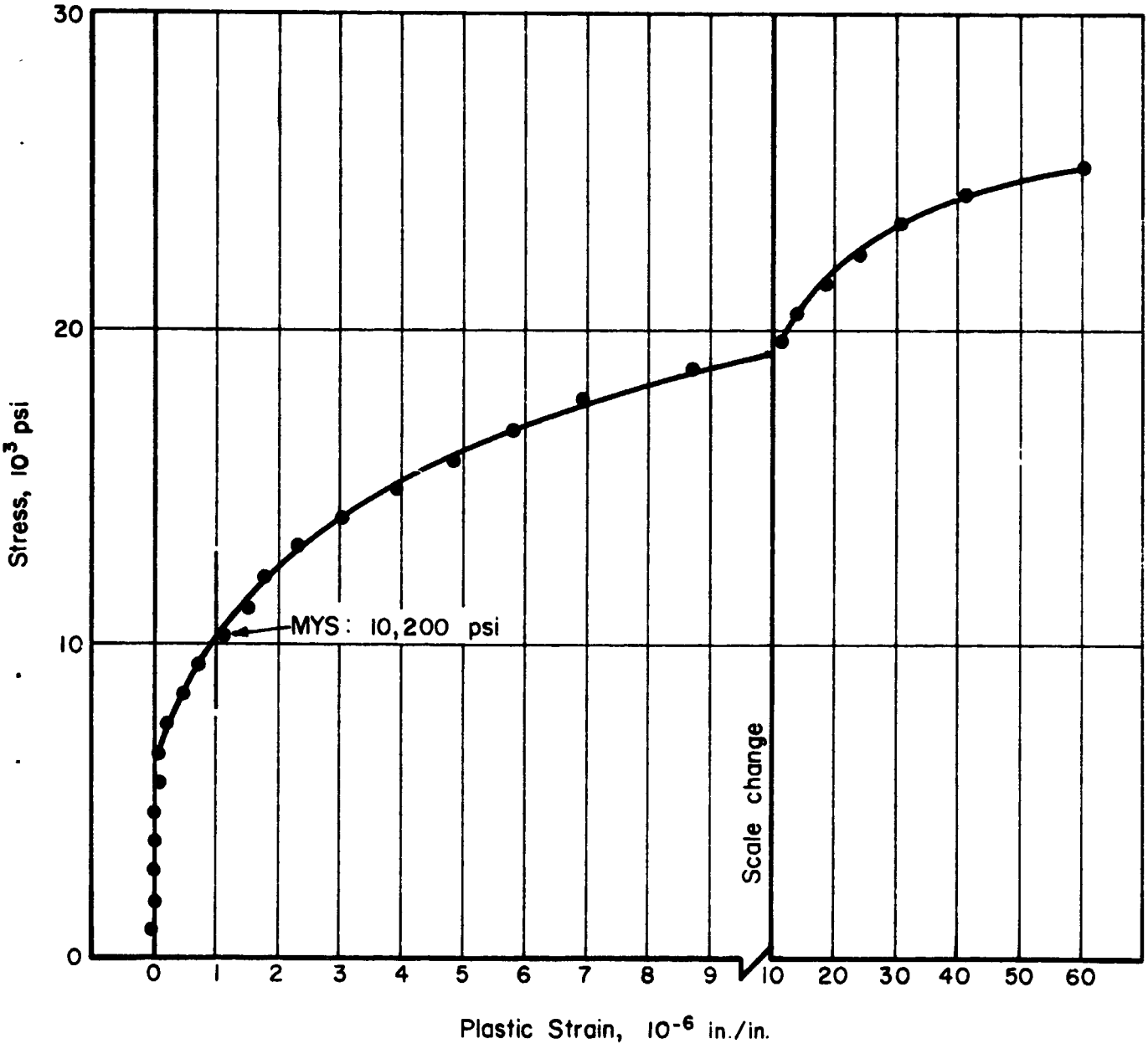

FIGURE A-23. MYS TEST ON 6061-T6 Al, SPECIMEN No. 25, HEAT TREATED AT 500 F FOR 1 HOUR

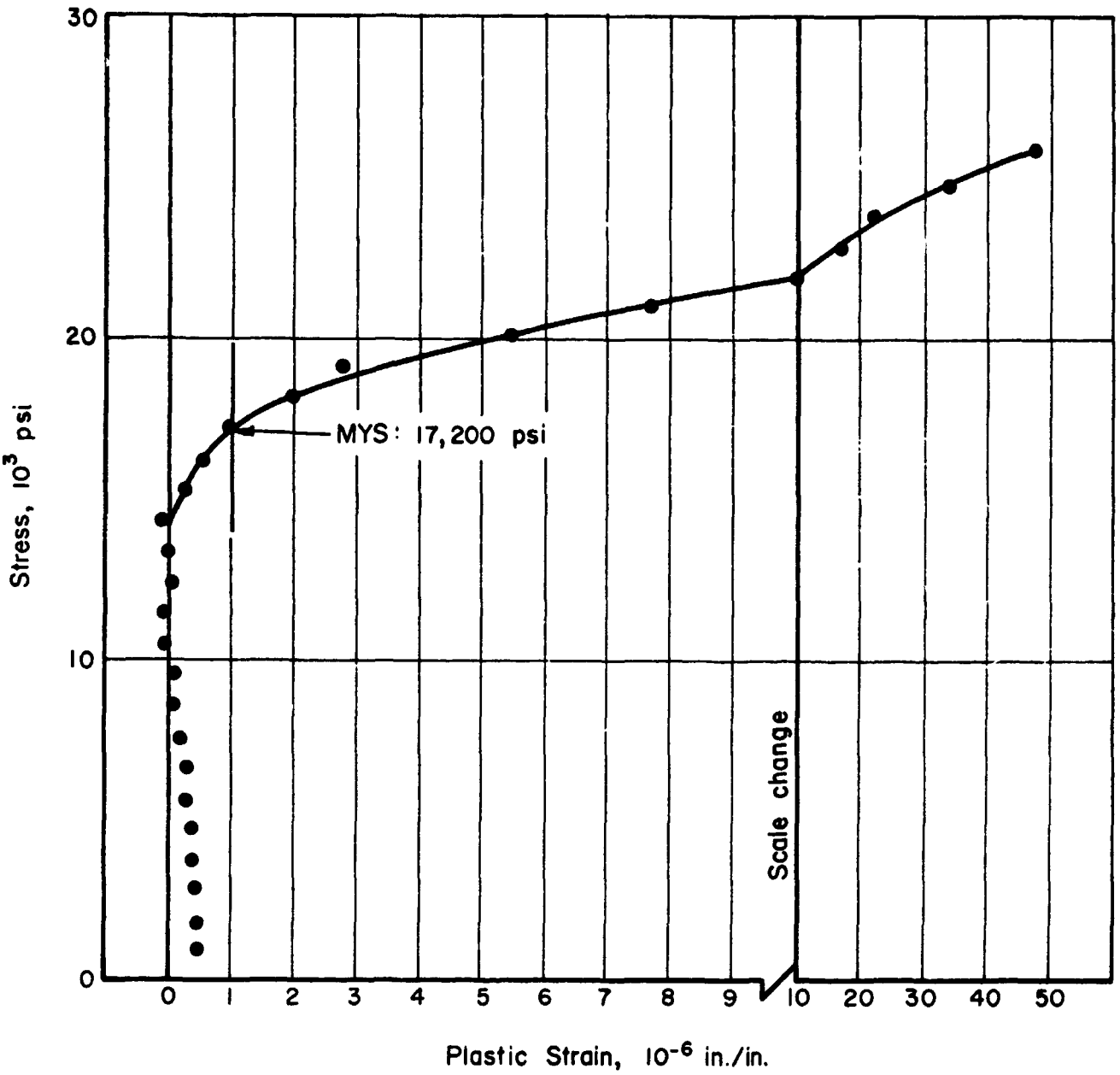

FIGURE A-24. MYS TEST ON 6061-T6 Al, SPECIMEN No. 24, HEAT TREATED AT 500 F FOR 1 HOUR

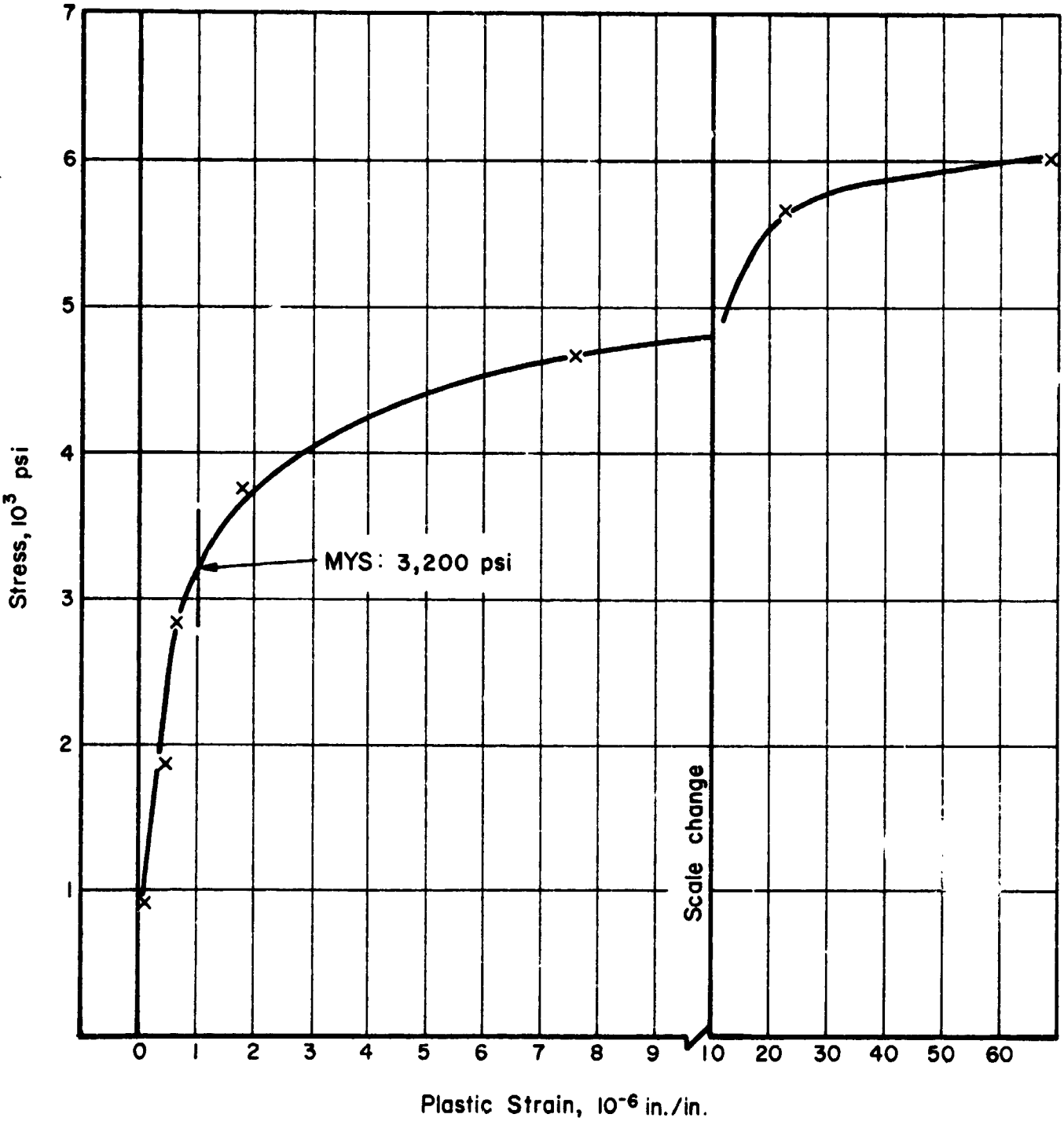

FIGURE A-25. MYS TEST ON AZ31Mg, SPECIMEN No. 1, AS RECEIVED

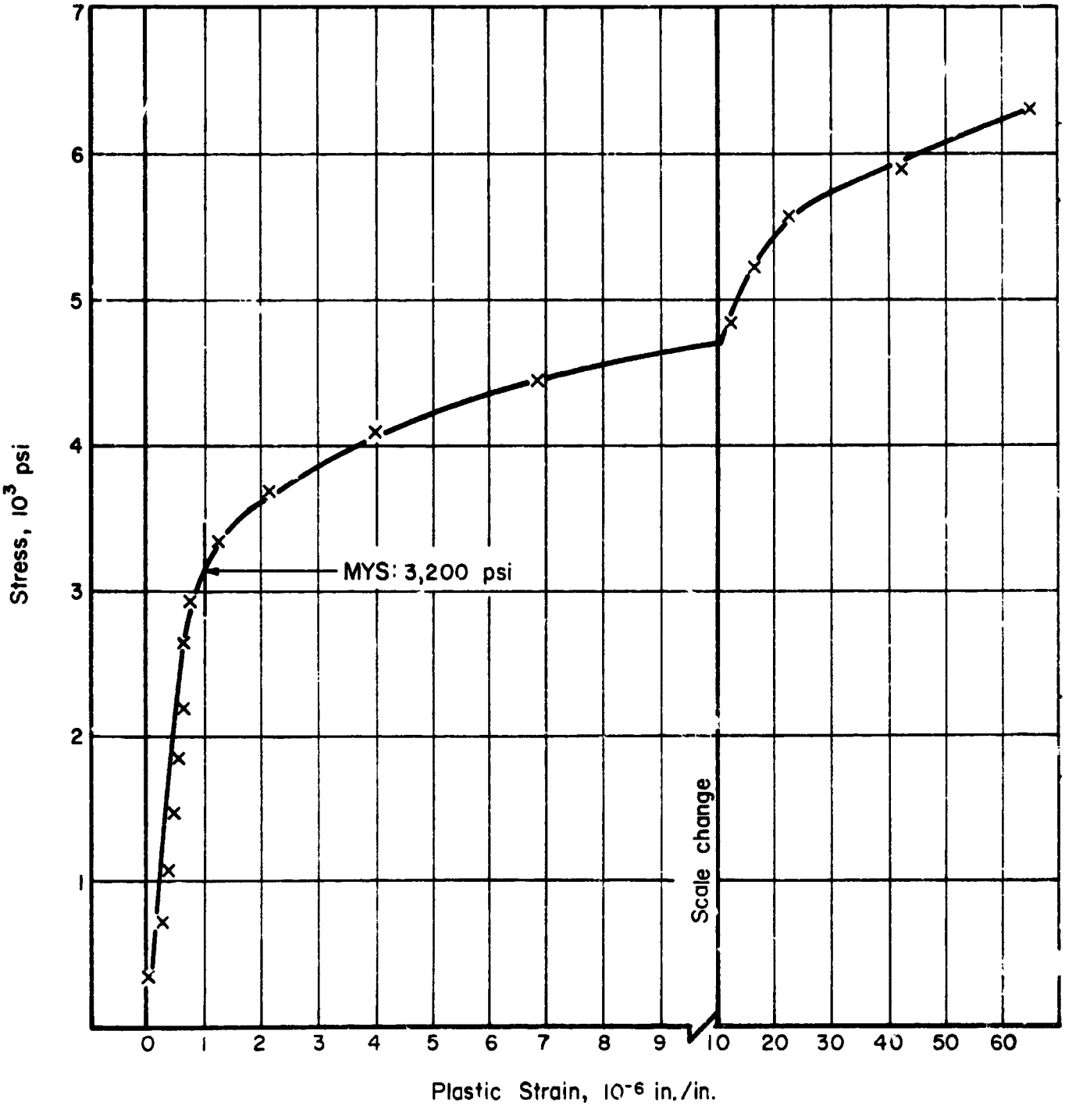

FIGURE A-26. MYS TEST ON AZ31-Mg, SPECIMEN No. 2, AS RECEIVED

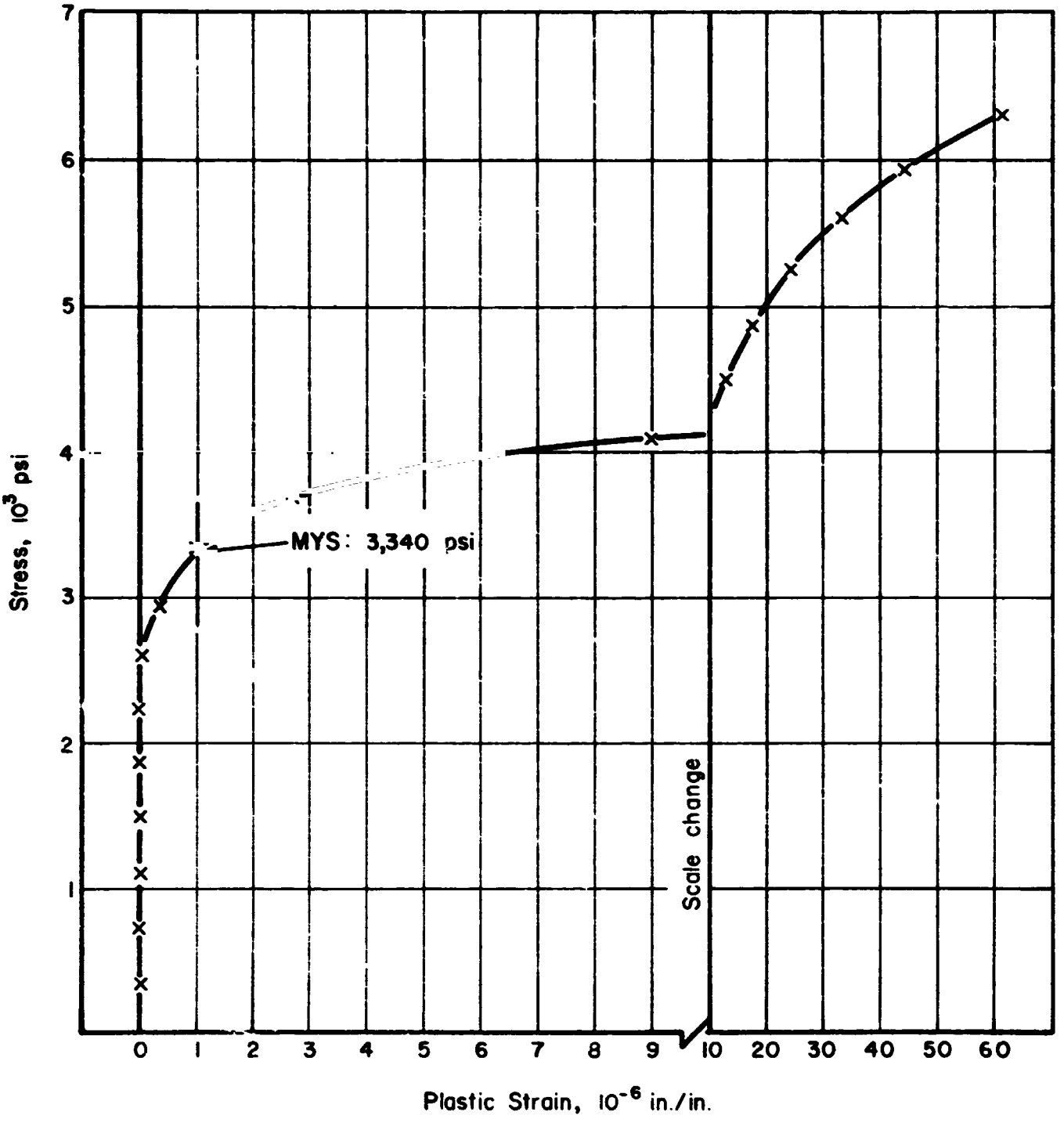

FIGURE A-27. MYS TEST ON AZ31-Mg, SPECIMEN No. 3, HEAT TREATED 1 HOUR AT 450 F

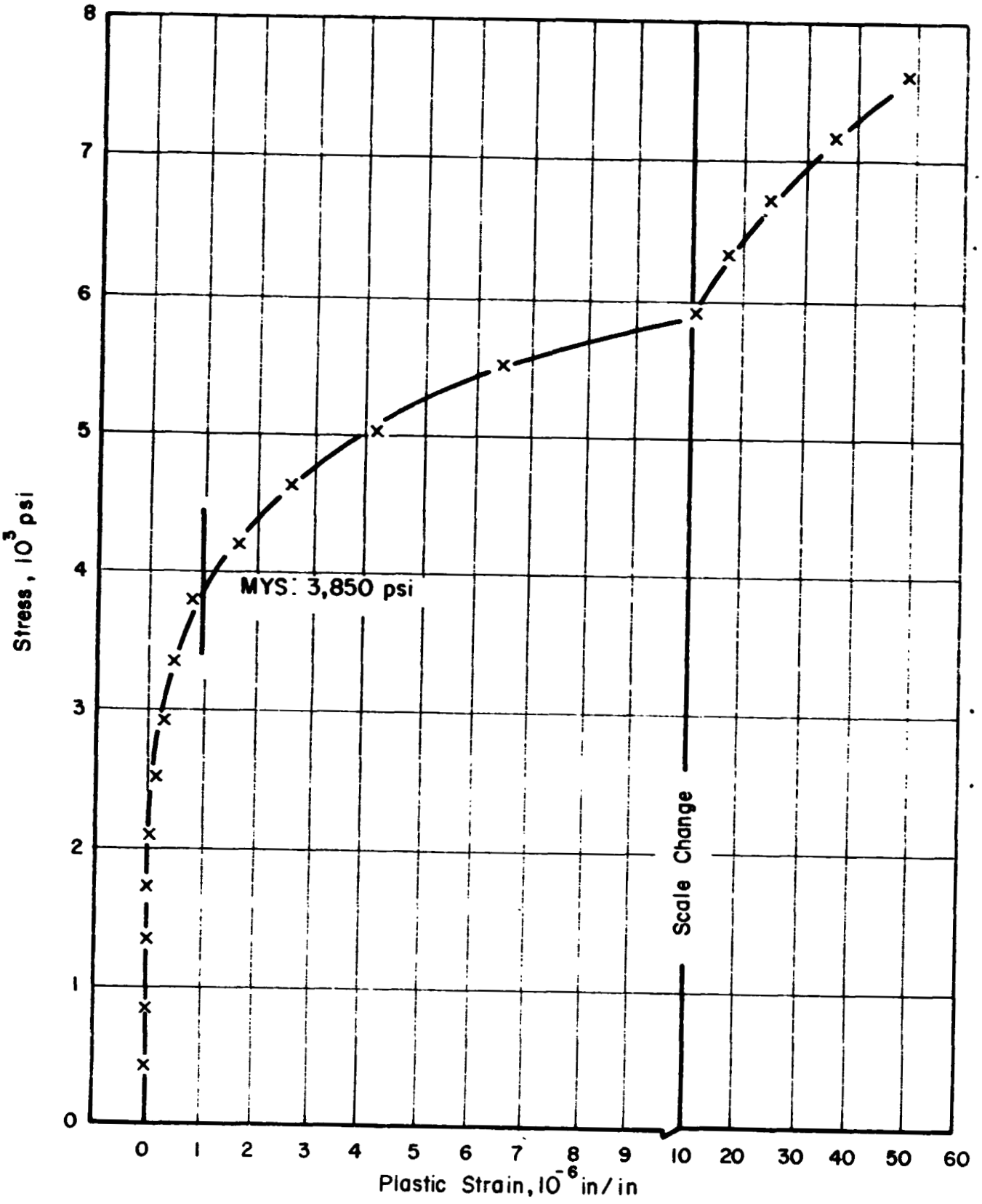

FIGURE A-28. MYS TEST ON AZ31-Mg, SPECIMEN No. 4, HEAT TREATED AT 450 F FOR 1 HOUR

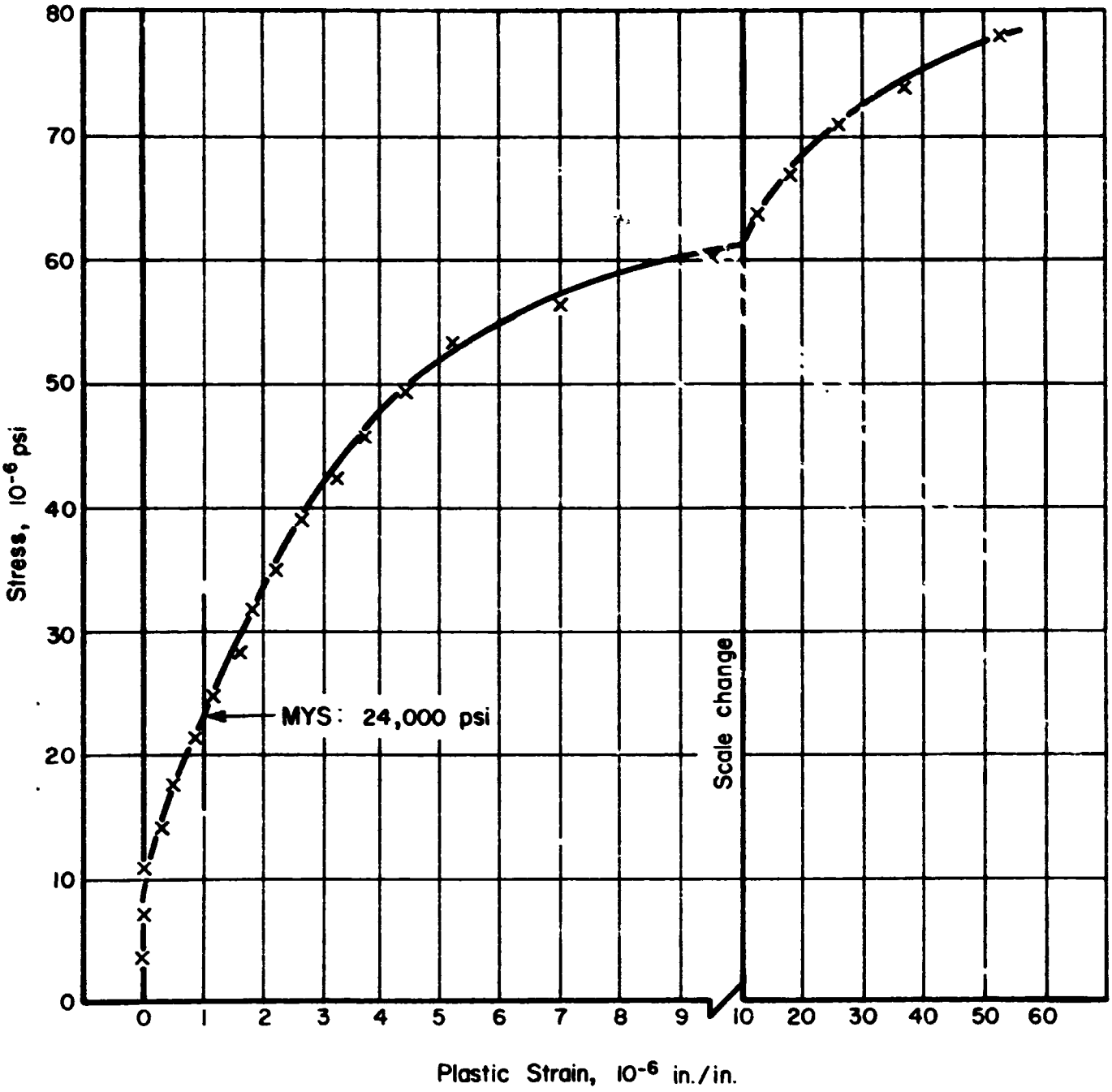

FIGURE A-29. MYS TEST ON TZM-Mo, SPECIMEN No. 1, AS RECEIVED

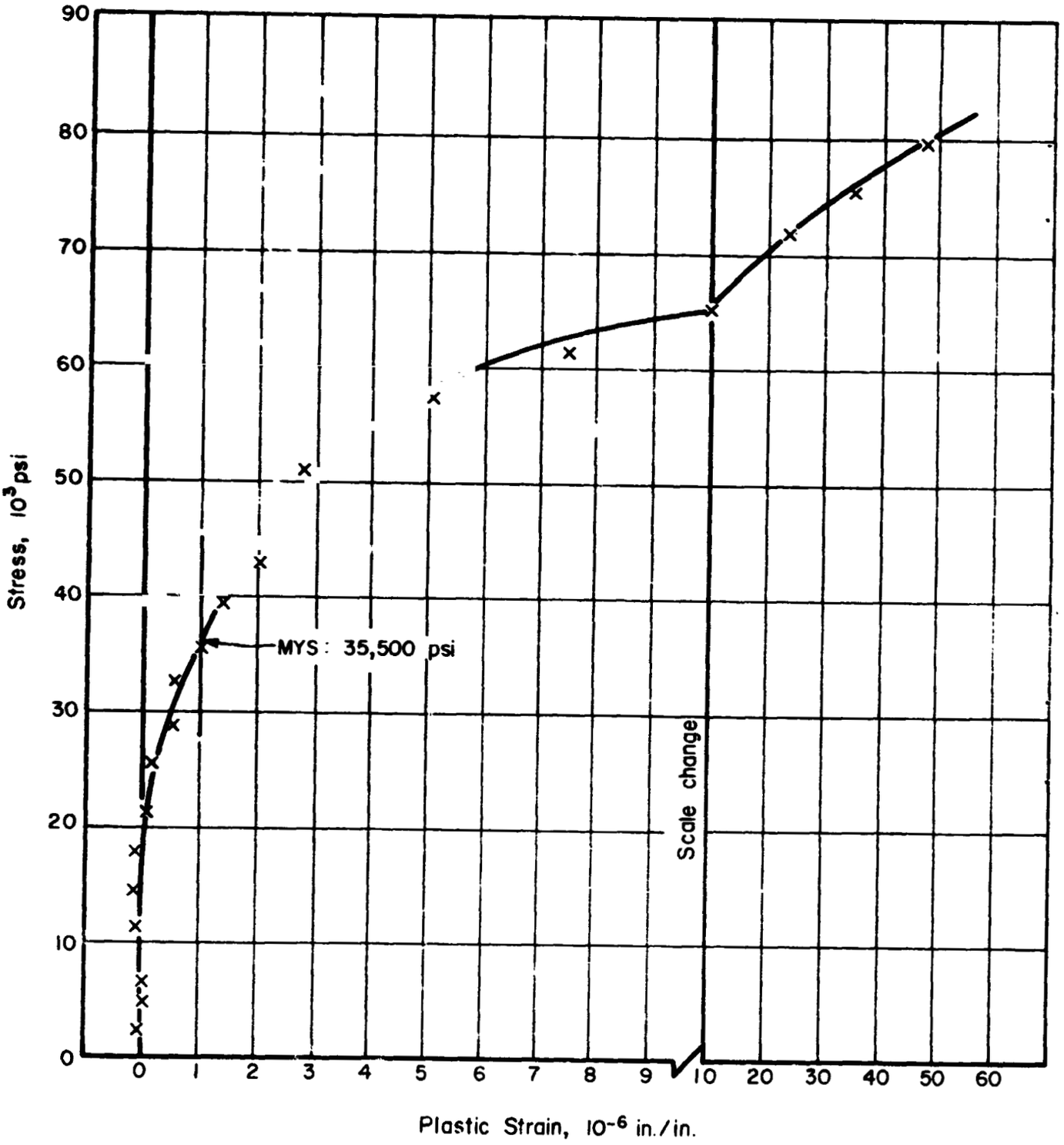

FIGURE A-30. MYS TEST ON TZM-Mo, SPECIMEN No. 2, AS RECEIVED

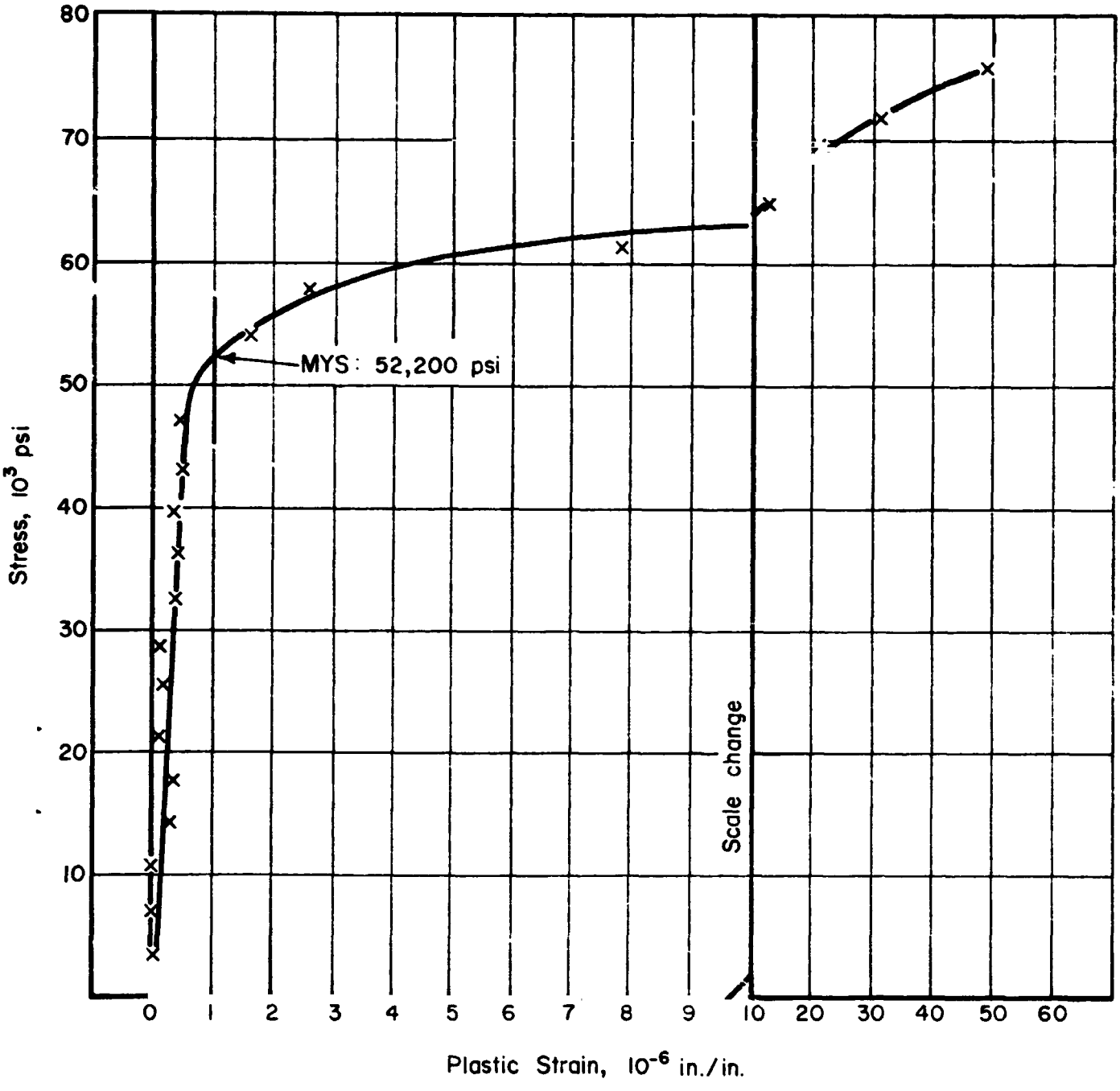

FIGURE A-31. MYS TEST ON TZM-Mo, SPECIMEN No. 4, HEAT TREATED AT 2200 F FOR 1 HOUR

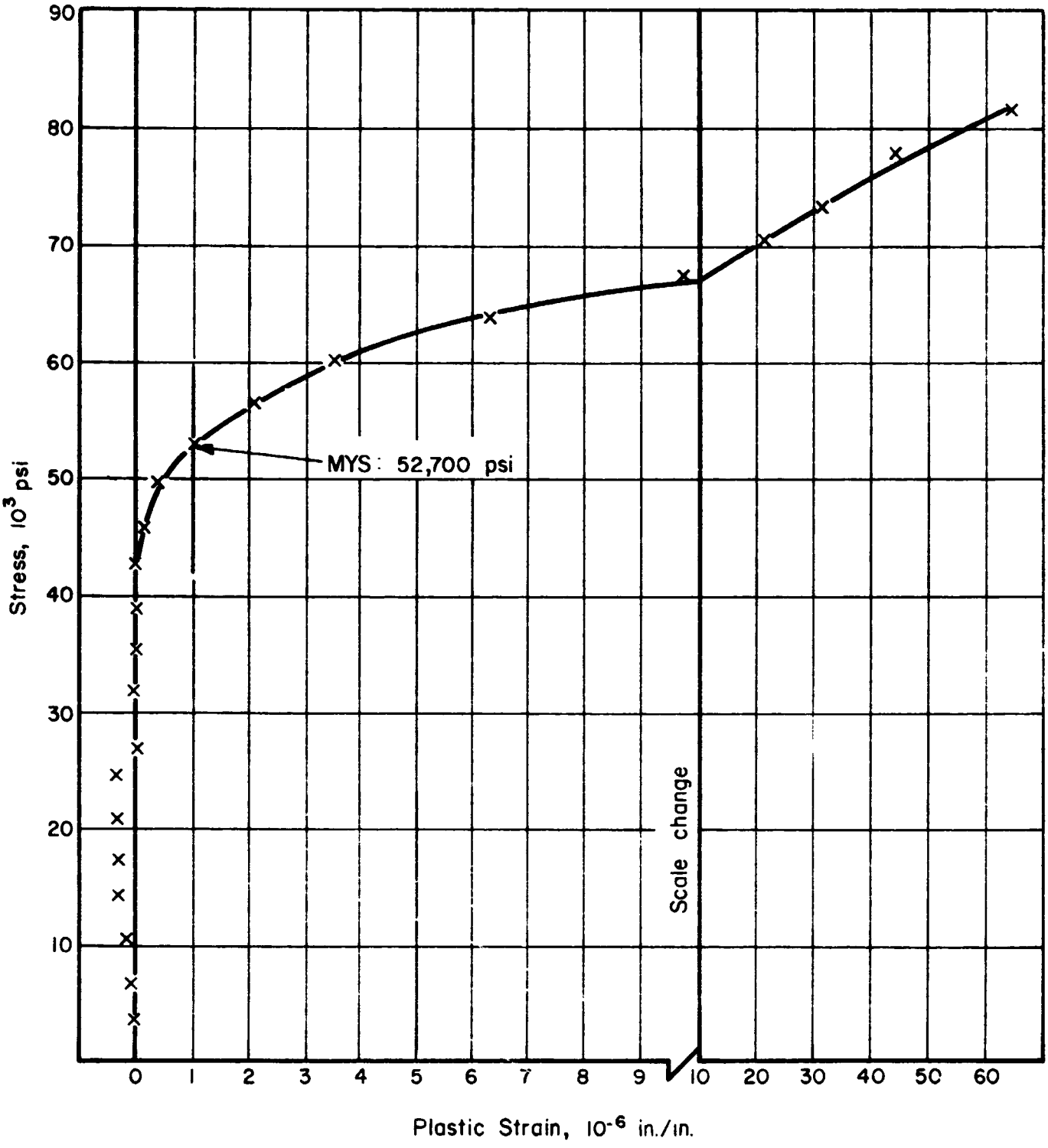

FIGURE A-32. MYS TEST ON TZM-Mo, SPECIMEN No. 5, HEAT TREATED AT 2200 F FOR 1 HOUR

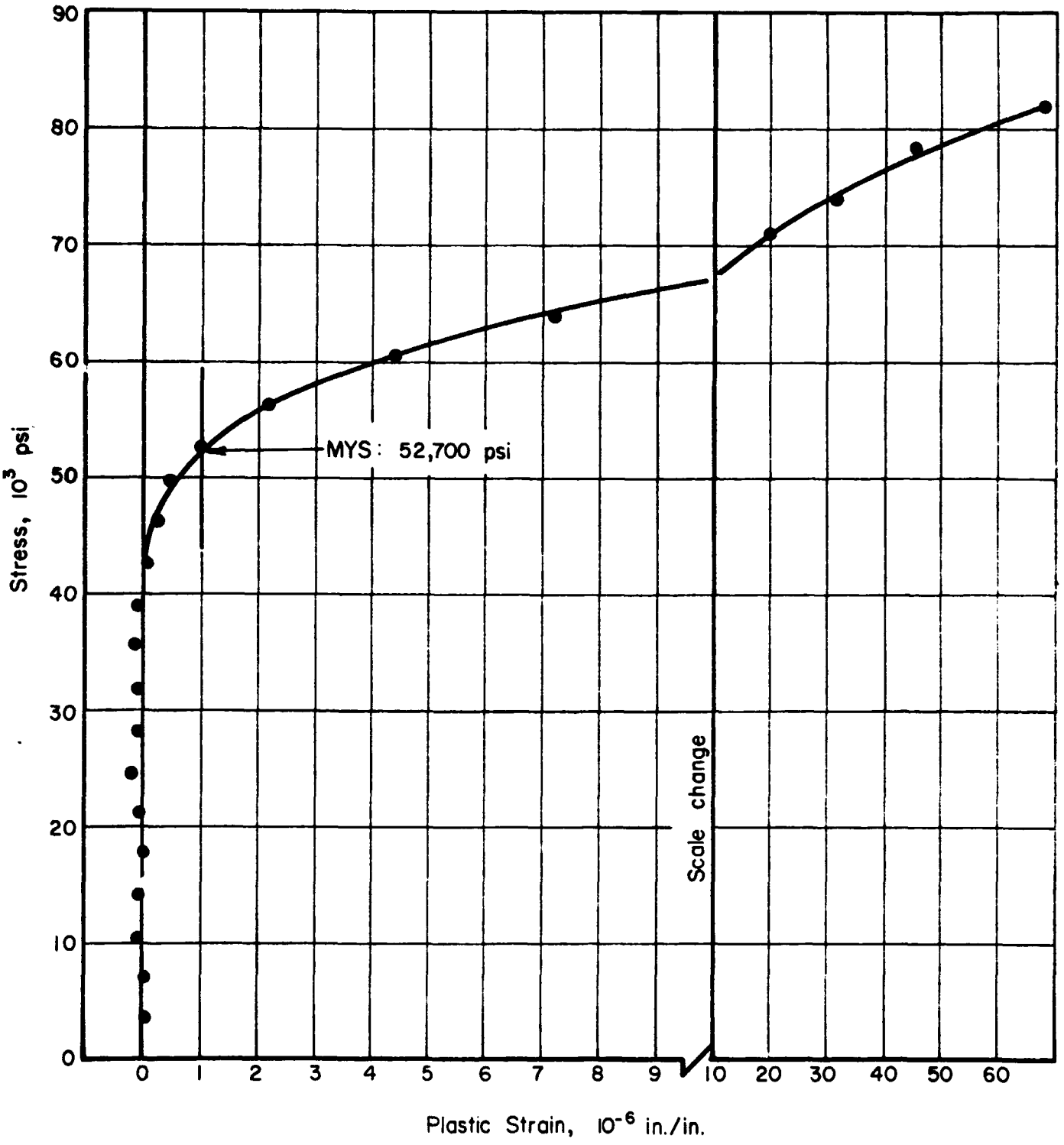

FIGURE A-33. MYS TEST ON TZM-Mo, SPECIMEN No. 6, HEAT TREATED AT 2200 F FOR 1 HOUR

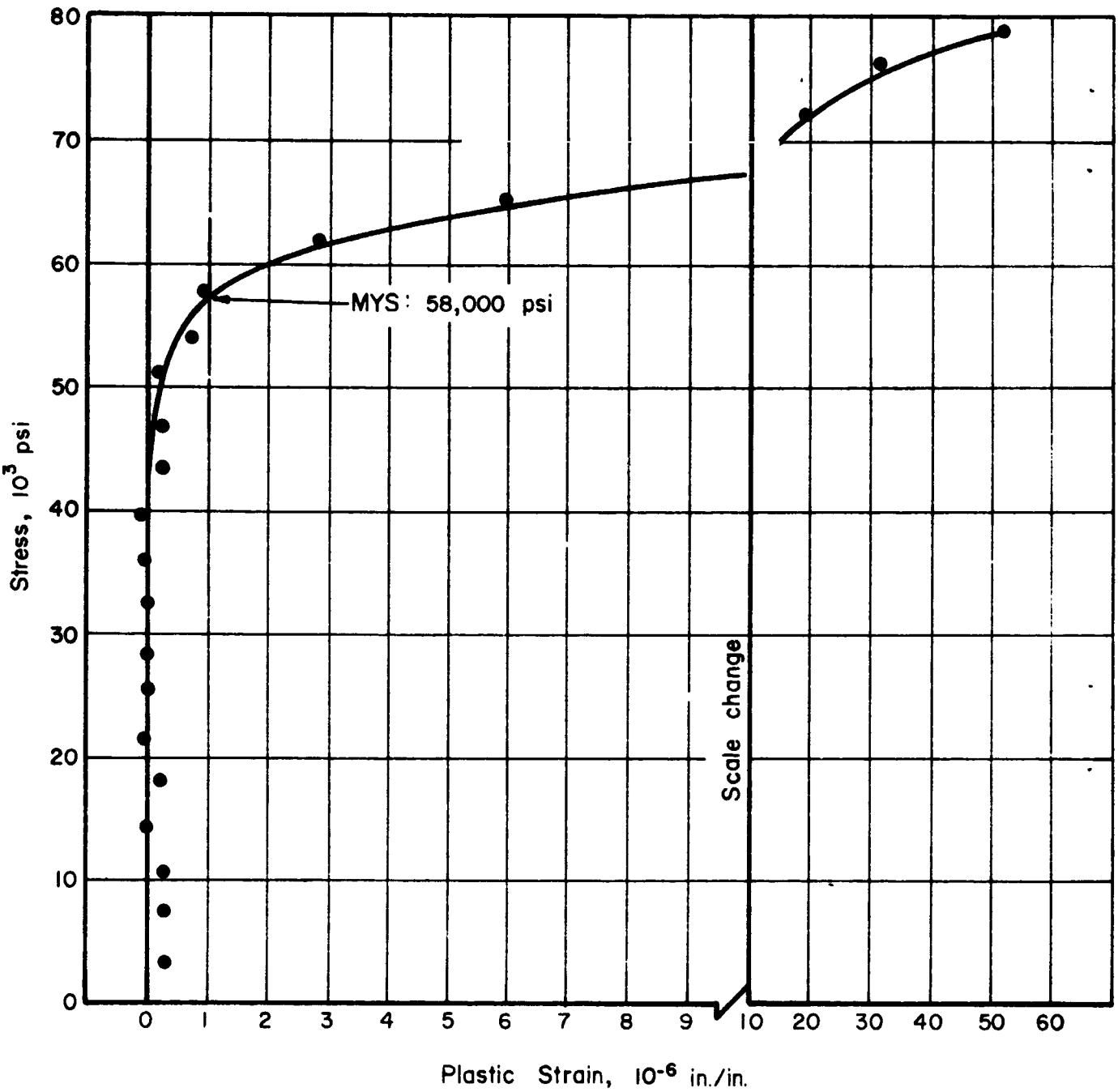

FIGURE A-34. MYS TEST ON TZM-Mo, SPECIMEN No. 7, HEAT TREATED AT 2200 F FOR 1 HOUR

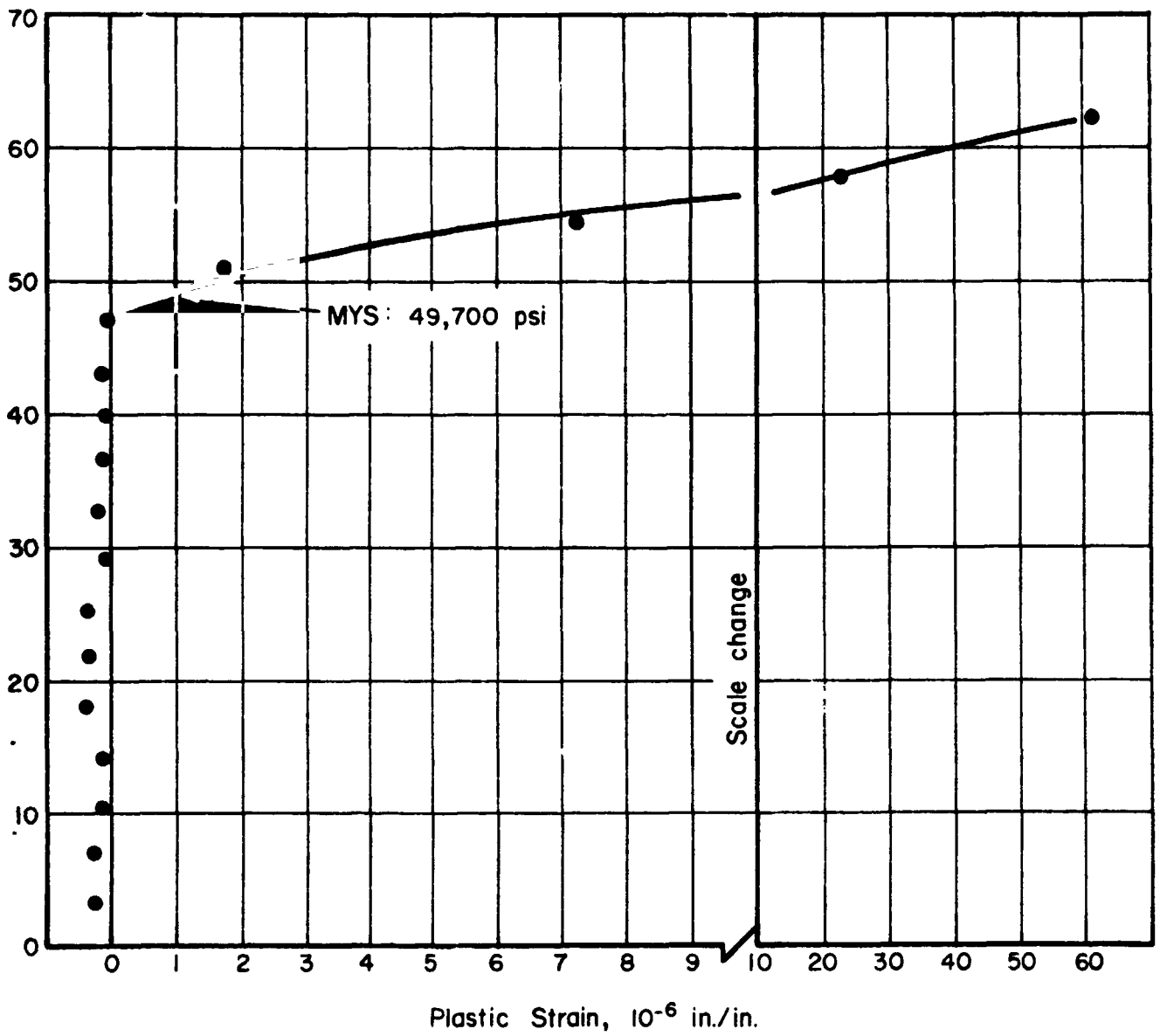

FIGURE A-35. MYS TEST ON TZM-Mo, SPECIMEN No. 8, HEAT TREATED AT 2600 F FOR 1 HOUR

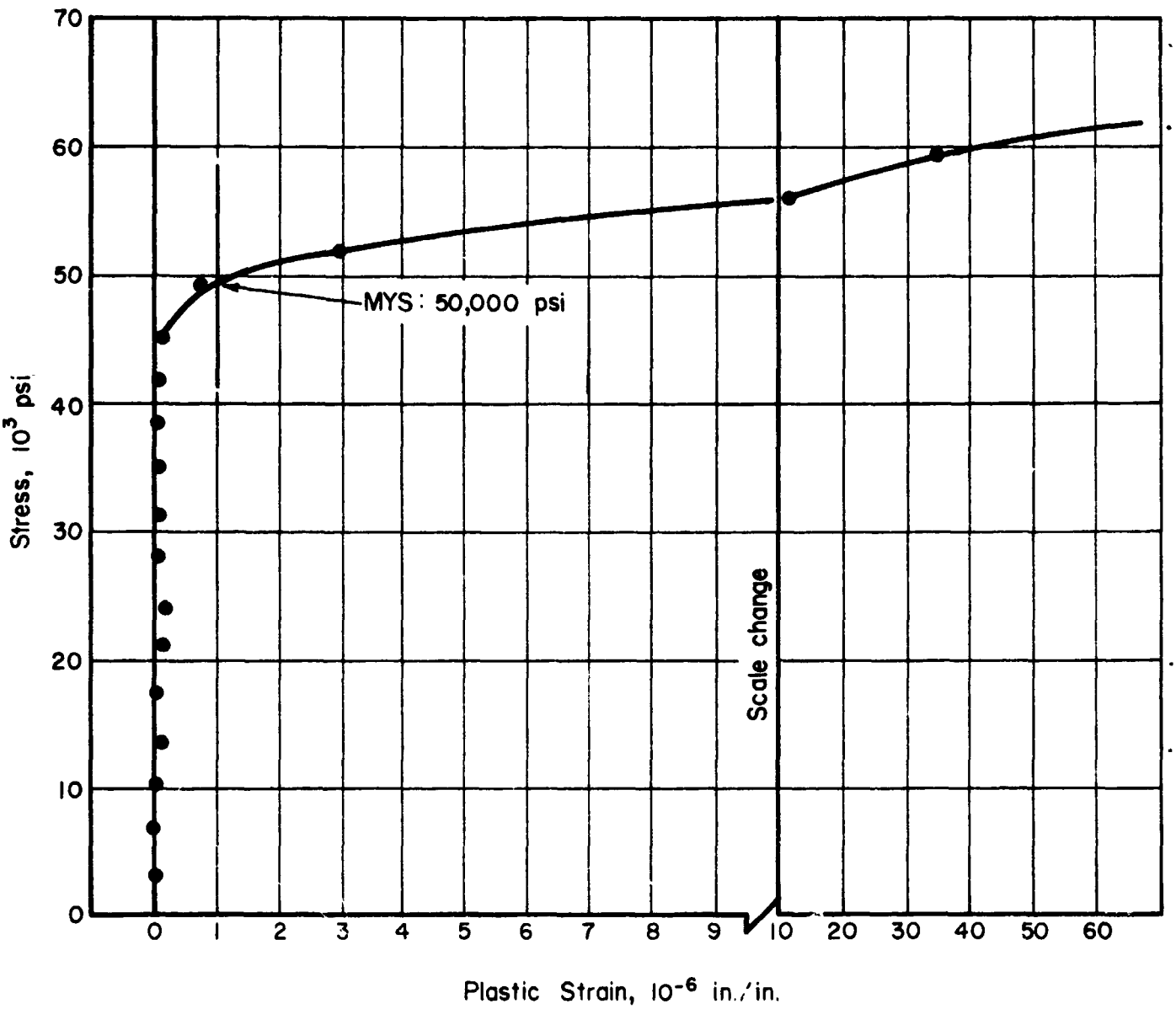

FIGURE A-36. MYS TEST ON TZM-Mo, SPECIMEN No. 9, HEAT TREATED AT 2600 F FOR 1 HOUR

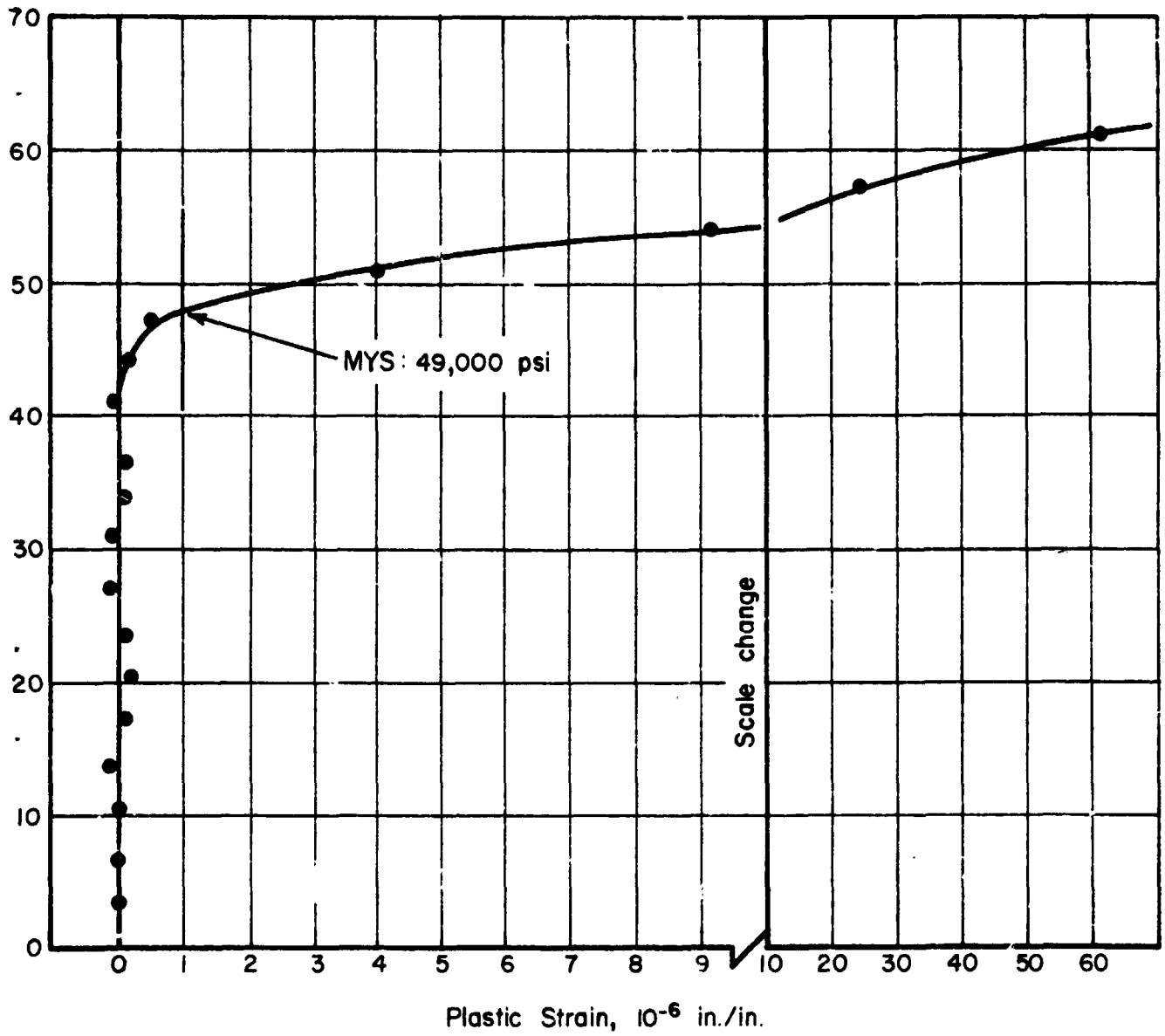

FIGURE A-37. MYS TEST ON TZM-Mo, SPECIMEN No. 10, HEAT TREATED AT 2600 F FOR 1 HOUR

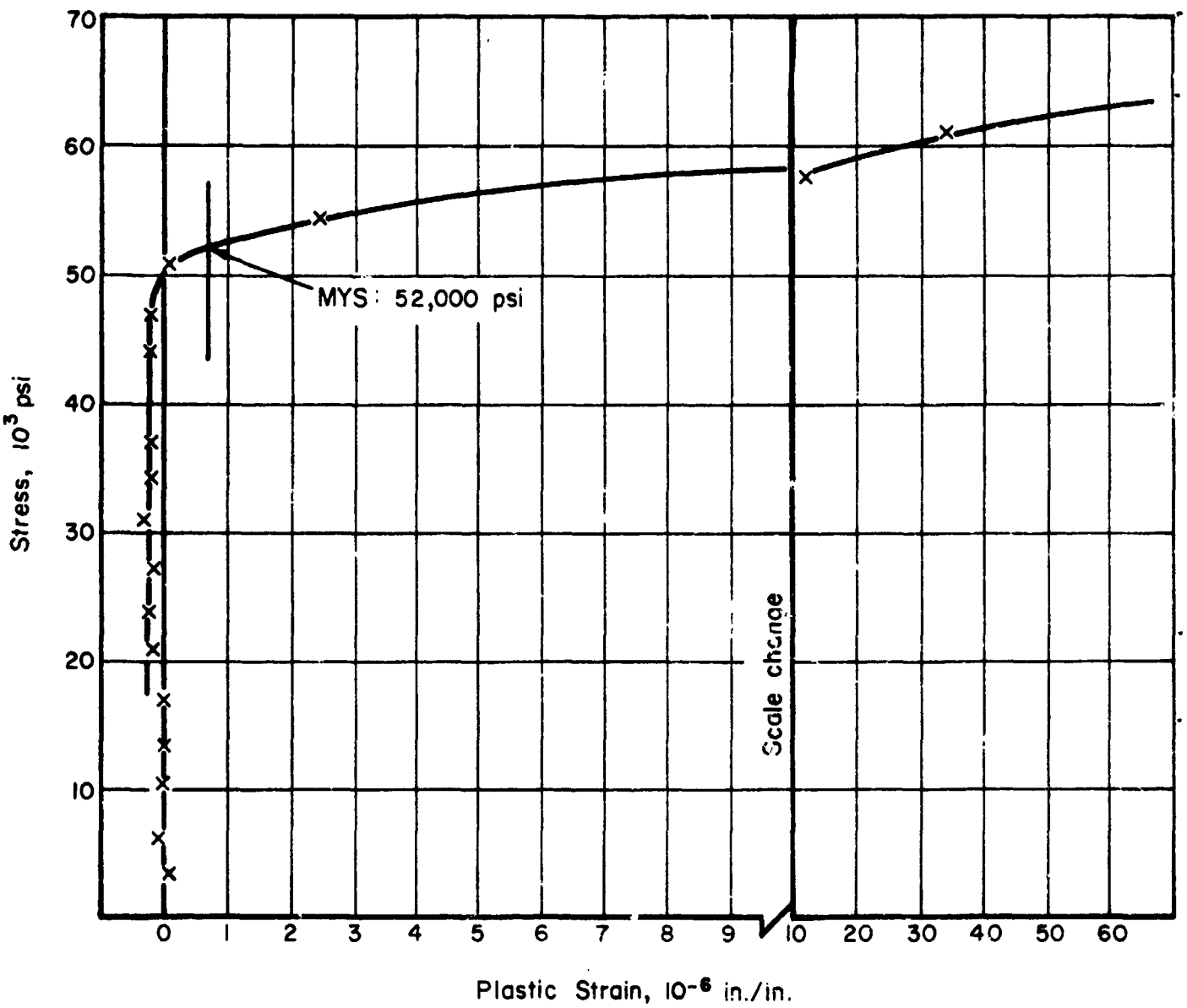

FIGURE A-38. MYS TEST ON TZM-Mo, SPECIMEN No. 11, HEAT TREATED AT 2600 F FOR 1 HOUR

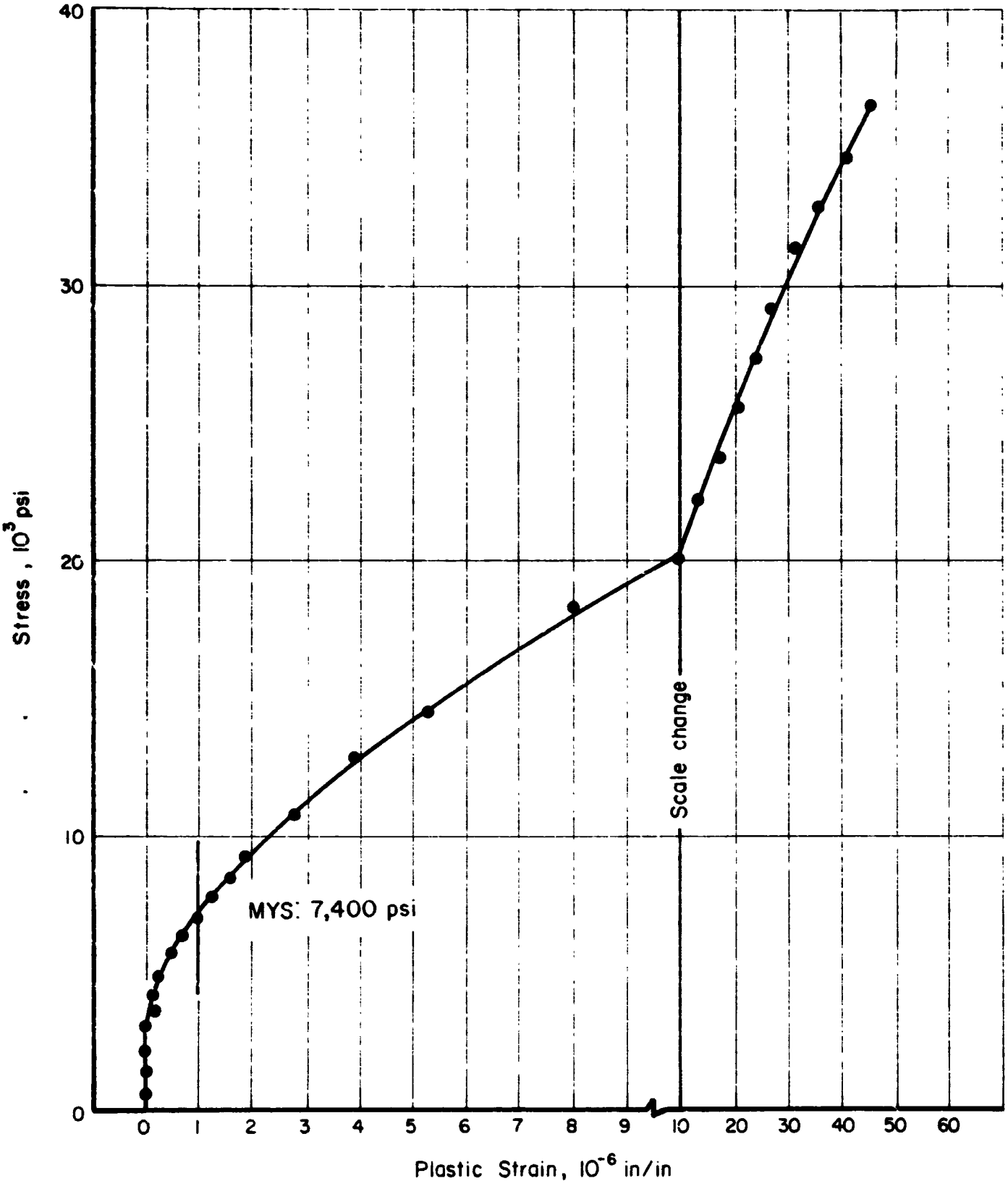

FIGURE A-39. MYS TEST ON I-400 Be, SPECIMEN No. 1, AS RECEIVED

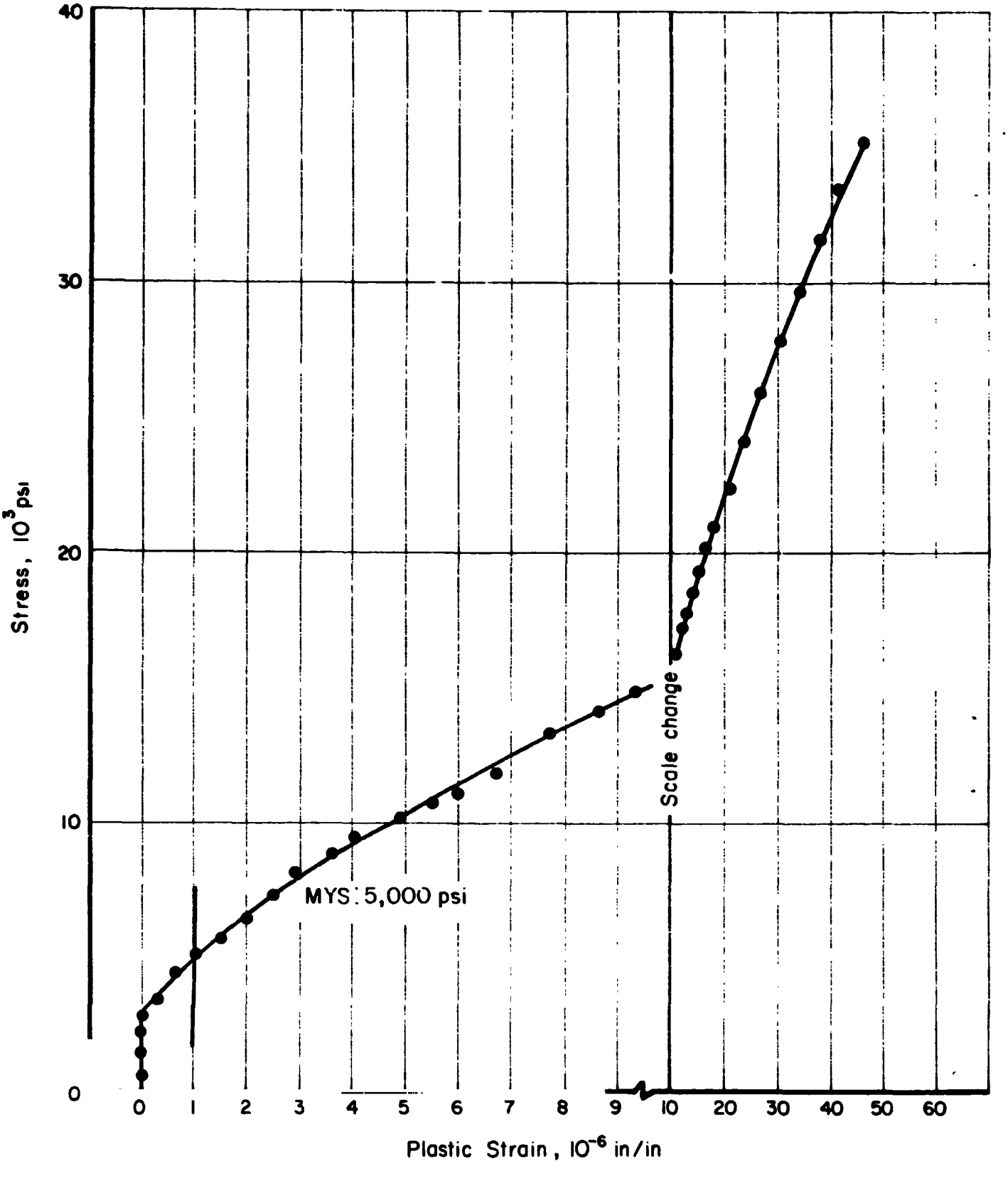

FIGURE A-40. MYS TEST ON I-400 Be, SPECIMEN No. 2, AS RECEIVED

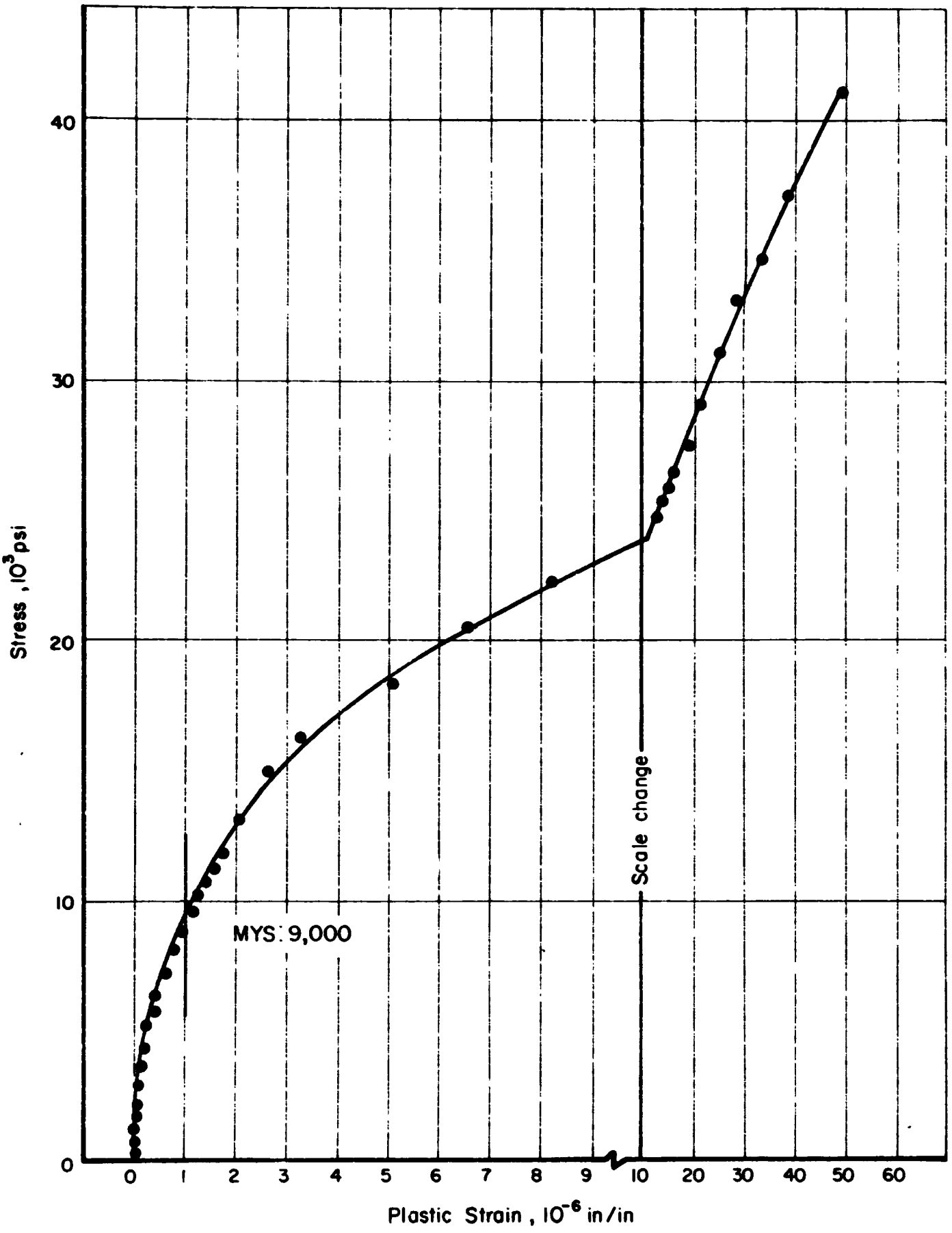

FIGURE A-41. MYS TEST ON I-400 Be, SPECIMEN No. 6, HEAT TREATED AT 1100 F FOR 1 HOUR

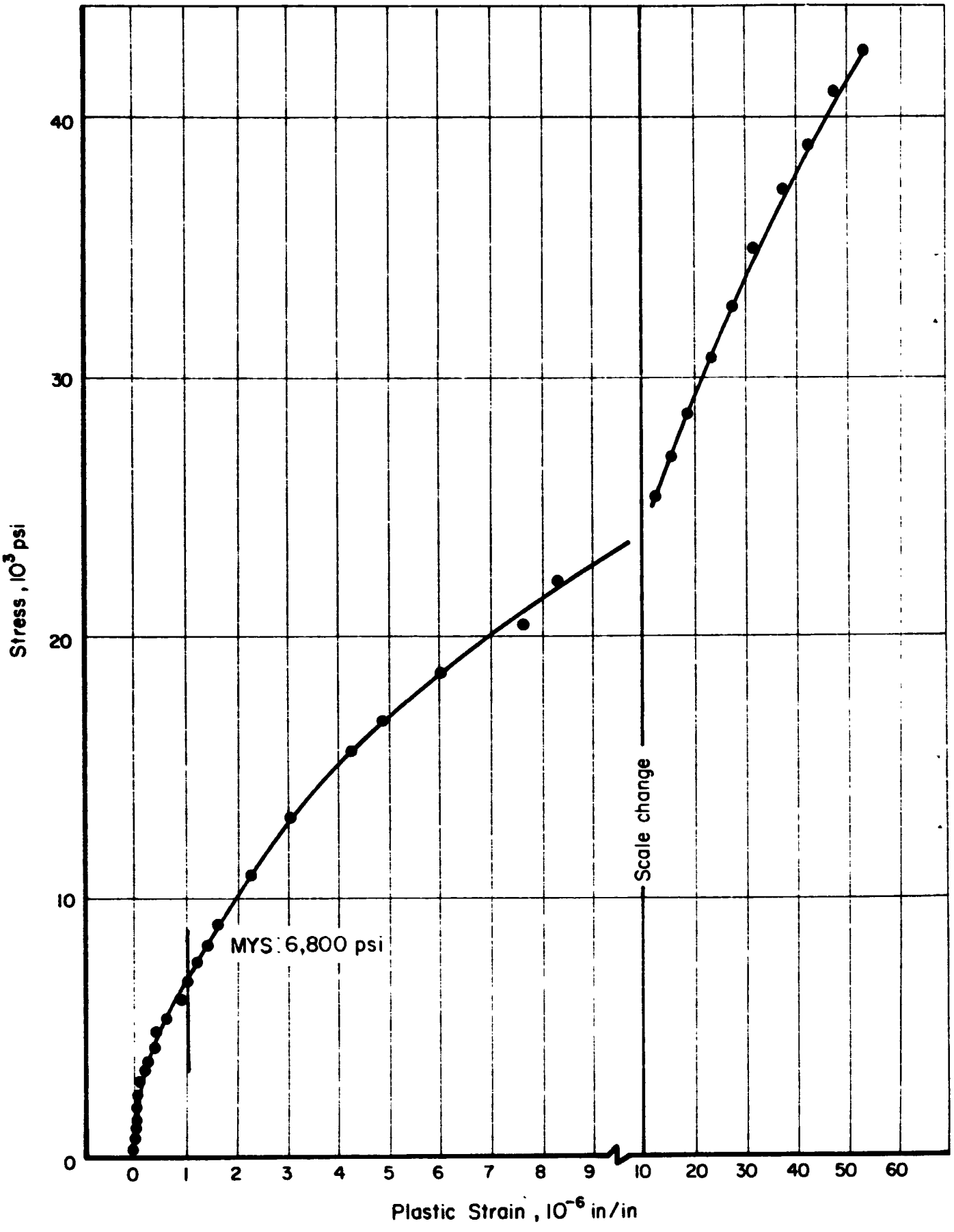

FIGURE A-42. MYS TEST ON I-400 Be, SPECIMEN No. 7, HEAT TREATED AT 1100 F FOR 1 HOUR

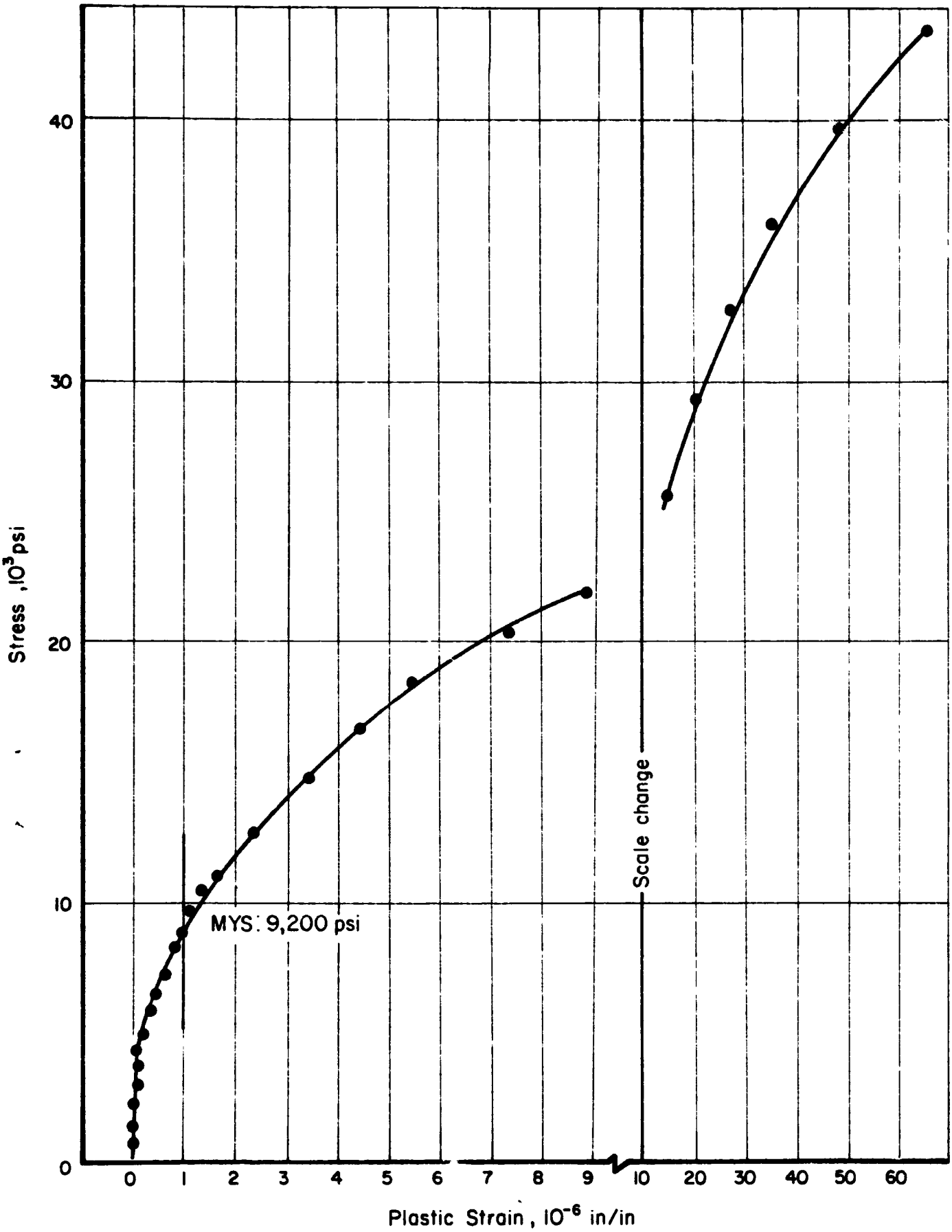

FIGURE A-43. MYS TEST ON I-400 Be, SPECIMEN No. 4, HEAT TREATED 1 HOUR AT 1500 F

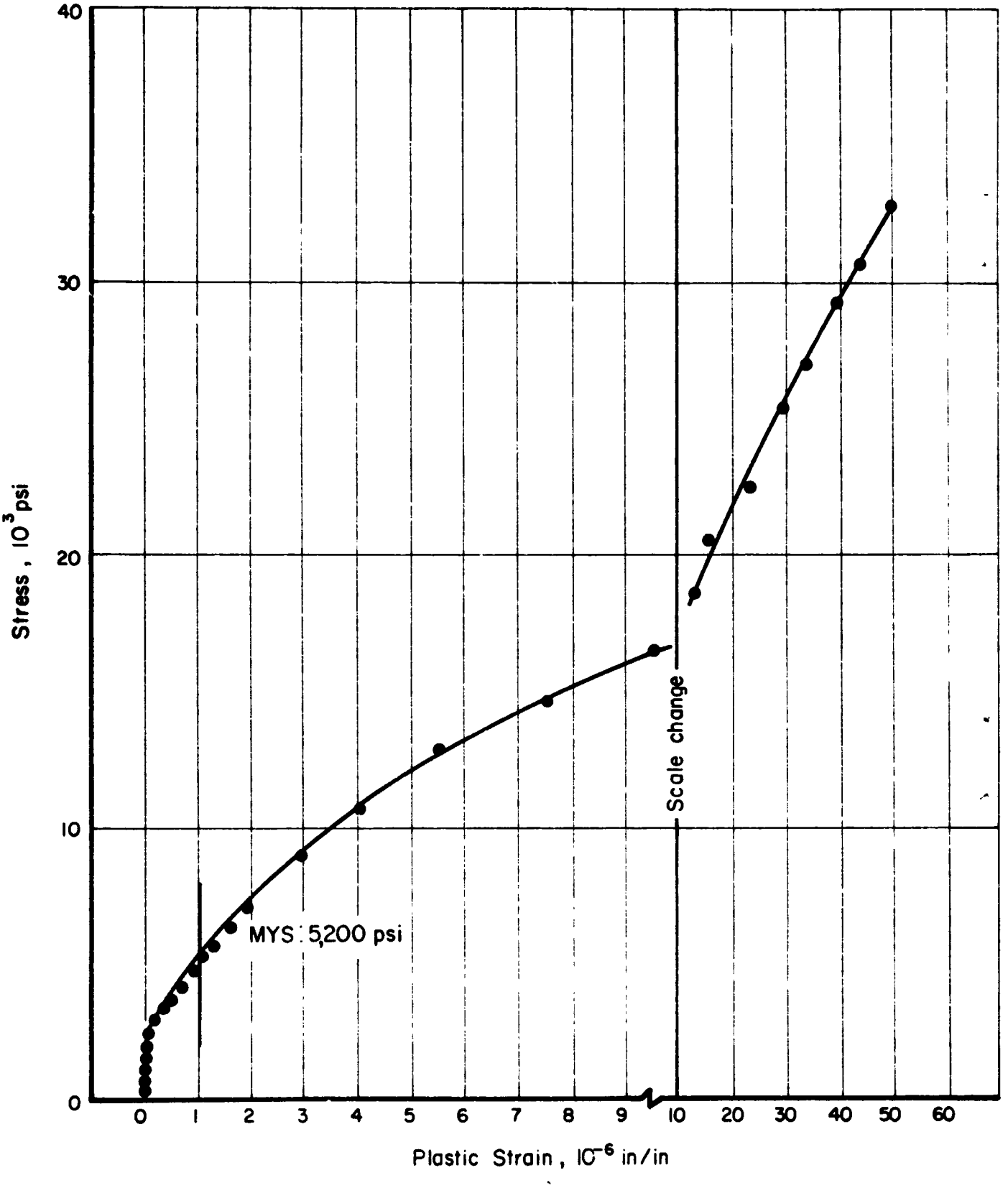

FIGURE A-44. MYS TEST ON I-400 Be, SPECIMEN No. 5, HEAT TREATED AT 1500 F FOR 1 HOUR

APPENDIX B

CREEP CURVES

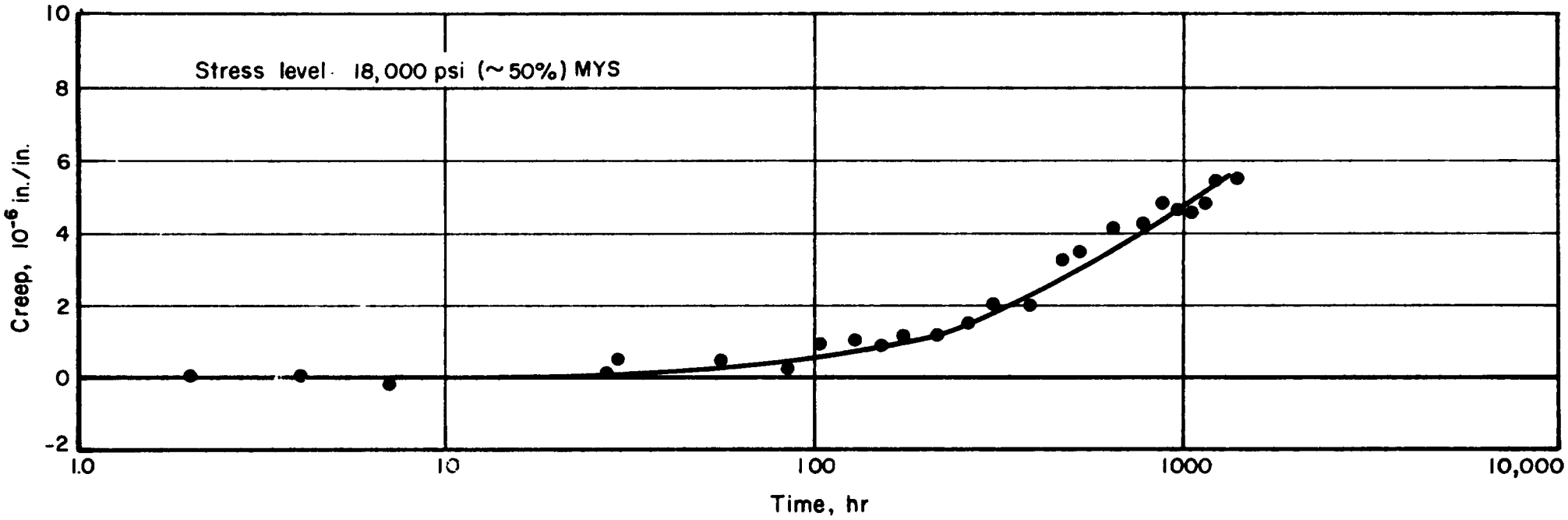

FIGURE B-1. MICROCREEP TEST ON 2024-T4 Al, SPECIMEN NO. 9, HEAT TREATED AT 400 F FOR 1 HOUR

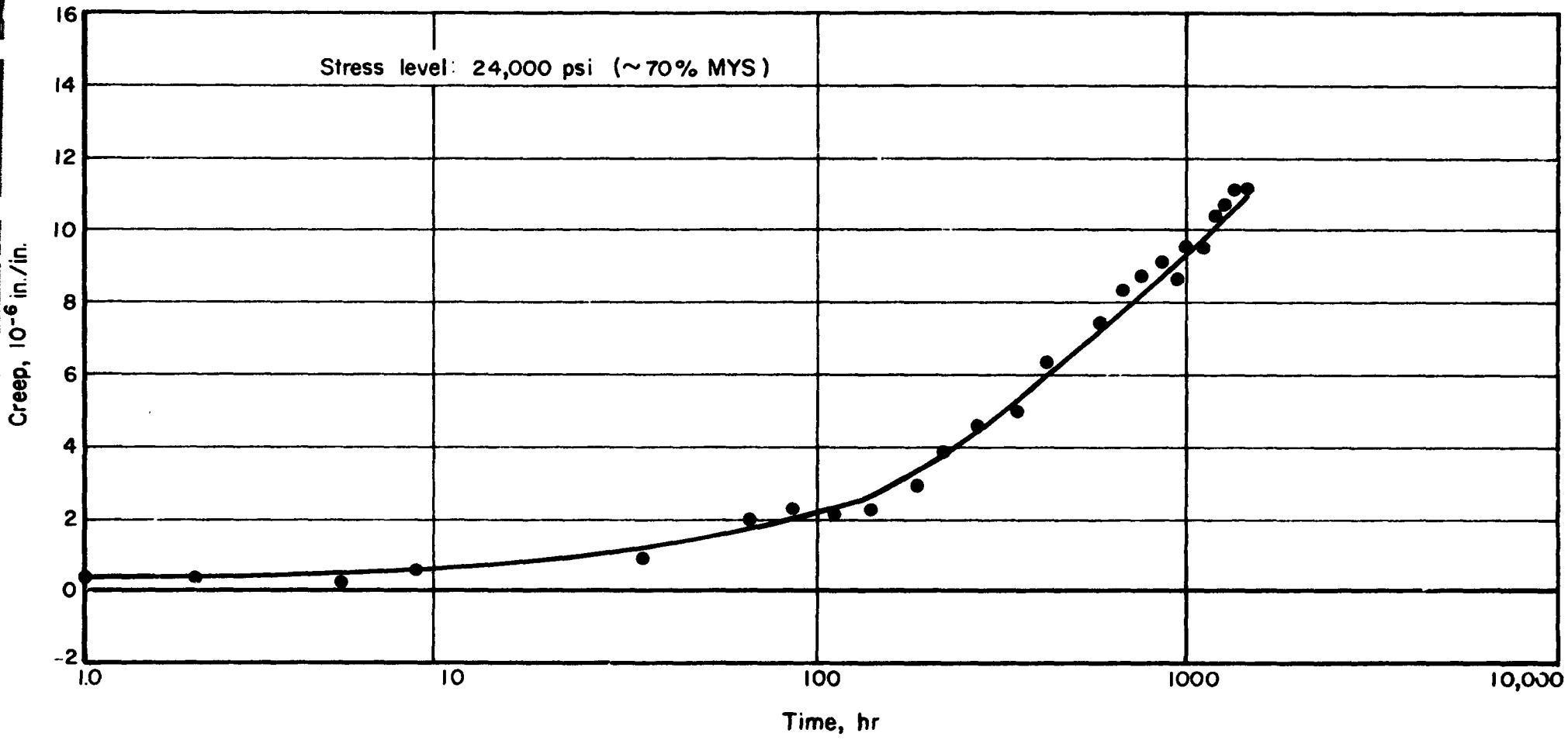

FIGURE B-2. MICROCREEP TEST ON 2024-T4 Al, SPECIMEN NO. 10, HEAT TREATED AT 400 F FOR 1 HOUR

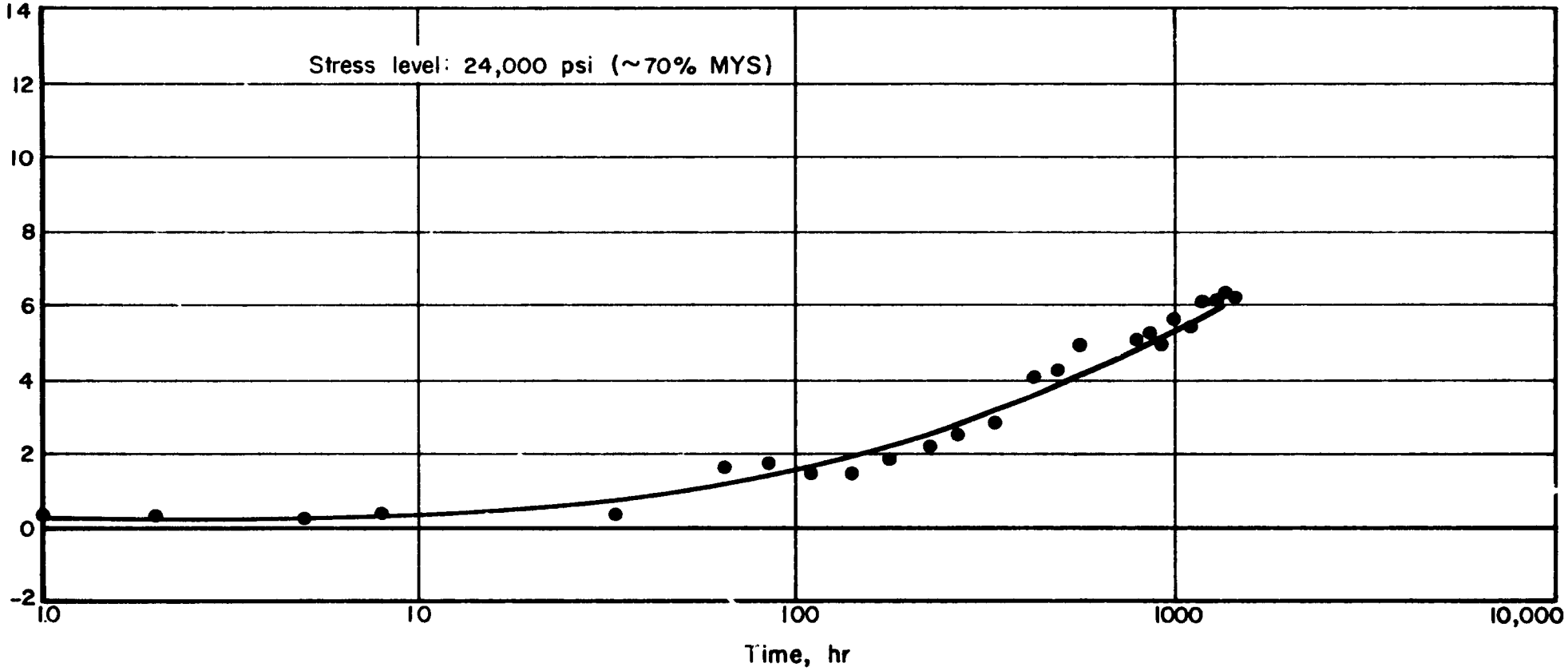

FIGURE B-3. MICROCREEP TEST ON 2024-T4 Al, SPECIMEN NO. 12, HEAT TREATED AT 400 F FOR 1 HOUR

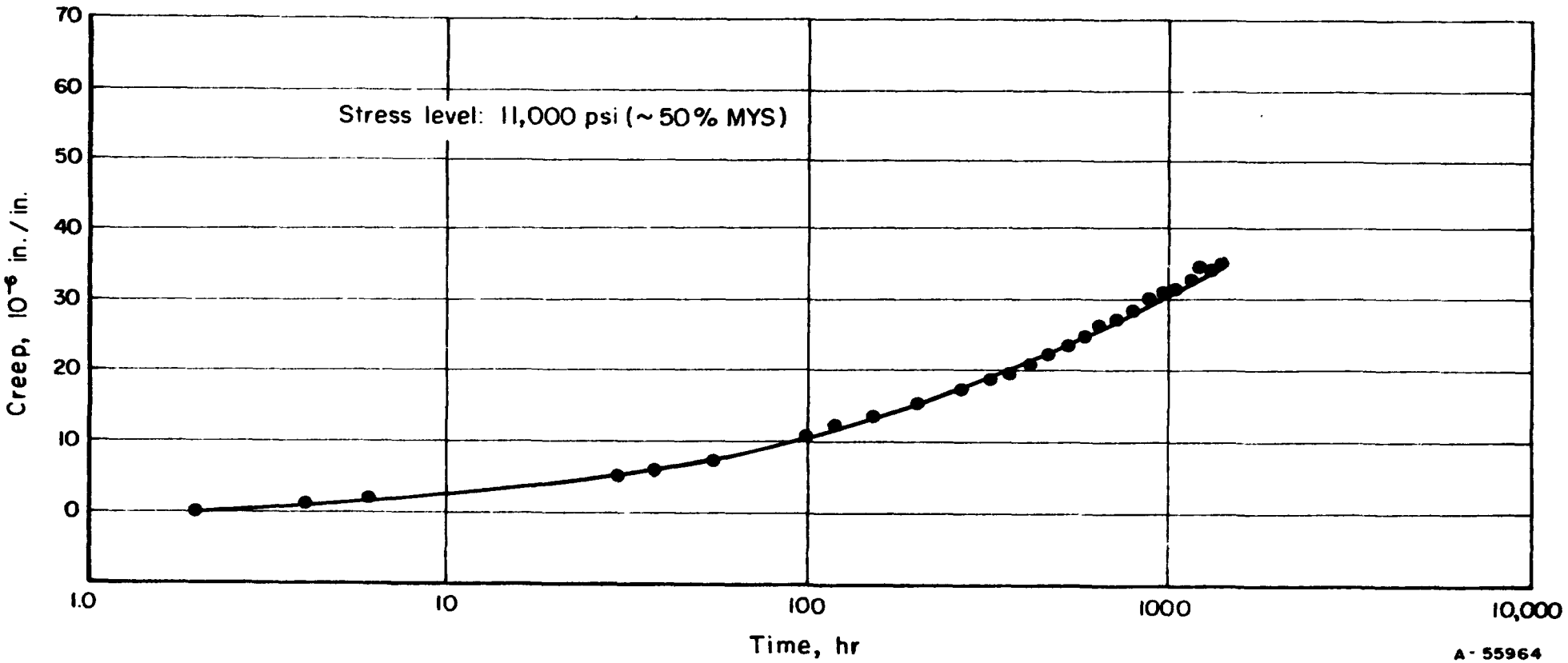

FIGURE B-4. MICROCREEP TEST ON 5456-H34 Al, SPECIMEN NO. 17, HEAT TREATED AT 400 F FOR 1 HOUR

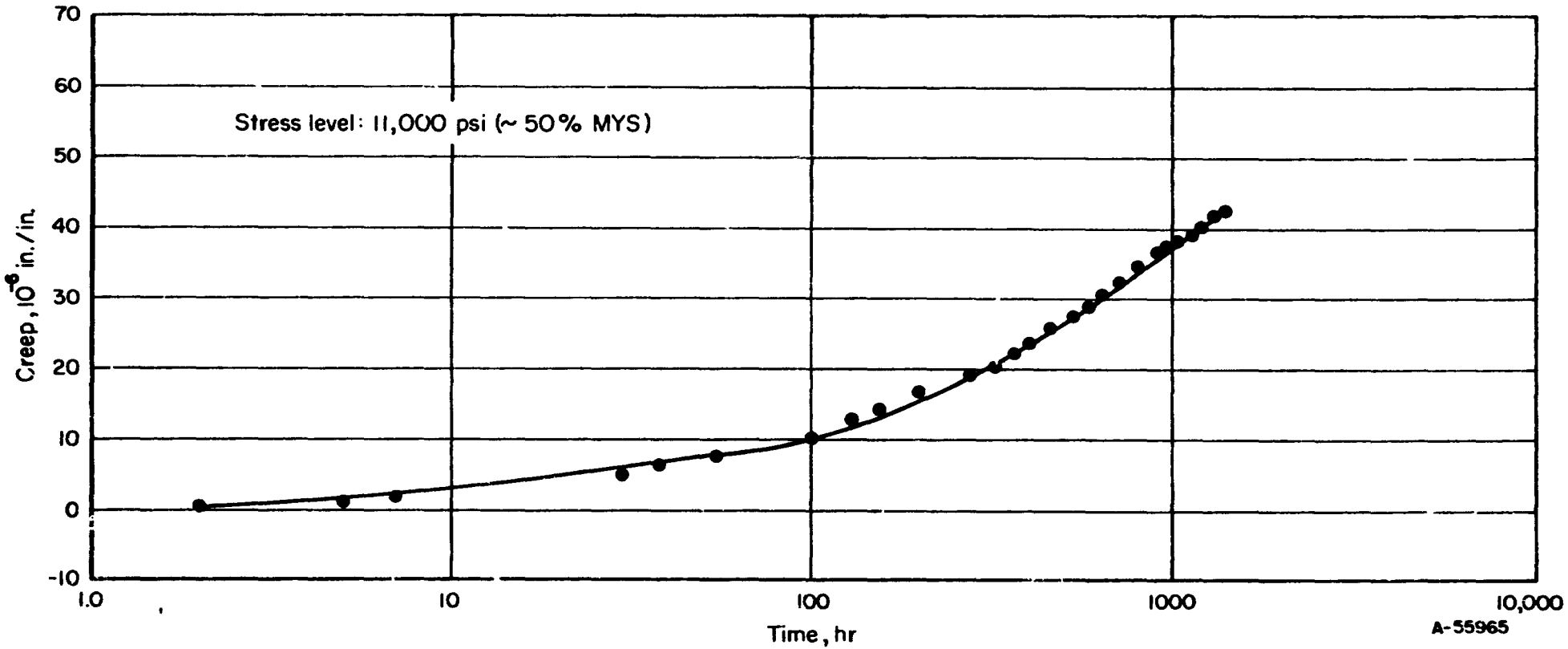

FIGURE B-5. MICROCREEP TEST ON 5456-H34 Al, SPECIMEN NO. 18, HEAT TREATED AT 400 F FOR 1 HOUR

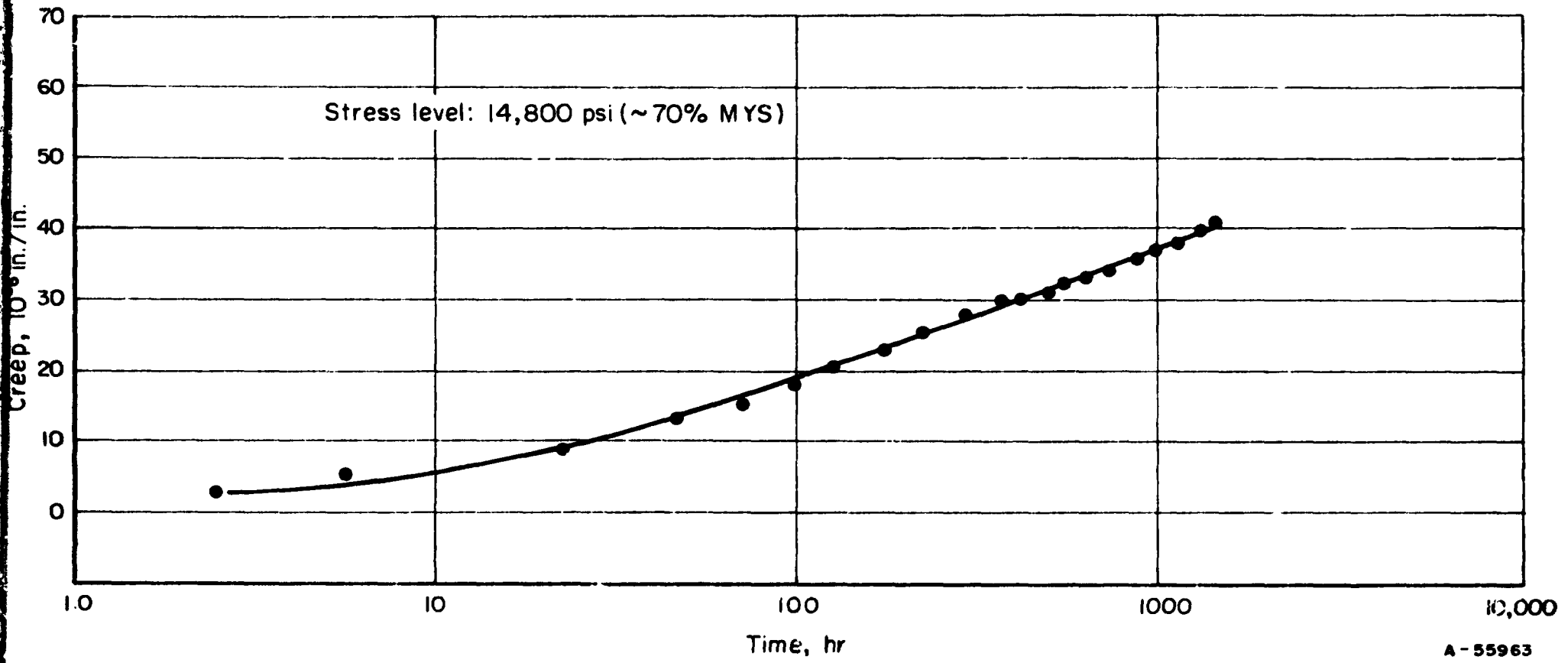

FIGURE B-6. MICROCREEP TEST ON 5456-H34 Al, SPECIMEN NO. 15, HEAT TREATED AT 400 F FOR 1 HOUR

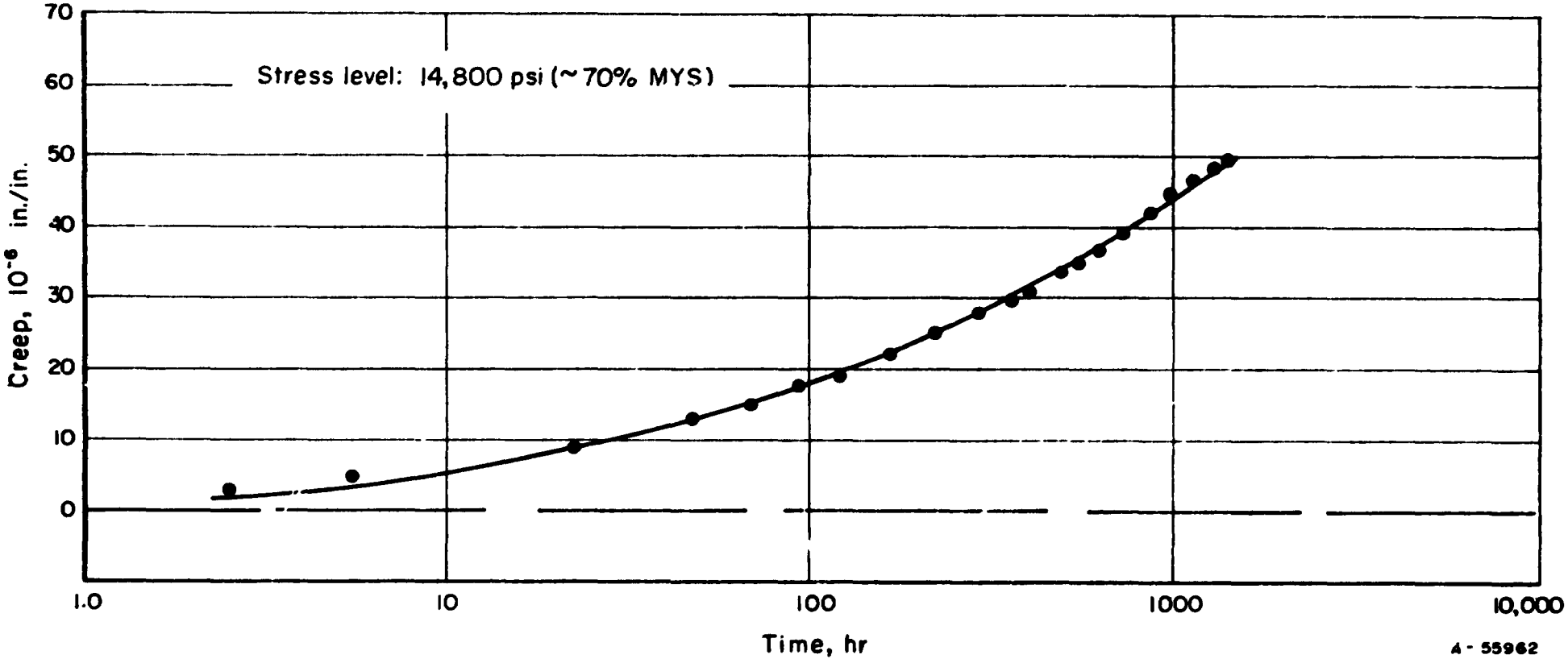

FIGURE B-7. MICROCREEP TEST ON 5456-H34 Al, SPECIMEN NO. 16, HEAT TREATED AT 400 F FOR 1 HOUR

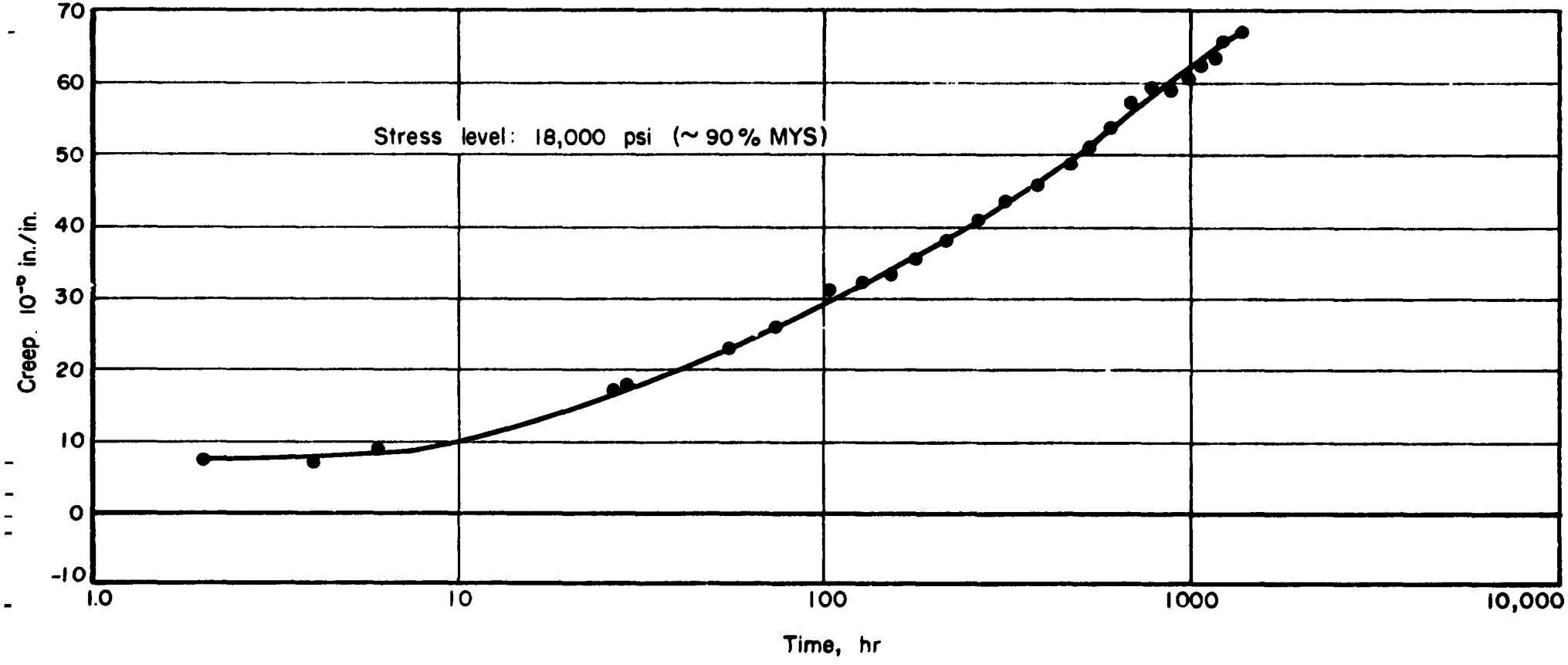

FIGURE B-8. MICROCREEP TEST ON 5456-H34 Al, SPECIMEN NO. 13, HEAT TREATED AT 400 F FOR 1 HOUR

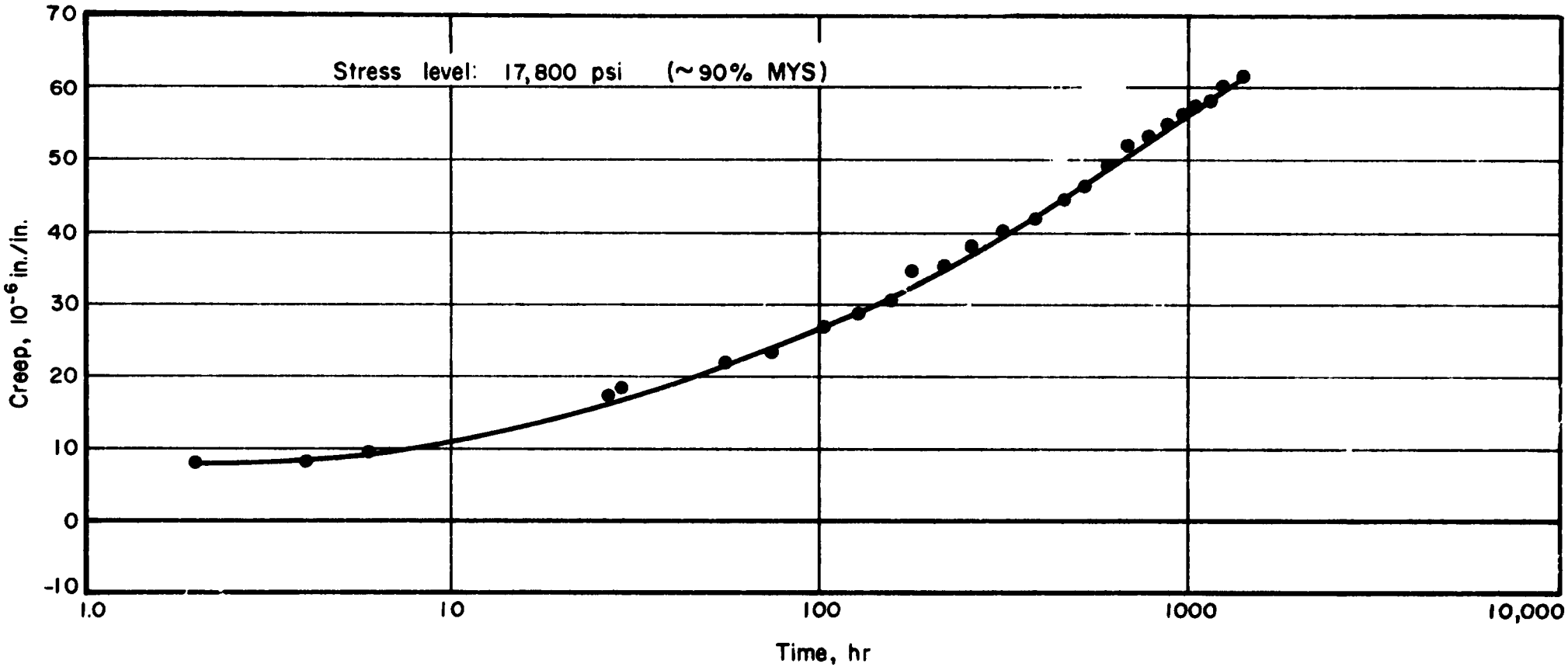

FIGURE B-9. MICROCREEP TEST ON 5456-H34 Al, SPECIMEN NO. 14, HEAT TREATED AT 400 F FOR 1 HOUR

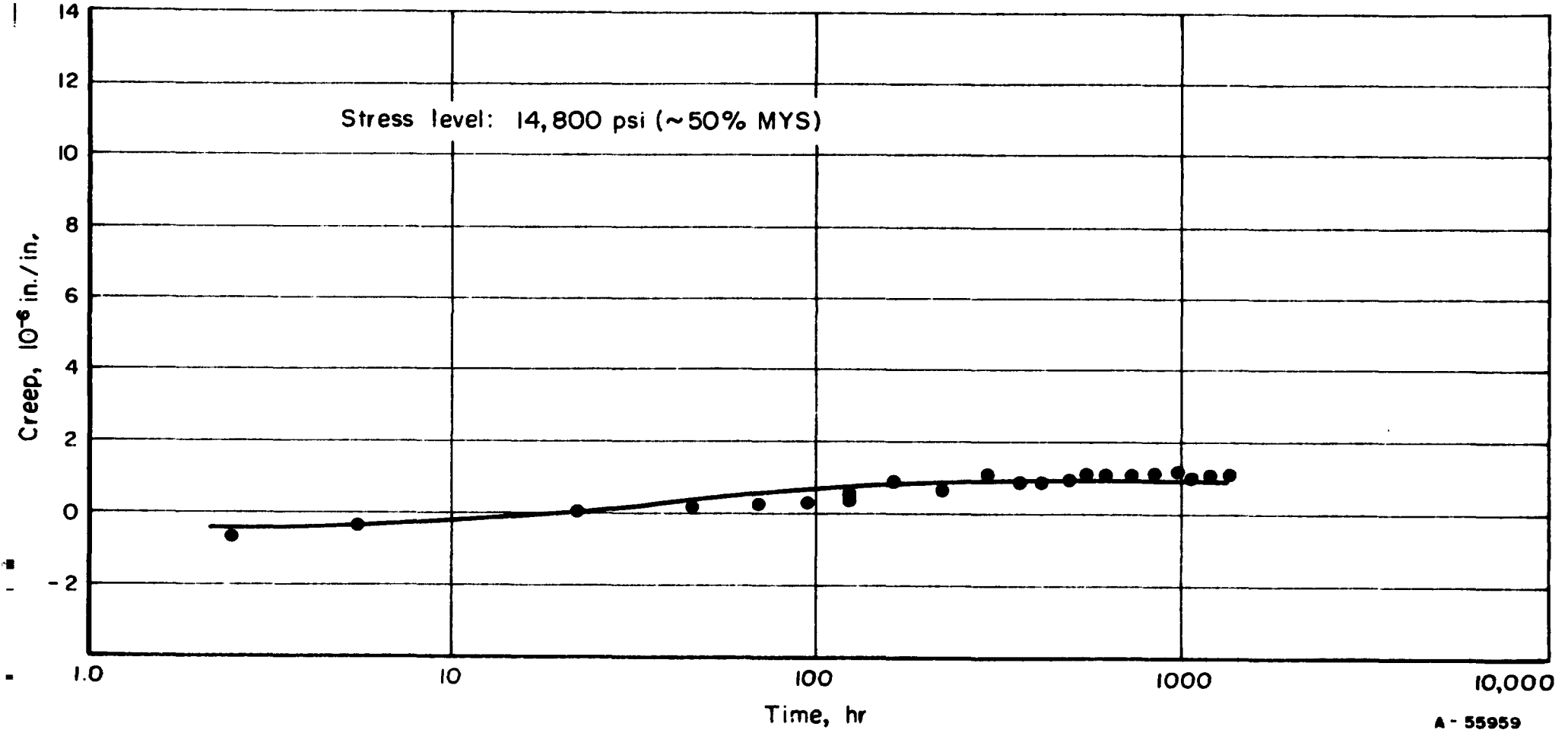

FIGURE B-10. MICROCREEP TEST ON 6061-T6 Al, SPECIMEN NO. 7, HEAT TREATED AT 400 F FOR 1 HOUR

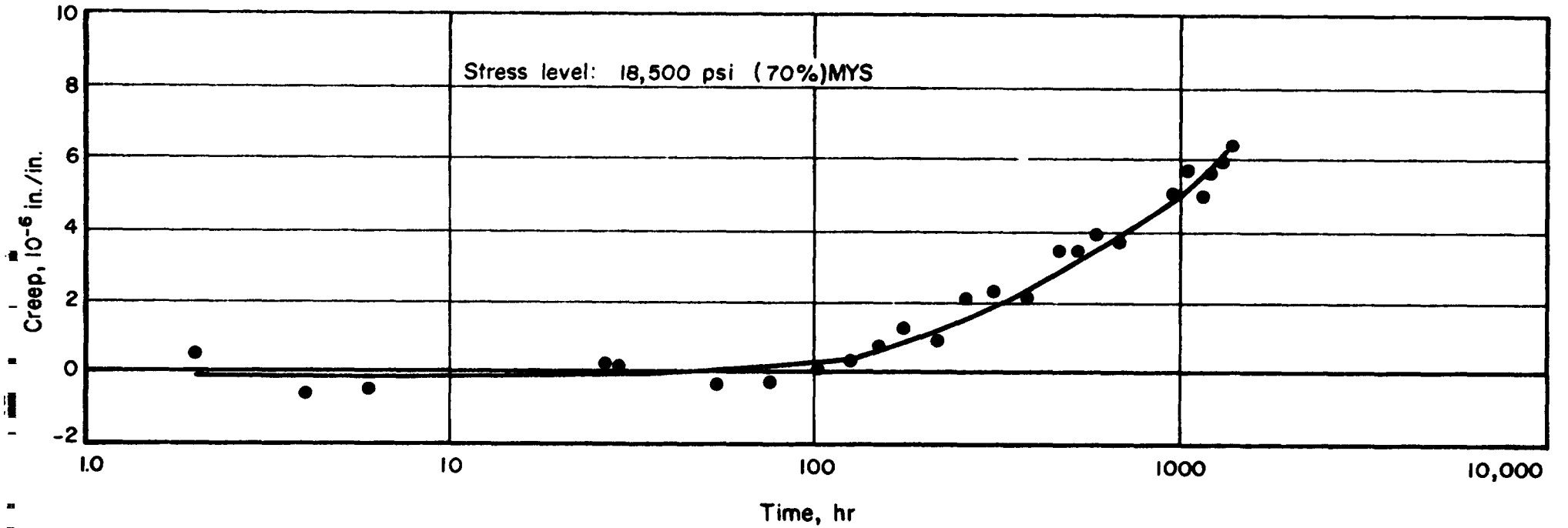

FIGURE B-11. MICROCREEP TEST ON 6061-T6 Al, SPECIMEN NO. 3, HEAT TREATED AT 400 F FOR 1 HOUR

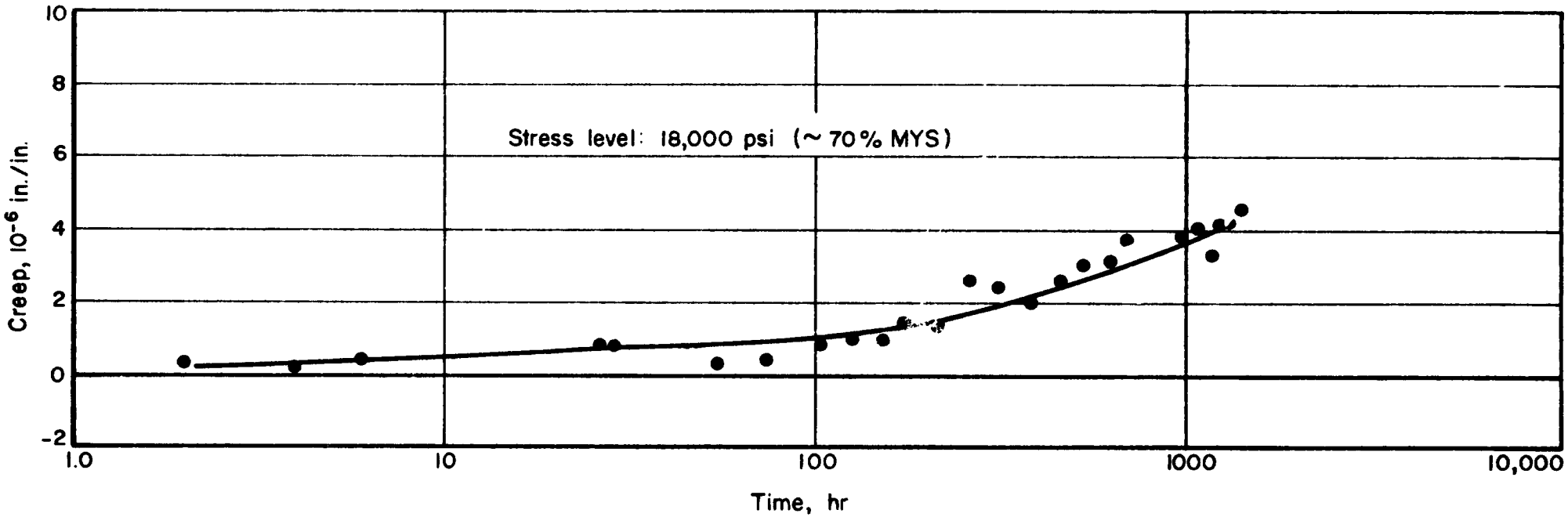

FIGURE B-12. MICROCREEP TEST ON 6061-T6 Al, SPECIMEN NO. 4, HEAT TREATED AT 400 F FOR 1 HOUR

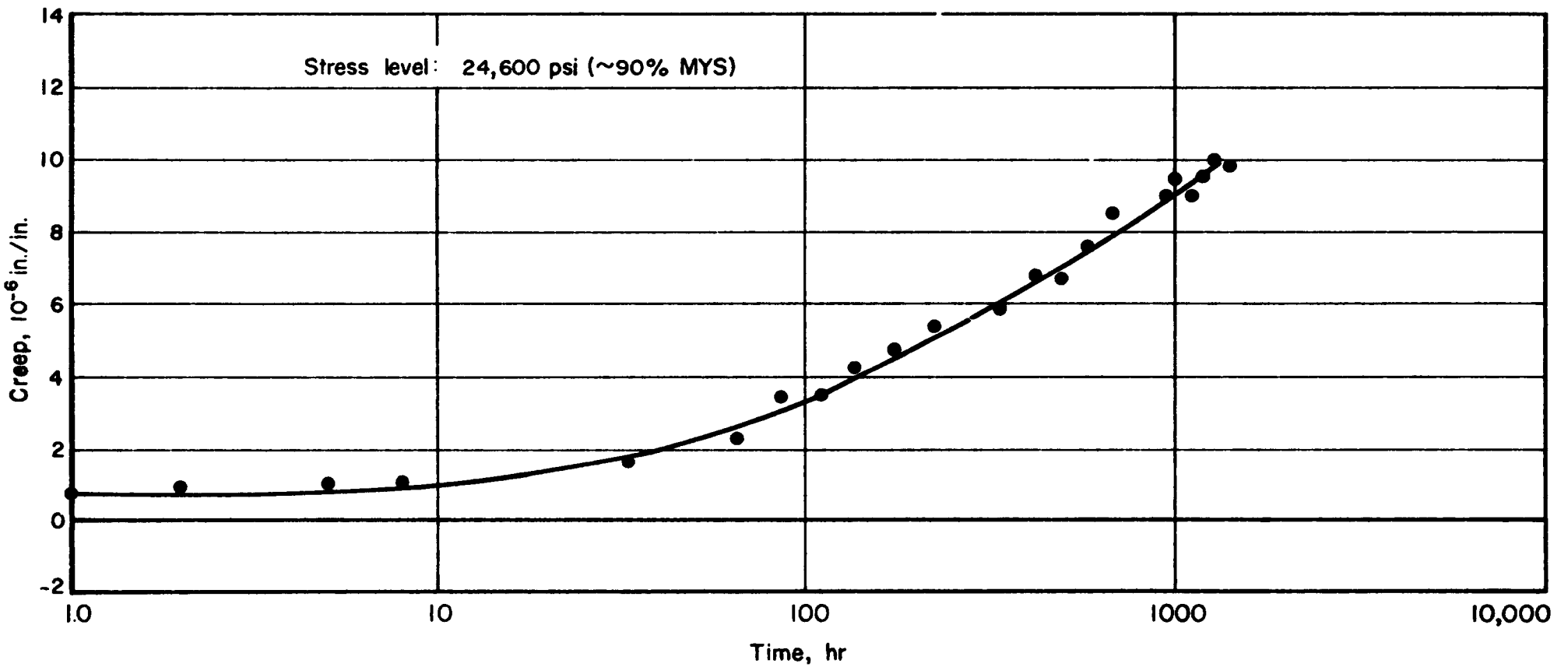

FIGURE B-13. MICROCREEP TEST ON 6061-T6 Al, SPECIMEN NO. 5, HEAT TREATED AT 400 F FOR 1 HOUR

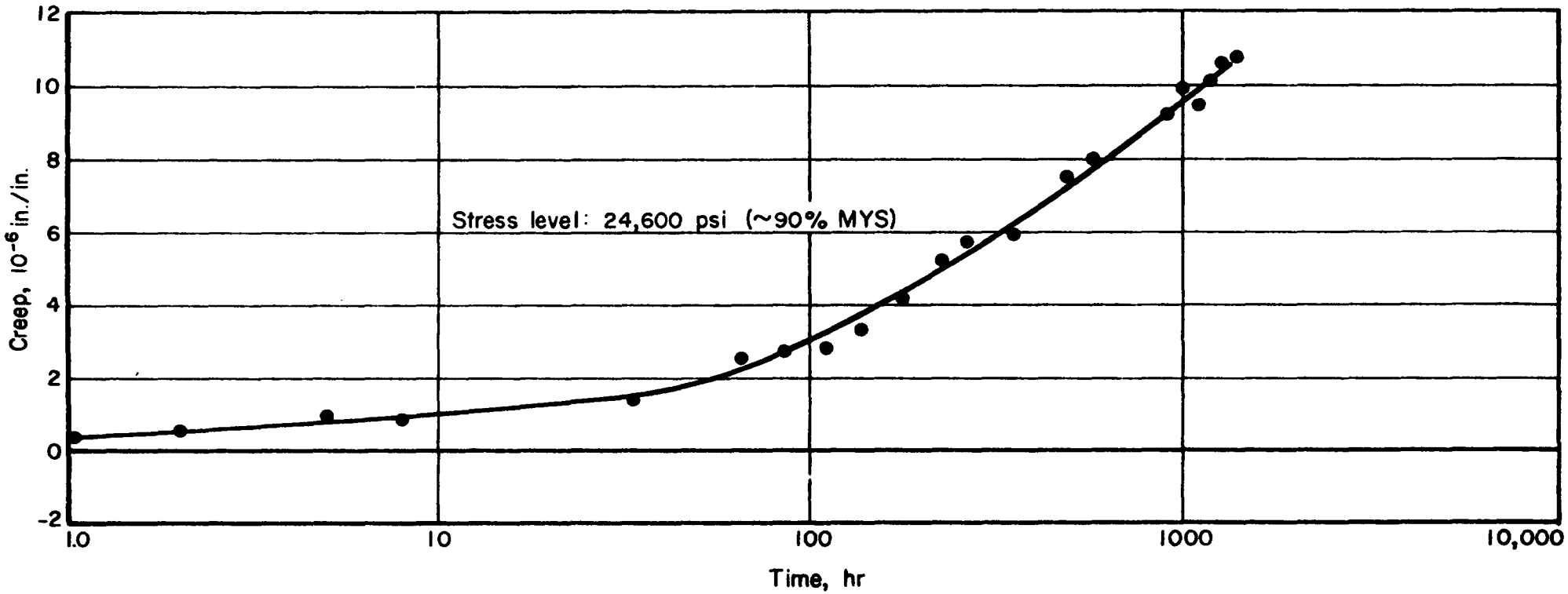

FIGURE B-14. MICROCREEP TEST ON 6061-T6 Al, SPECIMEN NO. 6, HEAT TREATED AT 400 F FOR 1 HOUR

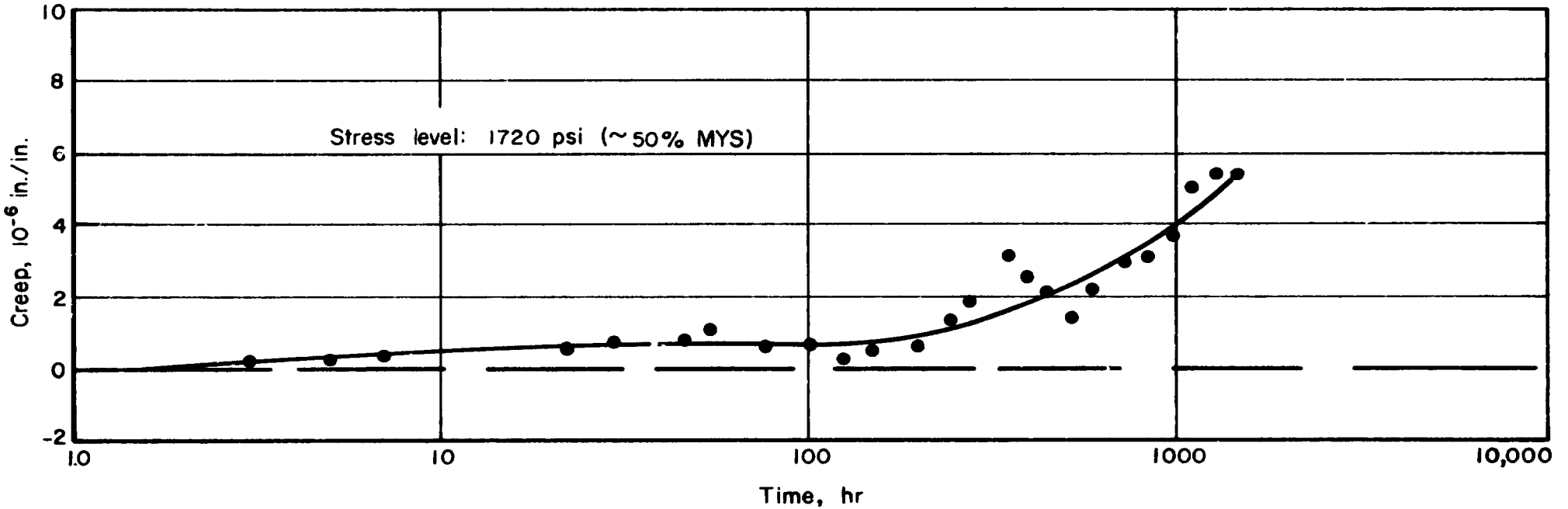

FIGURE B-15. MICROCREEP TEST ON AZ 31 Mg, SPECIMEN NO. 1, HEAT TREATED AT 450 F FOR 1 HOUR

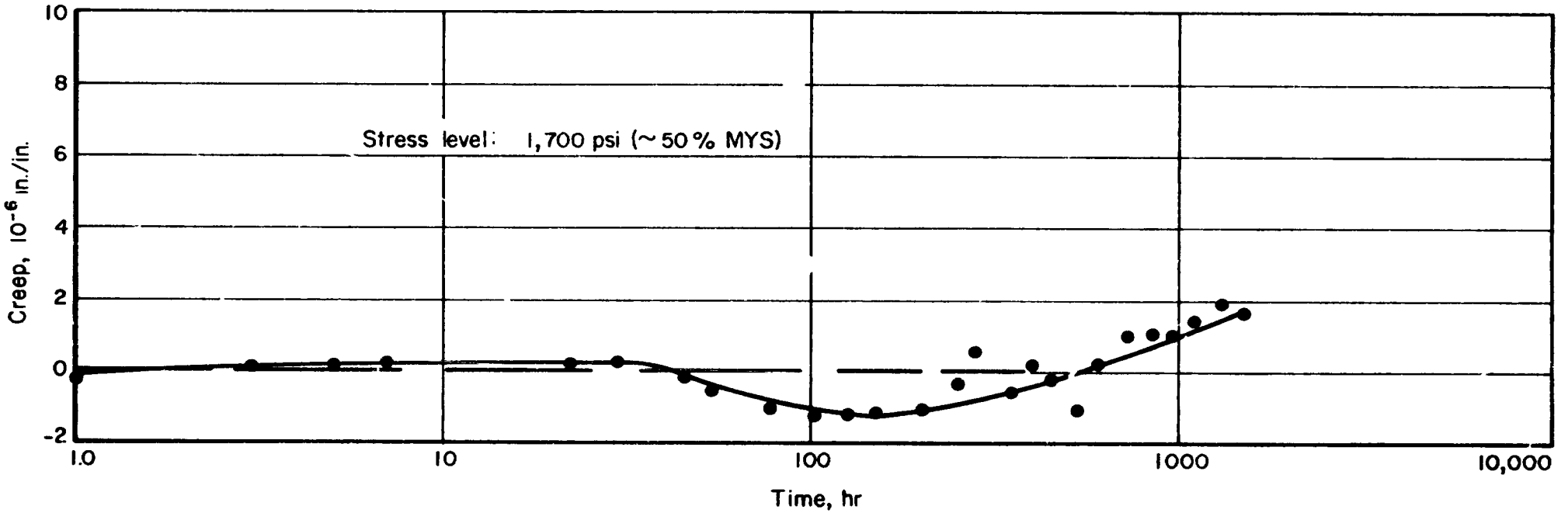

FIGURE B-16. MICROCREEP TEST ON AZ 31 Mg, SPECIMEN NO. 2, HEAT TREATED AT 450 F FOR 1 HOUR

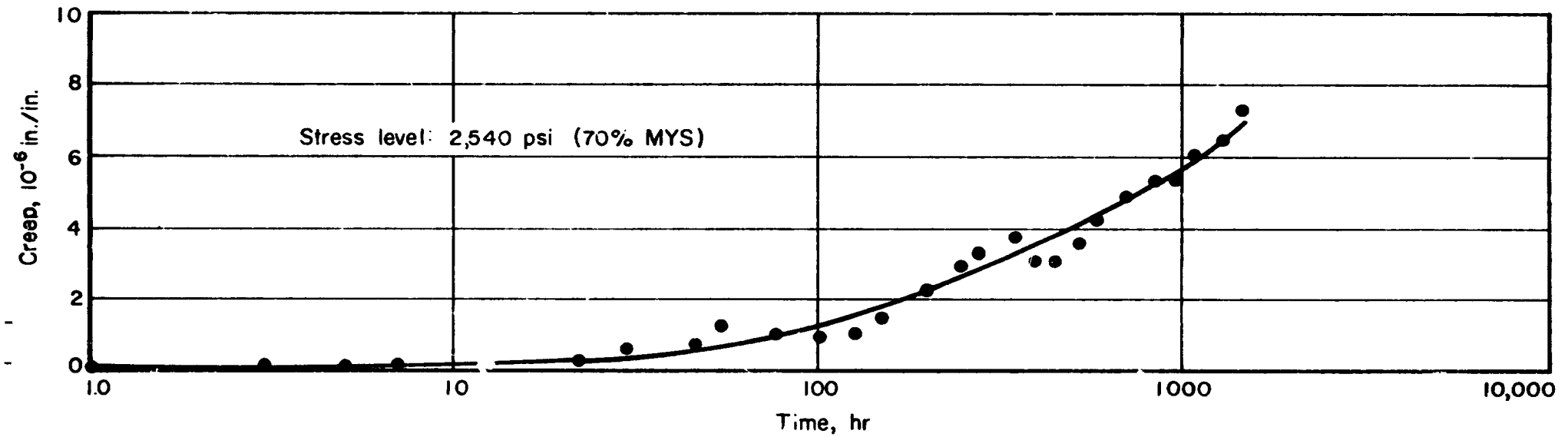

FIGURE B-17. MICRO CREEP TEST ON AZ 31 Mg, SPECIMEN NO. 3, HEAT TREATED AT 450 F FOR 1 HOUR

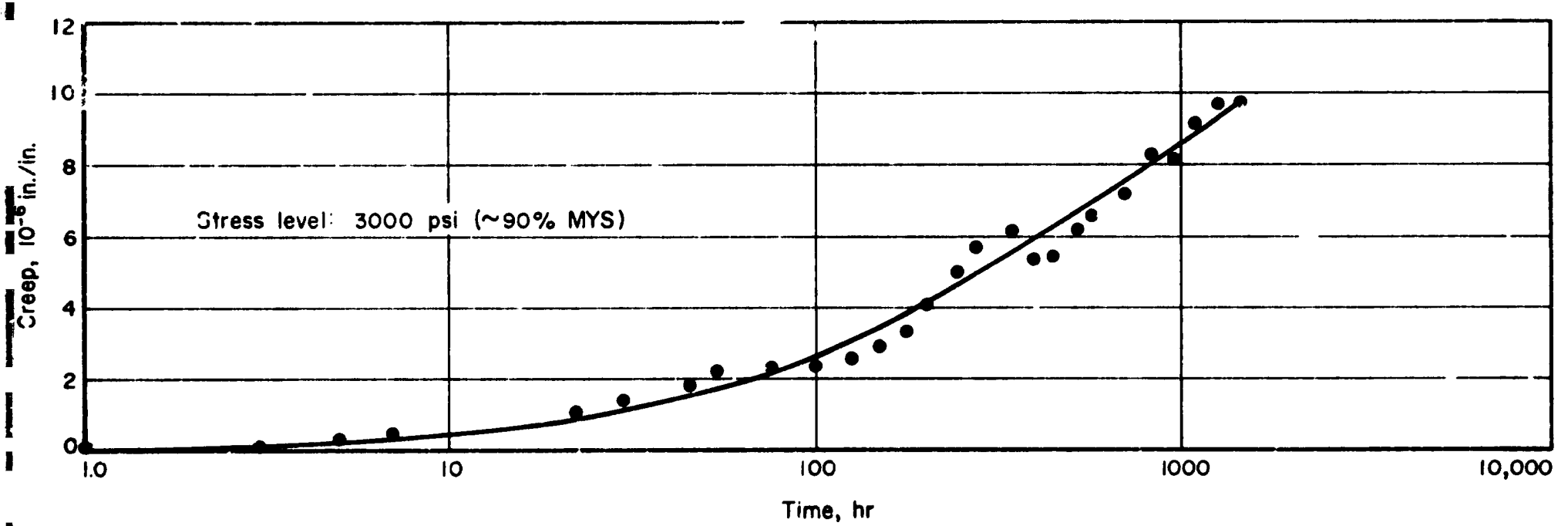

FIGURE B-18. MICROCREEP TEST ON AZ 31 Mg, SPECIMEN NO. 5, HEAT TREATED AT 450 F FOR 1 HOUR

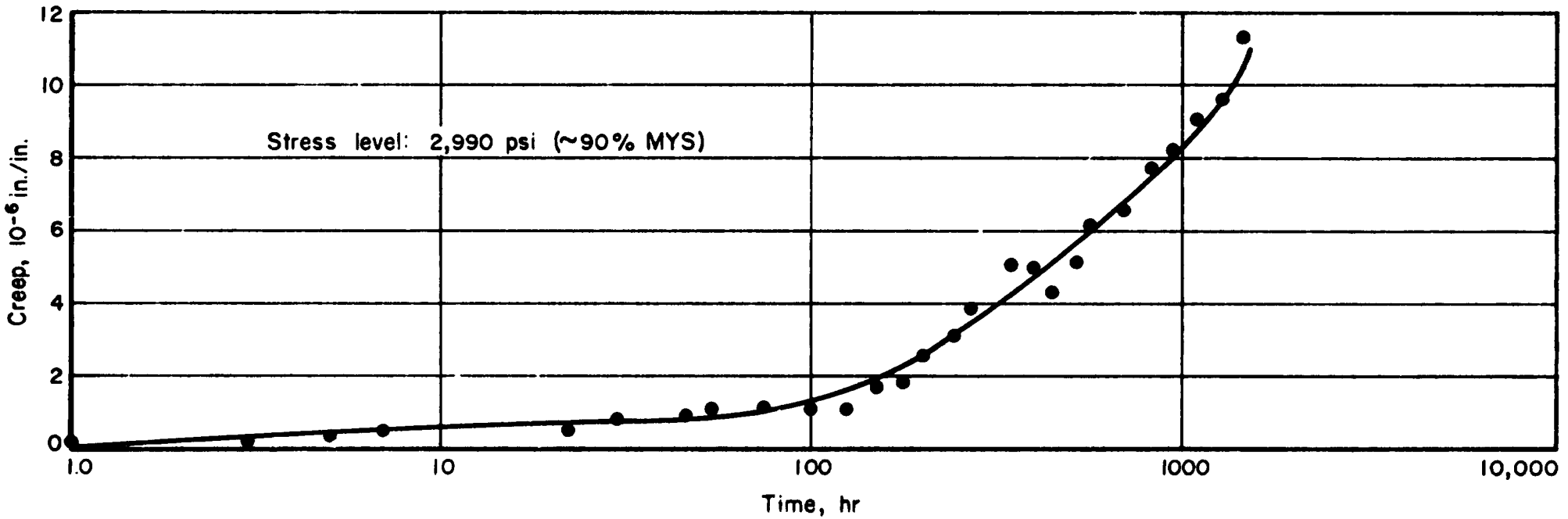

FIGURE B-19. MICROCREEP TEST ON AZ 31 Mg, SPECIMEN NO. 6, HEAT TREATED AT 450 F FOR 1 HOUR

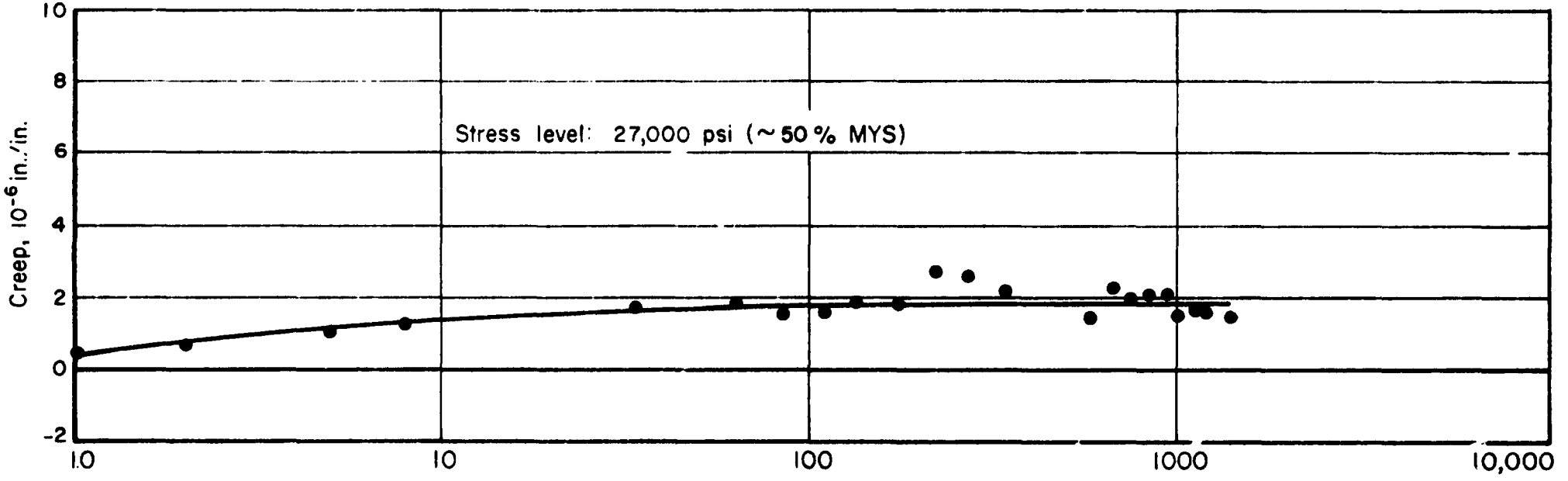

FIGURE B-20. MICROCREEP TEST ON TZM Mo, SPECIMEN NO. 1, HEAT TREATED AT 2200 F FOR 1 HOUR

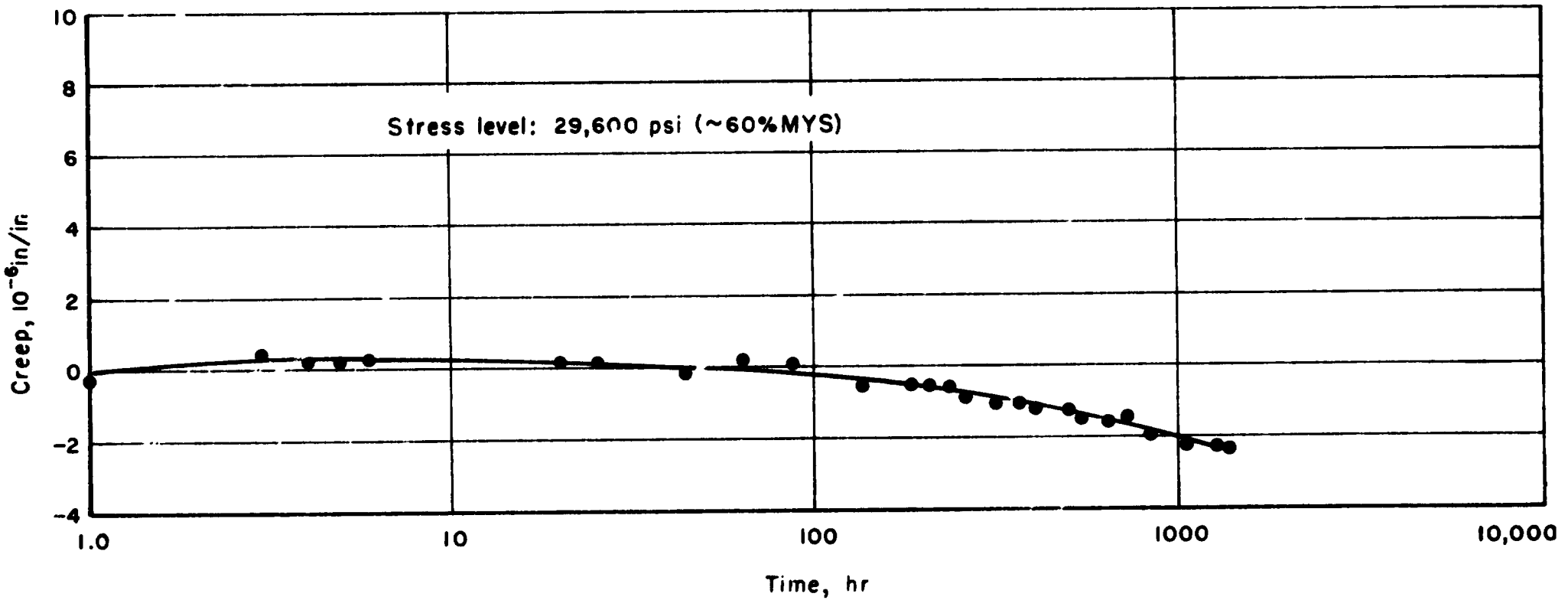

FIGURE B-21. MICROCREEP TEST ON TZM Mo, SPECIMEN NO. 3, HEAT TREATED AT 2200 F FOR 1 HOUR

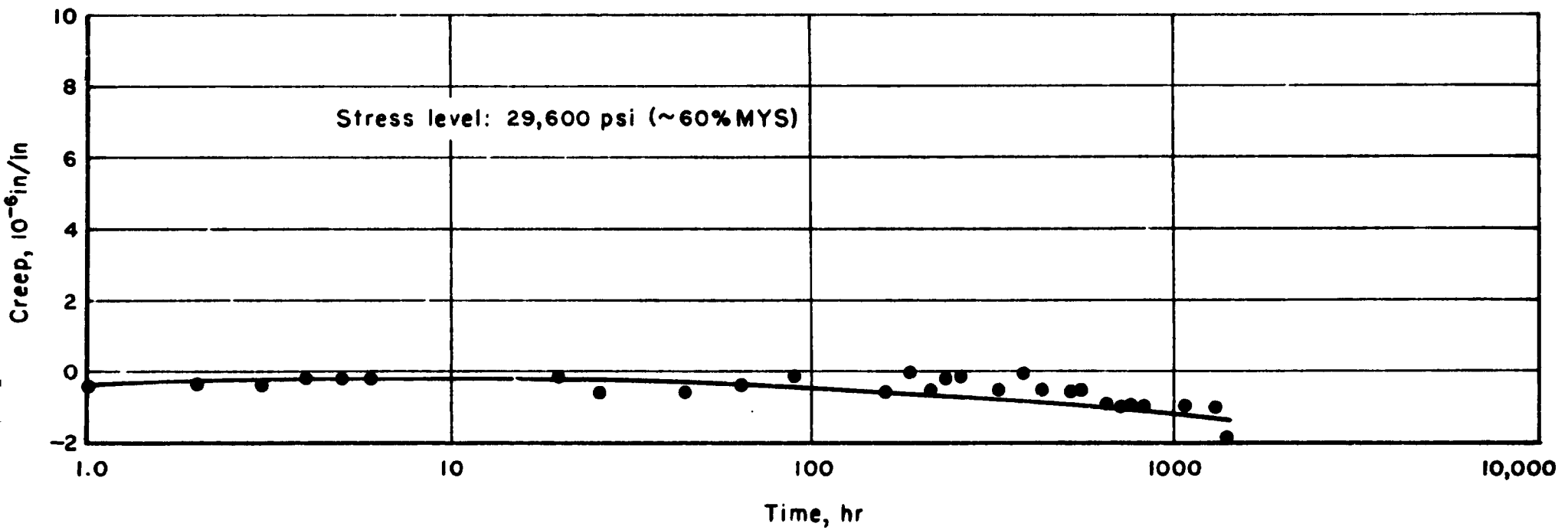

FIGURE B-22. MICROCREEP TEST ON TZM Mo, SPECIMEN NO. 8, HEAT TREATED AT 2200 F FOR 1 HOUR

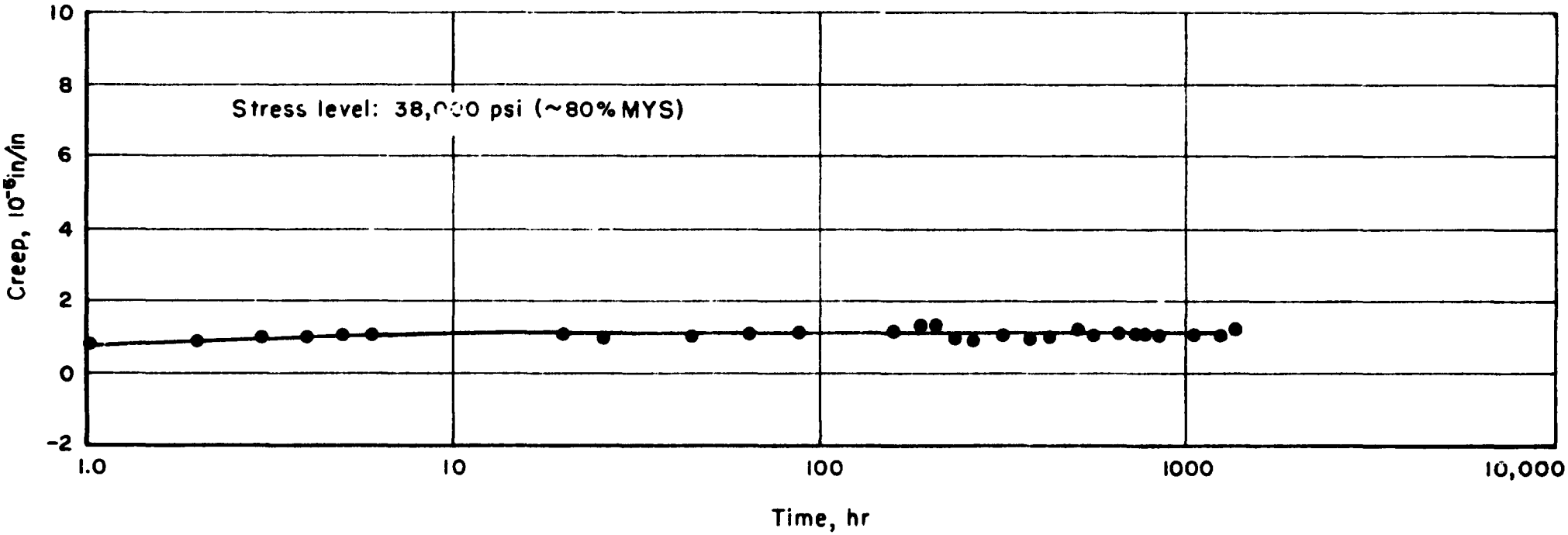

FIGURE B-23. MICROCREEP TEST ON TZM Mo, SPECIMEN NO. 2
HEAT TREATED AT 2200 F FOR 1 HOUR

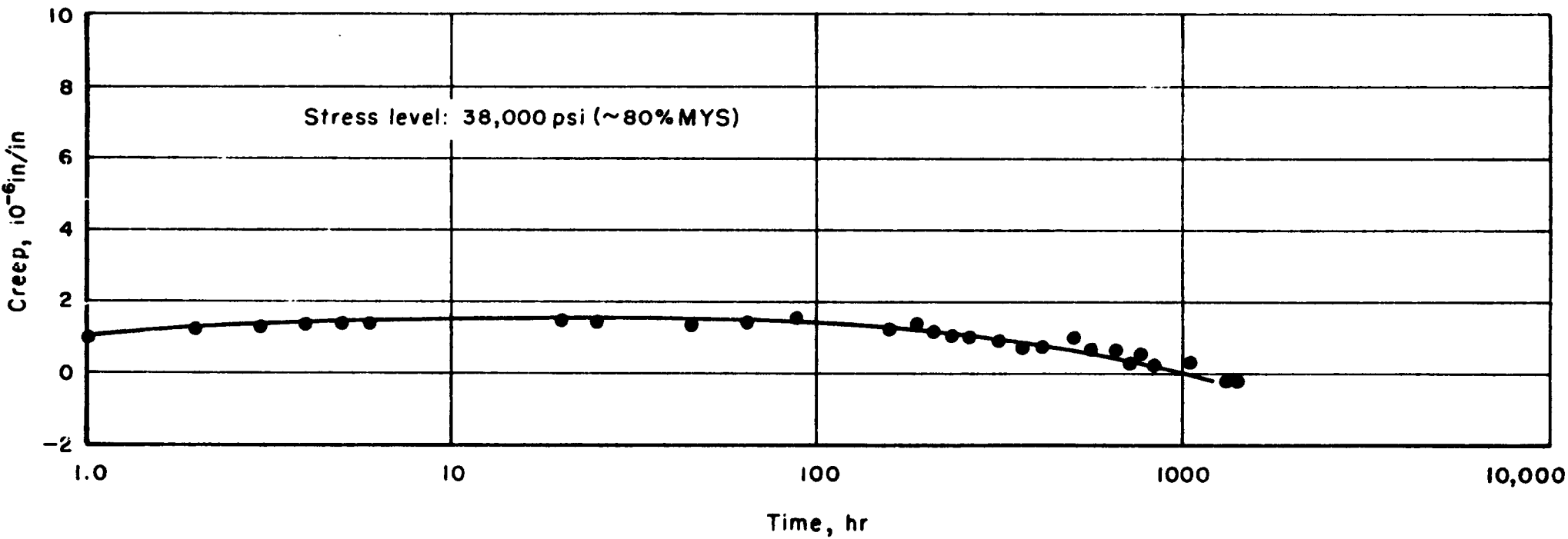

FIGURE B-24. MICROCREEP TEST ON TZM Mo, SPECIMEN NO. 4, HEAT TREATED AT 2200 F FOR 1 HOUR

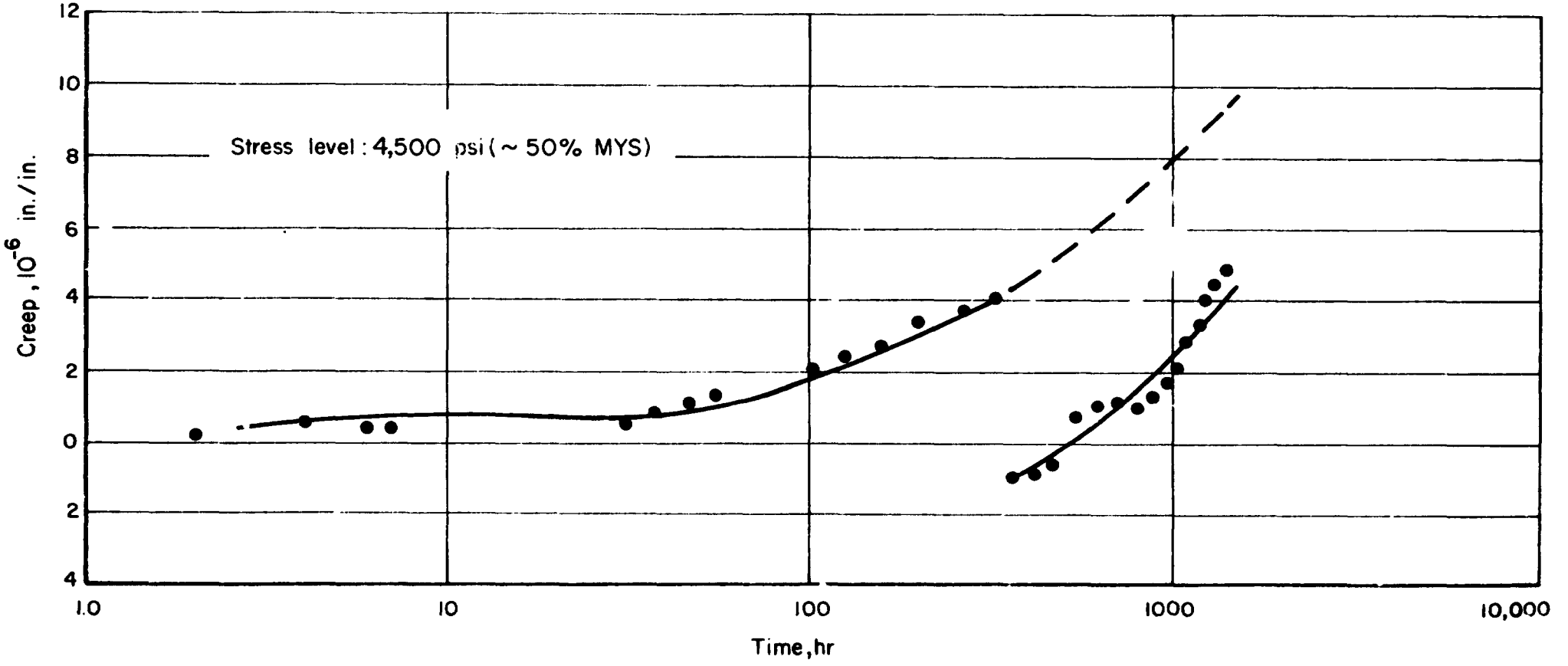

FIGURE B-25. MICROCREEP TEST ON I-400 Be, SPECIMEN NO. 2, HEAT TREATED AT 1100 F FOR 1 HOUR

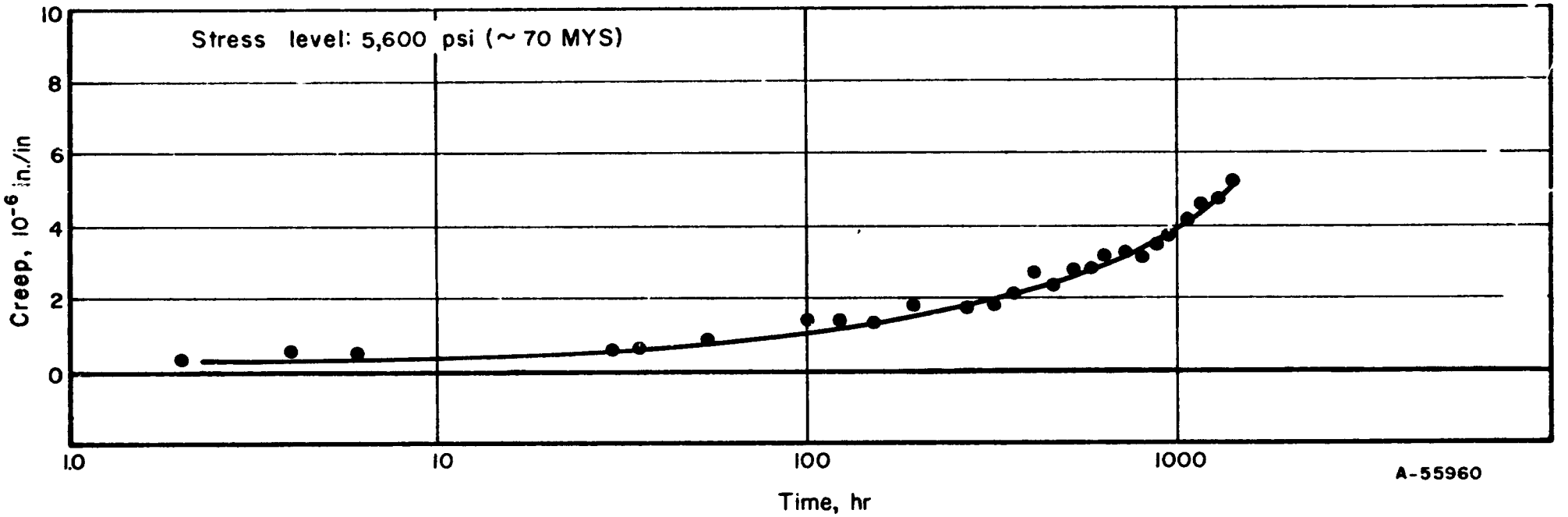

FIGURE B-26. MICROCREEP TEST ON I-400 Be, SPECIMEN NO. 3, HEAT TREATED AT 1100 F FOR 1 HOUR

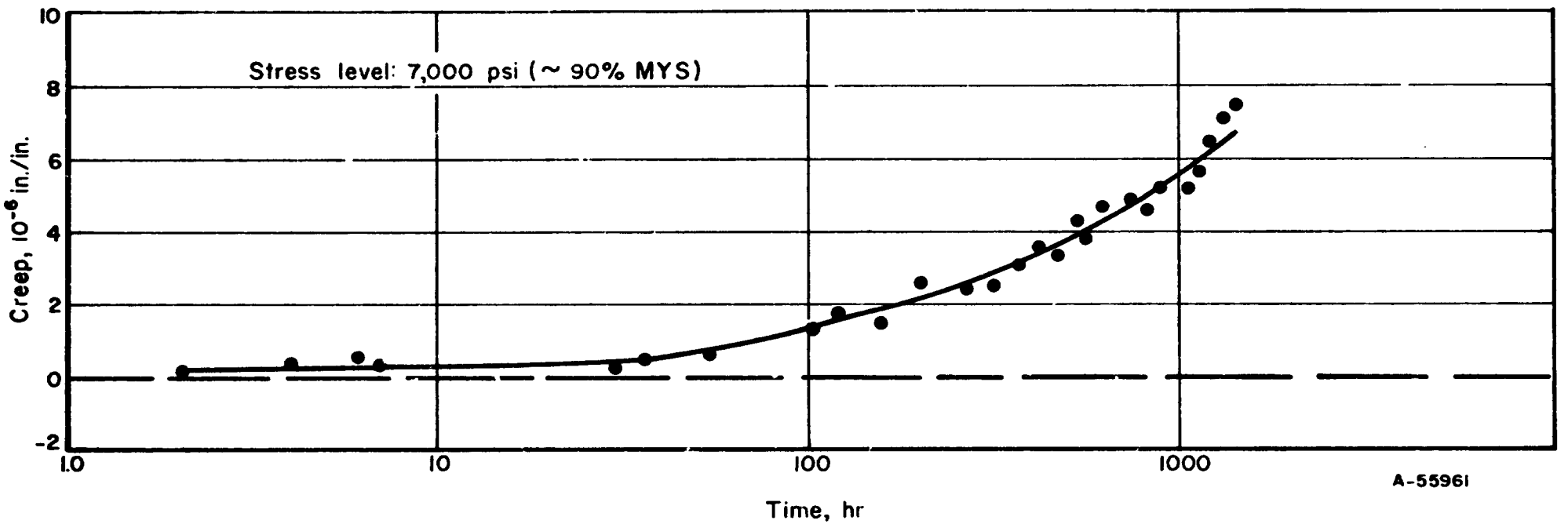

FIGURE B-27. MICROCREEP TEST ON I-400 Be, SPECIMEN NO. 1, HEAT TREATED AT 1100 F FOR 1 HOUR